

**Alabama Water Resources Research Institute
Annual Technical Report
FY 2011**

Introduction

The Alabama Water Resources Research Institute (AL-WRRI) was created in 1964 by the Alabama Legislature. In 2007 the AL-WRRI was combined with the newly created Auburn University Water Resources Center (AU-WRC), and in 2008 it was designated as part of the Auburn University Center of Excellence for Watershed Management by EPA. The AU-WRC and AL-WRRI function as a single university-based interdisciplinary, problem-oriented research and technology center under one Director with support from the federal government through the USGS that enables the programs to address broad national needs and relevant industrial technology.

The Alabama Water Resources Center and Research Institute coordinates research programs that contribute to the solutions of present and emerging water resources problems. In carrying out this mission, the Institute has developed a broadly based research, training, information transfer, and public service program involving personnel from many academic disciplines in the state's research universities

The Alabama Water Resources Center and Research Institute is one of 54 water resources institutes nationwide authorized by the federal Water Resources Research Act. The state-based Water Resources Research Institutes are located at land grant universities and function as a nation-wide network to promote research and information dissemination on the state's and nation's water resources problems

Research Program Introduction

The essential ingredient for determining proper policies and practices is factual information. Often such information must be obtained by means of scientific research. The Institute conducts a program that stimulates, sponsors, and provides for research, investigation, and experimentation in the fields of water and of resources as they affect water, and encourages the training of scientists in the fields related to water.

Objectives of the AU-WRC and AL-WRRI are:

To plan, conduct and otherwise arrange for competent research that fosters (a) the entry of new research scientists into the water resources fields, (b) the training and education of future water scientists, engineers and technicians, (c) the preliminary exploration of new ideas that address water problems or expand understanding of water and water-related phenomena, and (d) the dissemination of research results to water managers and the public

To identify major research needs and develop for Alabama and the Southeastern Region short- and long-term research priorities.

To encourage research applying to other environmental resources closely associated with water.

To maintain close consultation and collaboration with governmental agencies, public groups, and cooperate closely with other colleges and universities in the state that have demonstrated capabilities for research, information dissemination, and graduate training in order to develop a statewide program designed to resolve state and regional water and related land problems.

Development of an In-situ Capable Method for Detecting Pathogenic Bacteria in the Alabama Water Supplies

Basic Information

Title:	Development of an In-situ Capable Method for Detecting Pathogenic Bacteria in the Alabama Water Supplies
Project Number:	2010AL87B
Start Date:	3/1/2010
End Date:	2/28/2012
Funding Source:	104B
Congressional District:	Third
Research Category:	Engineering
Focus Category:	Surface Water, Water Quality, None
Descriptors:	None
Principal Investigators:	Ahjeong Son

Publications

There are no publications.

Project Report
for
Water Resources Research Institute Program
under
Section 104, Water Resources Research Act of 1984
to the
Alabama Water Resources Research Institute

DEVELOPMENT OF AN IN-SITU CAPABLE METHOD FOR DETECTING PATHOGENIC
BACTERIA IN THE ALABAMA WATER SUPPLIES

By

Ahjeong Son (Principal Investigator)
Assistant Professor
Department of Civil Engineering
Samuel Ginn College of Engineering
Auburn University
Telephone (334)-844-6260
Email: ason@auburn.edu

Submitted in May 20th 2011

- **Duration:** From March 1, 2010 to February 28, 2011
- **Fiscal Year 2011 Federal Funds:**

Total	Direct	Indirect
\$ 25,000	\$ 25,000	\$ 0
- **Non-Federal Funds Allocated:**

Total	Direct	Indirect
\$ 51,853	\$ 27,281	\$ 24,572
- **Name, University and City of Principal Investigators:**
Ahjeong Son, Auburn University, Auburn, Alabama (P.I.)
- **Congressional District of University performing the research:** Third

A. Statement of the problem:

Pathogenic contamination of Alabama surface water

Water is the vital resource that fuels Alabama's growth in agriculture, industrial output and technology. Gifted with more than a million acres of lakes, 1600 miles of rivers and an average annual rainfall of more than 50 inches, Alabama is able to provide precious water for growing commodity crops such as cotton and soy beans, steel production, aerospace and biomedical technologies. It also provides valuable recreation in the form of pristine lakes and rivers in state-parks. And of course, it is our source of drinking water. In other words, our water is such an indispensable resource that warrants no less than a *state of the art technology* to safeguard its integrity and to ensure its continual availability in a useable and safe form for future generations to come.

Alabama's economic base also consists of a sizeable poultry industry and more than a million head of cattle. This combination of large tracts of surface water and farms in proximity gives rise to a major problem: potential *bacterial pathogens contamination* via farm wastewater runoff. This problem is exacerbated by the frequent thunderstorms and occasional hurricanes. A water system contaminated with microbial pathogens from wastewater will have severe repercussions on Alabama's economic growth in terms of reputation and water reliability, and more importantly, it will jeopardize public health. Therefore it is critical that safe-guards must be set up without prior to a severe contamination incident.

In order to effectively mitigate the risk of pathogenic contamination, **low-cost and yet accurate pathogen detection tools must be made readily available and accessible for in-situ monitoring** of the water bodies to support timely management. **Sampling and off-site analysis is costly and more importantly will not be able to provide timely evaluation of the water quality.** Current techniques are also unable to identify specific pathogens such as *Escherichia coli* (*E. coli*) O157:H7 or *Giardia* without extensive sample preparations and incubations and therefore not feasible to be performed in-situ. In this proposal, **our aim is to push the technology envelope and develop a new rapid, accurate and yet robust technique that caters to the detection of specific pathogens in-situ.** The core basis of our technology is the novel use of advancing nanomaterials and genomic information of bacteria. The principle behind this technique is intended to permit eventual development of an enabling field tool, which will safeguard Alabama's water resources. To keep the proposed work in line with the resources available through the 104 program, we will concentrate on *E. coli* O157:H7 as the target pathogen. Other pathogens can be subsequently added relatively easily after the base technology has been developed.

E. coli are common bacteria in the intestines of human and warm-blooded animals and most of the strains are harmless. However some groups of *E. coli* are the causative agents of many enteric infections worldwide. As *E. coli* are supposed to be the natural reservoir of pathogenic strains [1], the presence of *E. coli* in water has been an indicator of recent fecal contamination. Among the hundreds of strains of the bacteria *E. coli*, the pathogenic *E. coli* O157:H7 is of particular interest. Ever since *E. coli* O157:H7 was first discovered in 1982, it is the most common pathogenic *E. coli* seen in the United States. *E. coli* O157:H7 is a food- and water- borne pathogenic bacterium that poses a significant concern in water supply systems [2-4]. In the United States, *E. coli* O157:H7 is responsible for 73,000 illnesses, 2,100 hospitalizations and 60 deaths annually [5].

The infective dose of *E. coli* O157:H7 is possibly fewer than 100 organisms [6]. The symptoms usually appear within 2-4 days from the uptake of contaminated water. It often results in acute kidney failure without quick diagnosis and intensive care. The only currently available test method specific for *E. coli* O157:H7 is based on Sorbitol-MacConky (SMAC) agar for human stool sample, which requires extensive incubation time and lacks specificity. Currently, **no available test has been adopted to detect specifically *E.coli* O157:H7 or other pathogenic bacteria in situ at water facilities**, even though those pathogens (e.g., *Giardia*, *Legionella*) are federally regulated as national primary drinking water standards.

Current technologies for pathogen detection

Traditionally, most probable number (MPN) method is commonly used for the detection of total coliforms or fecal coliforms in the water supply system. The MPN method is based on the empirical observation and the assumption that positive MPN is correlated to the existence of pathogens. This method requires numerous replicates and long incubation time. Unfortunately the greatest drawback of MPN method is the lack of specificity and therefore MPN cannot differentiate between benign and malignant species. It is vulnerable to both false positive and false negative. A false positive is costly and a false negative is deadly.

Recent improvement of biotechnology and genomics has developed a new DNA detection technology based on DNA amplification. Amplification techniques such as real-time PCR (also known as qPCR) are developed for the pathogen detection including *E. coli* O157:H7. It has a wide quantification range of at least 5 orders of

magnitude [7] and a relatively low detection limit [8-10]. However, it is unable to lend itself to in-situ application due to its susceptibility to contamination, which will result in the amplification of undesired DNA (i.e., contaminants) along with the target DNA. In order to avoid contamination, field samples have to undergo extensive preparations in a laboratory environment in order to quantify the target DNA by real-time PCR. Even with the recent development of an aid-reagent (e.g., chimeric polymerase), it is uncertain if it would work directly on unprocessed field samples. Furthermore, the amplicons (i.e., amplified products of DNA) are often required to be checked against the reference DNA via a gel electrophoresis to ensure that the target DNA has been amplified. Hence the real-time PCR requires extensive steps and apparatus, including a gel electrophoresis and a gel imaging apparatus and a clean bench, mainly owing to its vulnerability to contamination that is typical of gene amplification technique. These limitations rendered the in-situ application of real-time PCR near impossible (PCR: Polymerase Chain Reaction).

Research needs for developing new in-situ capable pathogen detection technique

Proper stewardship of Alabama's tremendous water resources relies on the amount of data and tools available to formulate and execute effective management strategies. In other words, **the availability of a miniaturized in-situ pathogen detection system will have enormous impact on the way we manage the contamination of our water resources.** It will open up numerous possibilities in terms of monitoring, tracing and rectifying the contamination source. However the development of such an in-situ pathogen detection system is contingent on the availability of a rapid, accurate, and economic detection technology. We will develop a rapid, accurate, in situ technique for the detection of pathogens in water at levels as low as 100 organisms per mL. The detection of our technique is based on the novel use of both fluorescent and magnetic nanoparticles which can be specifically assembled together only in the presence of the target pathogen DNA.

This technique, unlike PCR, must be able to maintain its selectivity in the presence of other contaminants. Its sensitivity should be also comparable to that of PCR such that it can detect the minimum infectious doses, which are 100 organisms per mL. A short analysis time from sample injection to pathogen quantification is also critical for efficient real-time monitoring. In other words, there must be minimal processing steps from sample injection to quantification. The reagents used in the technique must be stable over a range of temperature for an extended time in order for it to be viable for in-situ use. Most importantly, the technique must be able to lend itself readily to the detection of multiple pathogens such as *Giardia*, *Legionella* and *Campylobacter*. In terms of economic consideration, this technique should use only a small quantity of low cost reagents in order to limit the cost per test to a few dollars. The research proposed here will specifically allow us to further develop a technique that fulfills the above requirements.

B. Objectives of the research:

Scientific nature of the research

The basis of our technique is the novel use of both fluorescent and magnetic nanoparticles which will be specifically assembled together only in the presence of the target pathogen DNA. Magnetic manipulation is used to separate magnetic and fluorescent nanoparticles that are assembled (i.e., hybridized) to the target pathogen DNA from those that are not. Therefore the amount of fluorescent nanoparticles separated is quantified via their fluorescent intensity and correlated to the amount of target pathogen DNA.

Nanoparticles have large collective surface area per unit volume. They are ideal for the immobilization of bio-recognition materials such as DNA. They also allow easy manipulation/diffusion within samples, and their size range is compatible with the target DNA. As quantum dots nanoparticles (QDs) are inorganic crystals, they are exceptionally bright and photo-stable (photo-bleaching resistant). In this respect, QDs are very different from the organic fluorescent dyes that are currently employed in most of DNA detection assays [11-13]. DNA-conjugated QDs have also been shown to serve as sensitive and specific DNA labels for fluorescent in-situ hybridization [13], in single-nucleotide polymorphism and multi-parallel DNA detection [14].

Magnetic separation is popularly used for the rapid detection of DNA because it provides a rapid, simple and efficient method for separation/isolation without the need for centrifugation or filtration. Magnetic particles have also been used with fluorescent labels to enhance their functionality [15, 16]. The proposed technique has unparalleled specificity and therefore possesses negligible vulnerability to contamination. This technique has previously shown to be performed with similar sensitivity as the PCR in a laboratory using non-pathogenic target DNA [17]. The specificity of this technique will enable field samples to be analyzed with minimal preparation and therefore increasing the likelihood of implementing the in-situ pathogen detection system.

Scope of our research

In light of the need for the *in-situ* pathogen detection system and the limitations of the currently available methods, we envisioned the development of an *in-situ* capable pathogen detection method as outlined in Figure 1. The development of the *in-situ* capable pathogen system consists of three stages, however the research scope presented in this report *only includes STAGE 1*.

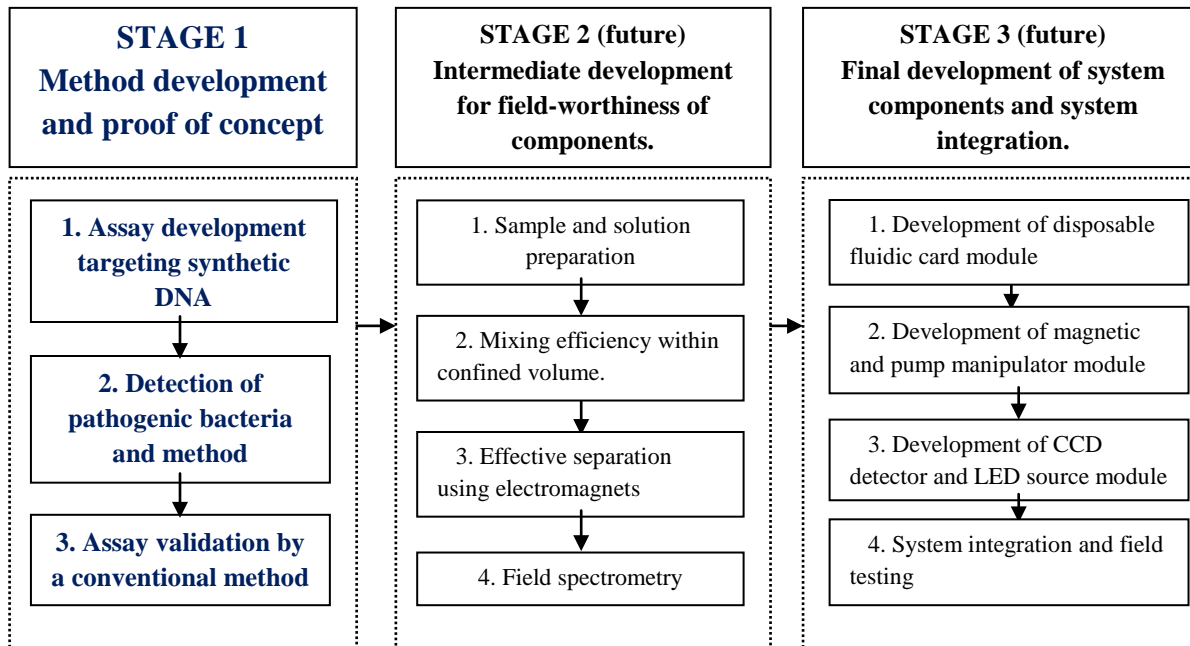


Figure 1. The overall flow scheme of our research with Stage 1 (blue-colored) being our scope for this proposal.

Stage 1 of the research (this report) consisted of three main tasks which also is the *complete scope* for this report.

Stage 1 is a proof-of-concept study in a laboratory setup to develop a novel, *in-situ* capable technique for rapid, accurate, and sensitive pathogen detection in water environments. The methodology is based on the specific DNA hybridization using our custom configured multi-functional nanoparticle labels. Our unique hybridization method was investigated for its ability to quantitatively detect pathogens in the forms of synthetic linear DNA (Task 1) and genomic DNA from bacterial culture (Task 2). Both tasks determined the quantitative parameters for pathogen DNA detection such as linearity (correlation coefficient and range of quantification), assay sensitivity (detection limits), specificity (mismatches), and rapidity of assay (reaction kinetics) in the laboratory. In Task 3, conventional plate counting method was used to verify our proof-of-concept as well as to mitigate the possibility of false positive results.

Stage 2 of the research (currently being funded for further study in 2011-2012) consists of the intermediate development of the technique and it *is not be part of the research scope* for this report. Parameters made known from Stage 1 will be used as preliminary data for Stage 2 research. The objective in this stage is to identify components of the techniques that are not field-ready and to perform further investigative studies as well as modifications to enable them for *in-situ* operation.

Stage 3 of the research (future work) consists of specific components design and development for the *in-situ* pathogen detection system. It *is not be part of the research scope* in this report. The schematic drawing for the envisioned *in-situ* pathogen detection kit is presented in Figure 2. The envisioned *In-situ* Pathogen Detection System (IPDS) will consist of 2 main components: disposable fluidic card and IPDS analyzer. The overall control of the system can be executed by a programmable logic control, microcontroller such as 8051 or a laptop computer. The controller will manage the air pump, electromagnets sequence, timing of mixing, movement of the linear actuator and the spectrometer unit itself. The entire unit will be powered by batteries. **The size of the IPDS will allow it to function as a handheld system.**

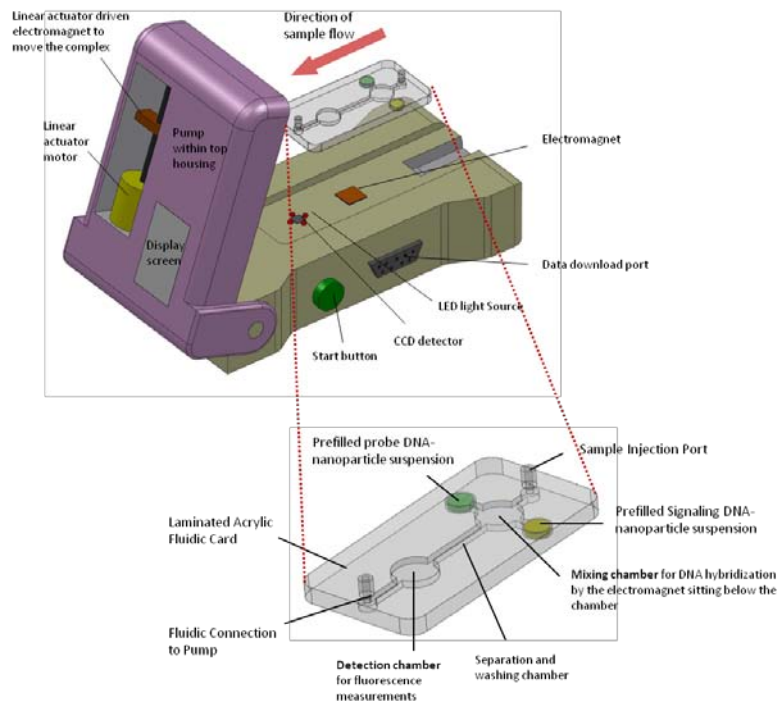


Figure 2. A schematic of a portable (hand-held) in-situ pathogen detection system (IPDS) with a disposable fluidic card (zoomed in lower side)

C. Principal findings and significance:

Achievements and publications

The proposed and funded research has resulted in two papers published thus far [18, 19]. The work has presented in three national (ACS and ASM) or regional meetings. The funded project served as a seed project for PI's research group, thus The PI has prepared two research proposals and submitted them to US federal agencies (DOE and NSF) for further funding. The details were described in Table 1.

Table 1. Academic achievements regarding this project during the funding period

•	Papers published in refereed journals.
1.	Kim, G. and Son, A. (2010) Development and characterization of a magnetic bead-quantum dot nanoparticles based assay capable of <i>Escherichia coli</i> O157:H7 quantification. <i>Analytica Chimica Acta</i> . 677 . 90-96.
2.	Kim, G. and Son, A. (2010) Quantitative detection of <i>E. coli</i> O157:H7 <i>eaeA</i> gene using quantum dots and magnetic particles. <i>Biotechnology and Bioprocess Engineering</i> . 15 . 669-676.
•	National/regional conferences attended.
1.	Kim, G. Wang, X. and Son, A. (2010) Separation and quantification of <i>E. coli</i> O157:H7 using magnetic bead-quantum dot nanoparticles. ACS 2010 , The 240th General Meeting of American Chemical Society, Boston, MA, USA, August 22-26.
2.	Kim, G., Wang, X. and Son, A. (2010) Quantitative detection of <i>E. coli</i> O157:H7 <i>eaeA</i> gene using quantum dots and magnetic particles. ASM 2010 , The 210th General Meeting of American Society for Microbiology, San Diego, CA, USA, May 23-27.
3.	Wang, X., Kim, G., and Son, A. (2010) Development of an inhibitor resistant gene monitoring method for the bacteria detection in water systems. The 24th Annual Alabama Water Resources Conference . Sep. 9-10.
•	Proposals to the federal agencies written.
1.	NSF CAREER proposal (July, 2010) Accepted for funding
2.	DOE SBR exploratory proposal (July, 2010)

Results and findings

Preliminary (a)-Optimization of particle configuration

The QD nanoparticles that are bonded to the MB serves as internal calibration for the assay by providing stable and long-lasting fluorescence. The stability of the MB-QD bonding is critical for successful quantification. The ratio of MB to the number of QDs together with the washing protocol was optimized to ensure maximum bonding of the QDs to the MB. Figure 3 [18] shows the presence of QDs encapsulated on the surface of MB. Field emission scanning electron microscopic (FE-SEM) energy disperse spectroscopy (EDS) mapping images of CdSe/ZnS QDs have shown four elements (Cd, Se, Zn, S) with four different colors. The results indicate that the covalent bonding between QDs and MB was successful, which also imply that the QDs were successfully immobilized on the surface of the MB. [18]

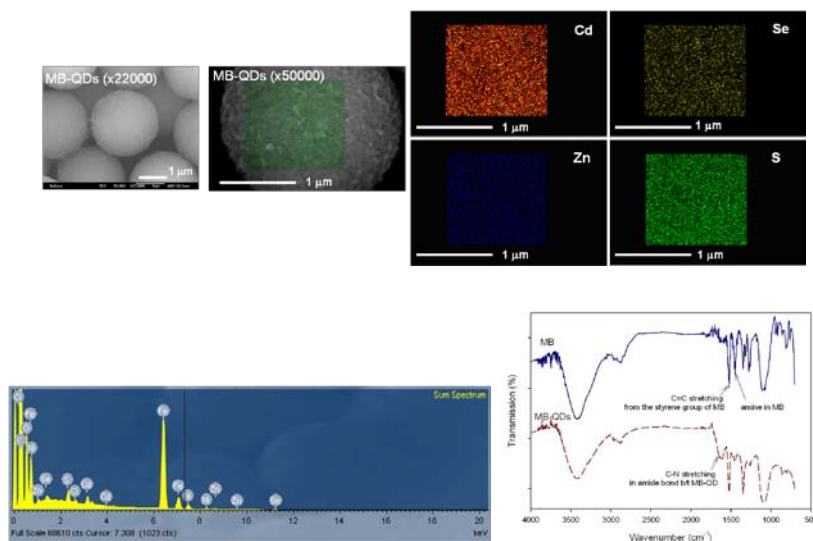


Figure 3. FE-SEM images of MB-QD complex (two in left, upper line) and corresponding energy disperse spectrometry (EDS) mapping images (right, upper line) of CdSe/ZnS QDs on the MB surface (scale bar = 1 μm). The color images of each elements (Cd: brown; Se: dark green; Zn: navy; S: light green) indicated the immobilization of QDs on the MB surface via covalent bonding was successful. [18]

Preliminary (b)-Photostability

The main advantage of using QD over organic fluorophore as a label for the assay is its photostability, which is defined as the resistance to photobleaching. Photostability of both QDs and Cy3 labeled DNAs was monitored via continuous measurement of the fluorescence intensity for 25 min. As shown in Figure 4, the fluorescence intensity of the signaling probe DNA with QDs maintained its initial intensity for the duration of the experiment, but that obtained from the DNA with Cy3 decreased to 75% after 25 min. The results showed that the **QD nanoparticles label has better stability for hybridization as compared to organic fluorophore, Cy3.**

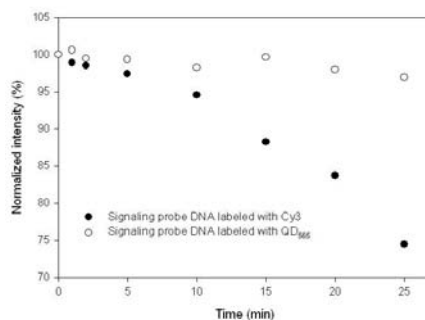


Figure 4. Comparison of signal photostability obtained by using signaling probe DNA labeled with Cy3 and QD565. The QDs nanocrystals that are made of semi-conducting materials have shown the excellent photostability over organic fluorophore, Cy3.

Preliminary (c)-Assay optimization

Washing. For further hybridization, the probe DNA conjugated MB-QDs particle complexes were washed with PB. The washing is required to remove non-hybridized DNA, non-bound QDs and residual hybridization reagents. However harsh washing could affect the bonds between particle and DNA or within DNA hybrids. In order to optimize the washing stringency, the fluorescence intensity was monitored in response to varying washing duration. As shown in Figure 5a, the similar fluorescence values were observed in the range of 100 through 500 pmoles of probe DNA labeled with Cy3 after a single wash. After 5 washes, there was no linear relationship between fluorescence signal and the concentration of probe DNA labeled with Cy3. After 3 washes, the normalized fluorescence values linearly increased and there was clear discrimination as the concentration of probe DNA labeled with Cy3 increased. Based on the experimental observations, even though stringent washing is advantageous for the complete removal of non-bound QDs and probe DNA, but it could also cause a loss of already bound QDs and probe DNA. In this regard the optimum washing stringency was determined to 3 times for the following experiments.

Passivation. Passivation is a common method for avoiding a non-specific binding (i.e., particle coagulations in this case) by inactivating the functional groups. The signaling probe DNA labeled with QD₅₆₅ was incubated in a NaBH₄ based blocking solution (0.5 g of NaBH₄ in the mixture of 10 mL 20×SSC, 0.5 mL 10% SDS, and 90 mL H₂O) at 42°C for 20 min to passivate the remained functional groups on the QD₅₆₅ surface, and washed with 1×SSC and 0.2×SSC twice. The signaling probe DNA with QD₅₆₅ was subsequently collected by centrifuging twice at 10,000 rpm for 5 min. In order to examine the passivation effect of the nanoparticle labels on DNA hybridization, both treated and non-treated QD₅₆₅ - signaling probe DNAs were compared during hybridization. The effect of passivation treatment for QD₅₆₅ labels (i.e., conjugated with a signaling probe DNA) is presented in Figure 15b. The passivation of QD₅₆₅ labels allowed the fluorescence output to increase accordingly when the amount of target ssDNA increases. This indicated that the quantification is only feasible with the use of passivated nanoparticle labels. For non-passivated labels, no change of fluorescence was observed with a various amount of target ssDNA. One possible cause involves particle aggregation via non-specific binding which can be induced by the remaining functional groups on the surface of non-treated QD₅₆₅ labels. The passivation of QDs in the signaling probe DNA can prevent particle agglomeration which is caused by the unoccupied functional groups of QD₅₆₅.

Molar ratio of QDs and signaling probe DNA. The molar ratio effect of QD₅₆₅ to signaling probe DNA (i.e., 1:3, 1:10, and 1:30) on the hybridization efficiency was examined. The optimum molar ratio of signaling probe DNA and QD₅₆₅ was determined by the highest output signal of fluorescence after hybridization. The quantification of target DNA is based on sandwich hybridization between the probe and signaling probe DNAs. The capturing MB-QD₆₅₅ particles' functional groups (i.e., carboxyl) should be linked to a large number of probe DNAs' functional groups (i.e., amine) to maximize available counterparts for the target DNA. Since the target and signaling probe DNAs are simultaneously hybridized with the probe DNA, the successful hybridization between the target and the signaling probe DNAs is essential for the complete hybridization. The ratio between the numbers of signaling probe DNA and label has to be optimized to maximize the output of the assay. The effect of QD₅₆₅ to signaling probe DNA molar ratio on DNA quantification is shown in Figure 5c. The maximum output of assay was observed at the signaling probe DNA to QD₅₆₅ molar ratio of 10. For our assay format the optimum molar ratio was established at 10. The signaling probe DNA and labels were optimized in terms of molar ratio and passivation prior to the subsequent quantification experiments in later sections.

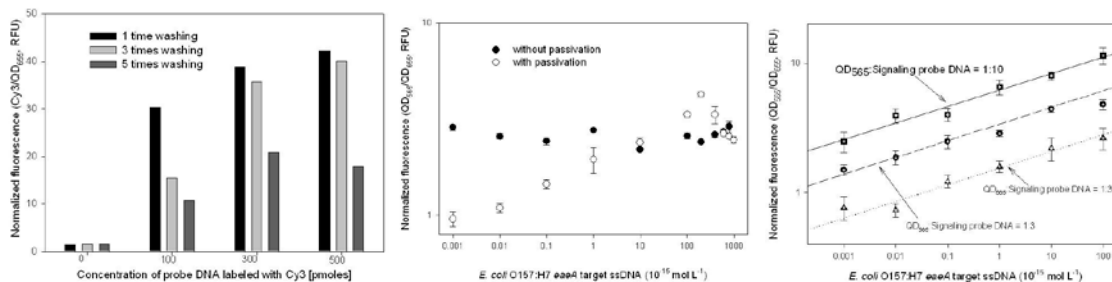


Figure 5. (a) The washing effect, (b) passivation effect, and (c) optimized molar ratio between QDs and probe DNAs for MB-QD assay.

Task 1 – Synthetic DNA (ssDNA) quantification

Quantification results and assay sensitivity. In order to characterize the quantification range and linearity of the MB-QD assay, hybridization was performed using ssDNA as the target. The quantification result is presented in Figure 6. A linear quantitative relationship was observed in the range of 10^{-18} to 10^{-13} mol L⁻¹. The normalized fluorescence (i.e., QD₅₆₅/QD₆₅₅) showed a linearity ($R^2 = 0.929$) of over 5 orders of magnitude with the LOD of 890 zeptomolar concentration (i.e., zM = 10^{-21} mol L⁻¹). The detection of ssDNA in various formats was reported in several prior literatures: 2×10^{-9} mol L⁻¹ in the gold nanoparticle based fluorescence quenching method [20]; 1×10^{-10} mol L⁻¹ by MB-functionalized fluorescent microspheres [21]; 1×10^{-12} mol L⁻¹ in the format of gold nanoparticles coupled light scattering [22]; 8×10^{-13} mol L⁻¹ in the dye-doped silica nanoparticle based hybridization [23]; 5×10^{-15} mol L⁻¹ in the silver nanoparticle based chemiluminescent method [24]; and 8.3×10^{-18} mol L⁻¹ by the magnetic particles with electrogenerated chemiluminescent detection [25]. Recently Liu *et al.* [26] reported the feasibility of detecting ssDNA of 250 zM (i.e., 2.5×10^{-19} mol L⁻¹) by QD nanoparticle labeling. The result however was preliminary. The assay had only three points examined and no LOD reported. More importantly there was no internal standard to normalize the assay output, thereby potentially resulting in the poor reproducibility of the assay. As compared to the previous studies listed above, the MB-QD assay demonstrated excellent sensitivity for the detection of ssDNA.

Table 2. The linear equation and concentration range, R2, and detection limit of nanoparticle-based gene quantification assay.

Parameters	
Regression equation	$y = 0.0329x + 3.391$
Correlation coefficient (R^2)	0.992
Linear range	10 – 1000 fM
Detection limit	9.72 fM

Assay specificity. In order to evaluate the discrimination capability of DNA sequence variations of our assay, 1-, 2-, and 41-bp mismatched (out of total 55-bp) ssDNAs targets were hybridized with probe DNA as compared to perfectly matched target DNA. DNAs of different concentrations (50 - 400 fM) were analyzed based on the normalized fluorescence signal (Figure 6b). The various mismatched DNAs were clearly discriminated from perfectly matched target for the range of concentration. Assuming the difference of fluorescence signals between perfectly matched and 41-bp mismatched DNA at 400 fM is 100%, the fluorescence intensity of 1- and 2-bp mismatched DNA target corresponded to 30 and 20% of that of the perfectly matched target, respectively. The significant difference among them was verified by a statistical test. All the obtained *P*-values were smaller than 0.1 by the two-sided *t*-test with 95% confidence level. Moreover, the fluorescence signal among mismatches tended to be consistent regardless of varying concentrations of target DNA (50 - 400 fM). Bacteria represented by 1- and 2-bp mismatched DNAs are phylogenetically close but not identical to the bacterium represented by perfectly matched DNA. In contrast, the 41-bp mismatched DNA is of entirely different species. This demonstrates that our developed technique is capable of screening through the DNA sequences of pathogenic and non-pathogenic bacteria species and detecting the pathogens. Our assay has shown excellent selectivity in discriminating a phylogenetically similar gene to *eaeA* gene. Furthermore, the use of our technique can be expanded to encompass the detection of single-nucleotide polymorphisms (SNPs) in biomedical science.

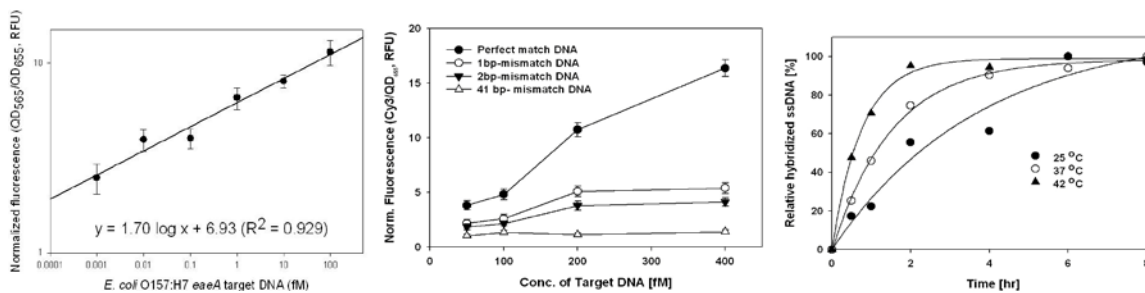


Figure 6. (a) Linearity, dynamic range, and sensitivity of the assay, (b) specificity using mismatch DNAs, and (c) rapidity of the assay based on the kinetics in various temperatures.

Assay rapidity (kinetics). In order to examine the kinetic parameters of the presented technique, the effects of target DNA concentration and hybridization temperature were investigated as described earlier. The results are illustrated in Figure 6c and detailed in Table 3. The rate constants of hybridization reactions were obtained from the linear regression analysis based on second-order kinetic model with the assumption of negligible dissociation reaction and excess signaling probe DNA concentration. The governing equation is as follows:

$$\ln\left(\frac{C_{i,p} - C_{h,p}}{C_{i,t} - C_{h,t}}\right) = -k_h \cdot (C_{i,t} - C_{i,p}) \cdot t$$

where, $C_{i,t}$ and $C_{h,t}$ is the initial and hybridized concentration of target DNA, respectively, $C_{i,p}$ and $C_{h,p}$ is the initial and hybridized concentration of probe DNA, t is time, and k_h is the hybridization rate constant. Herein, the initial concentration of probe DNA was 1.25 μM . As shown in Table 3, the correlation coefficient (R^2) indicated that the kinetics of DNA hybridization follows the second-order reaction. Please note that the result is consistent with the previous studies [27, 28]. It was due to the rate-limiting step of DNA hybridization is the prior formation of a few base pairs from each strand into a transient intermediate (i.e., nucleus). Then the remaining base quickly forms a complete helix [29]. The hybridization rate increased with the concentration of target DNA, indicating the target concentration is another rate-limiting factor in a hybridization reaction.

Figure 6c shows the normalized hybridized amount of ssDNA target depending on the various hybridization temperatures. The percentage was calculated by assuming each plateau value as 100%. This assumption is reasonable because each measurement is relative. The result indicated that the reaction rate constant increased as the hybridization temperature increased, which is consistent with Table 3. In other words, the higher hybridization temperature would allow hybridization equilibrium to be reached in a shorter period of time. For example, the equilibrium time for hybridization was 5 hrs at 25°C, and it was 2 h at 42°C. From a practical perspective, it is concluded that at sufficiently high target concentration, the required amount of target DNA could be hybridized at ambient temperature. However higher temperature will be required to expedite DNA hybridization for low DNA concentrations. The adjustment of hybridization temperature in accordance to the amount of target DNA is required for the maximum efficiency of DNA hybridization.

Table 3. The hybridization rate constants and R^2 values measured from the linear regression analysis based on the second order kinetic models. R^2 values were presented in brackets.

Target DNA (fM)	Second order rate constant (k_h) ($\times 10^6 \text{ M}^{-1} \text{ h}^{-1}$)		
	25°C	37°C	25°C
100	0.211 (0.929)	0.450 (0.781)	0.676 (0.902)
400	0.366 (0.971)	0.699 (0.998)	0.801 (0.908)
800	0.335 (0.957)	0.682 (0.995)	1.073 (0.931)

Task 2 – Bacterial DNA (dsDNA) quantification

Assay sensitivity. The characterization of the MB-QD assay's sensitivity was carried out via dsDNA quantification. The standard curve constructed by the serial dilution of dsDNA fragments (i.e., 151 bp of PCR amplicon) and the quantification result are presented in Figure 7a and Table 4. The linear quantification range was $2 \times 10^2 - 2 \times 10^7$ with the LOD of 87 gene copies. The dynamic range was 5 orders of magnitude. The lower detection limit of dsDNA in the developed MB-QD assay (i.e., 87 gene copies) presented here is a significant improvement over previously reported assay for the nanoparticle based DNA quantification. For example, Storhoff *et al.* [30] demonstrated the detection of at least 6×10^6 gene copies of the PCR product from human gDNA using silver amplified gold nanoparticles in DNA microarray format; Eastman *et al.* [31] developed a QD nanobarcode-based magnetic microbead array for gene expression analysis with a sensitivity of $10^4 - 10^6$ gene copies; and Hill *et al.* [32] reported that $2.5 \times 10^{-15} \text{ mol L}^{-1}$ (i.e., 7.5×10^4 gene copies) of bacterial gDNA was detected at the bio-bar-code assay using gold nanoparticles. To evaluate the quantification capability of the MB-QD assay, real-time PCR analysis was conducted. The linear range of real-time PCR was $2 \times 10^2 - 2 \times 10^9$ with the LOD of 47 gene copies.

Table 4. Quantification performance of the MB-QD assay. (CV: coefficient of variation)

Parameters	
Dynamic range (gene copies)	$2 \times 10^2 - 2 \times 10^7$
Regression equation	$\text{RFU} = 0.670 \log(\text{gene copies}) - 0.729$
Correlation coefficient (R^2)	0.929
Limit of detection (gene copies)	87
Inter-assay CV (%)	2.01
Intra-assay CV (%)	5.74

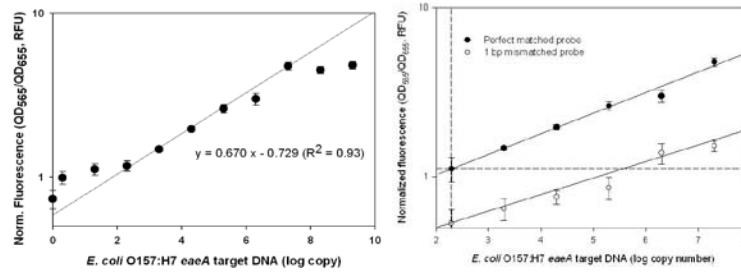


Figure 7. (a) Quantification of *E. coli* O157:H7 *eaeA* target dsDNA in the MB-QDs assay. The normalized fluorescence is plotted against the corresponding *E. coli* O157:H7 *eaeA* gene copy numbers. (b) Assay specificity of the MB-QDs assay.

Assay specificity. The specificity of the MB-QD assay was characterized by varying the amount of PCR amplicon hybridized with both perfectly matched and 1 bp nucleotide mismatched probe DNAs. The specificity result is presented in Figure 7b. By comparing the fluorescence signal, 1 bp mismatched probe DNA was clearly discriminated from the perfectly matched probe DNA. When the 1 bp mismatch was used, the quantification results were observed to be below the LOD (i.e., $\text{RFU} = 1.17$) in the range of $2 \times 10^2 - 2 \times 10^5$ target gene copies. This result demonstrated our developed method is capable of screening and detecting pathogenic bacteria with an excellent selectivity among other non-pathogenic but phylogenetically similar bacteria. Real-time PCR assay (graph not shown) was implemented to validate the specificity of MB-QD assay. In the real-time PCR assay, 1 bp nucleotide mismatched forward primer was adopted to simulate the 1 bp nucleotide mismatch effect. When the 1 bp mismatched primer was used, the limit of quantification increased from 2×10^2 to 2×10^4 and the dynamic range shifted accordingly.

Task 3 - Validation of the assay using *E. coli* O157:H7 bacteria culture

Genomic DNA quantification. In order to demonstrate the assay's capability to perform quantification without the need of amplification, non-amplified genomic DNA of *E. coli* O157:H7 culture was used as the target. Target gDNA with various gene copies were hybridized and the quantification result is shown in Fig. 8.

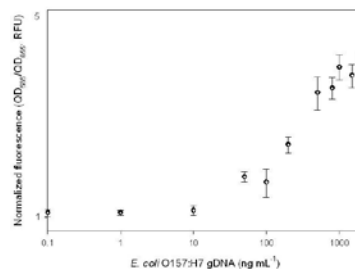


Figure 8. Quantitative detection of *E. coli* O157:H7 using gDNA without amplification.

Comparison with the traditional plate counting method. A standard culture based bacteria quantification method (plate counting) was employed to correlate the DNA-based quantification and conventional bacterial cell counts. The output of the assay, depicted in the y-axis (Figure 9a), is the normalized fluorescence. The serial dilutions of

bacterial culture was inoculated on trypticase soy agar plates and incubated at 37°C for 24 hrs. Figure 9b shows the picture taken during the plate counting and the yellow dots (i.e., colony) are bacteria grown on the surface of agar plates. The colonies were counted to determine the number of colony-forming units per mL of culture (CFU/mL).

Gene copy numbers (i.e., a variable of assay) were converted to the number of bacterial cells (CFU mL⁻¹) based on the result of the plate counting method and subsequently depicted in the *x*-axis. Plate counting method was implemented using active *E. coli* O157:H7 cells and correlated with gene quantification results. 4×10⁹ CFU per mL was determined to be equivalent to 2×10¹² gene copy numbers of the *eaeA* per mL. The dynamic range of the assay was 4×10 – 4×10⁵ CFU mL⁻¹ (R² = 0.980) with the LOD of 25 CFU mL⁻¹. The infectious dose (> 100 organisms) [33, 34] was indicated by the vertical dashed line in Figure 9a. The minimum infectious dose of *E. coli* O157:H7 was within the range of quantification of the MB-QD assay. In comparison, other studies have shown that their LODs were similar or more than 100 CFU mL⁻¹ [35–39], indicating the MB-QD assay has higher sensitivity for the detection of pathogens. Similar techniques have been recently developed and they are based on DNA aptamer or liposome. Bruno *et al.* [40] have developed DNA aptamer based sandwich hybridization approach with magnetic bead and QDs. Zaytseva *et al.* [41] used fluorescent liposome as a reporter for the detection of viral nucleic acids. Even though these developments have demonstrated the integration of the assay with portable devices such as microfluidics, they are still in the early stage of development.

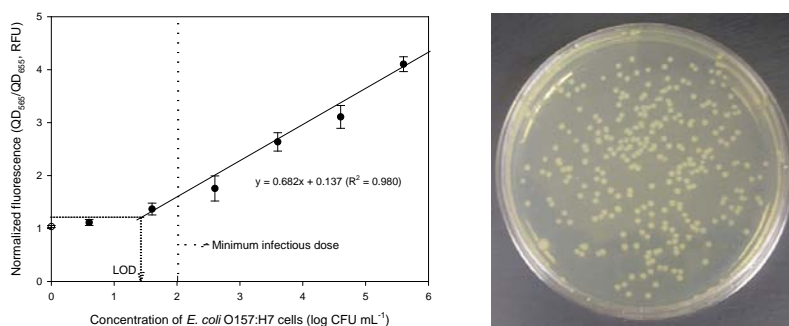


Figure 9. (a) Quantitative detection of *E. coli* O157:H7 using genomic DNA without amplification (y-axis) in comparison to the conventional plate counting methods (x-axis). This technique is able to detect below the minimum infectious limit (100 cells) as indicated by the vertical dashed line. (b) Example of a plate counting method using agar plates. The colonies shown above indicate *E. coli* O157:H7 cultured on trypticase soy agar plates.

D. Conclusion

We have developed a highly sensitive DNA assay using magnetic and quantum dot nanoparticles for the quantification of pathogenic *E. coli* O157:H7 bacteria in water. The use of QD₅₆₅ for the label of signaling probe DNA resulted in increased photostability and also allowed the assay to be used with a single, short-wavelength excitation source. The new format of QDs configuration (i.e., QD₅₆₅/QD₆₅₅) as both a fluorescence label and an internal standard increased the sensitivity of the assay. This MB-QD assay was able to detect ssDNA and dsDNA fragment up to 890 zptomolar concentration and 87 gene copies, respectively. The specificity of the assay was also demonstrated via the discrimination of target DNA with 1 bp nucleotide mismatch. Finally the MB-QD assay was able to detect *E. coli* O157:H7 with 25 cells/mL of the detection limit which is below the minimum infectious dose in water. This sensitive nanoparticle based DNA quantification assay is potentially applicable for in-situ monitoring of pathogenic bacteria in the aquatic environment.

E. REFERENCES

1. Neidhardt, F.C., Ed.; , *American Society for Microbiology*. 1996, Washington, DC.
2. Lin, Y.-H., et al., *Disposable amperometric immunosensing strips fabricated by Au nanoparticles-modified screen-printed carbon electrodes for the detection of foodborne pathogen Escherichia coli O157:H7*. *Biosensors and Bioelectronics*, 2008. **23**: p. 1832-1837.
3. Mao, X., et al., *A nanoparticle amplification based quartz crystal microbalance DNA sensor for detection of Escherichia coli O157:H7*. *Biosensors and Bioelectronics*, 2006. **21**: p. 1178-1185.
4. Chi-Fang Wu, J.J.V., William E. Bentley, Jennifer W. Sekowski, *DNA microarray for discrimination between pathogenic O157:H7 EDL933 and non-pathogenic Escherichia coli strains*. *Biosensors and Bioelectronics* 2003. **19**(1): p. 1-8.
5. Wang, L., et al., *A novel electrochemical biosensor based on dynamic polymerase-extending hybridization for E. coli O157:H7 DNA detection*. *Talanta* 2009. **78**(3): p. 647-652.
6. Tuttle, J., et al., *Lessons from a large outbreak of Escherichia coli O157:H7 infections: Insights into the infectious dose and method of widespread contamination of hamburger patties*. *Epidemiology and Infection*, 1999. **122**(2): p. 185-192.
7. Sharma, V.K. and E.A. Dean-Nystrom, *Detection of enterohemorrhagic Escherichia coli O157:H7 by using a multiplex real-time PCR assay for genes encoding intimin and Shiga toxins*. *Veterinary Microbiology* 2003. **93**(3): p. 247-260.
8. Bhagwat, A.A., *Simultaneous detection of Escherichia coli O157:H7, Listeria monocytogenes and Salmonella strains by real-time PCR*. *International Journal of Food Microbiology*, 2003. **84**(2): p. 217-224.
9. Jothikumar, N. and M.W. Griffiths, *Rapid Detection of Escherichia coli O157:H7 with Multiplex Real-Time PCR Assays*. *Applied and Environmental Microbiology* 2002. **68**(6): p. 3169-3171.
10. Ibekwe, A.M. and C.M. Grieve, *Detection and quantification of Escherichia coli O147:H7 in environmental samples by real-time PCR*. *Journal of Applied Microbiology*, 2003. **94**: p. 421-431.
11. Medintz, I.L., et al., *Quantum dot bioconjugates for imaging, labelling and sensing*. *Nature Material*, 2005. **4**: p. 435-446.
12. Bruchez, M.J., et al., *Semiconductor nanocrystals as fluorescent biological labels*. *Science*, 1998. **281**: p. 2013-2016.
13. Pathak, S., et al., *Hydroxylated quantum dots as luminescent probes for in situ hybridization*. *Journal of American Chemical Society*, 2001. **123**: p. 4103-4104.
14. Gerion, D., et al., *Room-temperature single-nucleotide polymorphism and multiallele DNA detection using fluorescent nanocrystals and microarrays*. *Analytical Chemistry*, 2003. **75**: p. 4766-4772.
15. Eastman, P.S., et al., *Qdot nanobarcodes for multiplexed gene expression analysis*. *Nano Letters*, 2006. **6**: p. 1059-1064.
16. Kouassi, G.K. and J. Irudayaraj, *Magnetic and gold-coated magnetic nanoparticles as a DNA sensor*. *Analytical Chemistry*, 2006. **78**: p. 3234-3241.
17. Son, A., et al., *Quantitative gene monitoring of microbial tetracycline resistance using magnetic luminescent nanoparticles*. *Journal of Environmental Monitoring*, 2010. **12**: p. 1362-1367.
18. Kim, G.Y. and A. Son, *Quantitative detection of E.coli O157:H7 eaeA gene using quantum dots and magnetic particles*. *Biotechnology and Bioprocess Engineering*, 2010. **15**(6): p. 1084-1093.
19. Kim, G.Y. and A. Son, *Development and characterization of a magnetic bead-quantum dot nanoparticles based assay capable of Escherichia coli O157:H7 quantification*. *Analytica Chimica Acta*, 2010. **677**: p. 90-96.
20. Wu, Z.-S., et al., *Optical detection of DNA hybridization based on fluorescence quenching of tagged oligonucleotide probes by gold nanoparticles*. *Anal. Biochem.*, 2006. **353**(1): p. 22-29.
21. Ferguson, J.A., F.J. Steemers, and D.R. Walt, *High-density fiber-optic DNA random microsphere array*. *Anal. Chem.*, 2000. **72**: p. 5618-5624.
22. Dai, Q., et al., *A one-step highly sensitive method for DNA detection using dynamic light scattering*. *J. Am. Chem. Soc.*, 2008. **130**: p. 8138-8139.
23. Zhao, X., R. Tapeç-Dytioco, and W. Tan, *Ultrasensitive DNA detection using highly fluorescent bioconjugated nanoparticles*. *J. Am. Chem. Soc.*, 2003. **125**: p. 11474-11475.
24. Liu, C.-H., et al., *Silver nanoparticle-based ultrasensitive chemiluminescent detection of DNA hybridization and single-nucleotide polymorphisms*. *Anal. Chem.*, 2006. **78**: p. 3738-3744.

25. Patolsky, F., et al., *Magnetically amplified DNA assays (MADA): sensing of viral DNA and single-base mismatches by using nucleic acid modified magnetic particles*. *Angew. Chem. Int. Ed.*, 2003. **42**: p. 2372-2376.
26. Liu, Y.-J., et al., *Magnetic bead-based DNA detection with multi-layers quantum dots labeling for rapid detection of Escherichia coli O157:H7*. *Biosens. Bioelectron.*, 2008. **24**: p. 558-565.
27. Chunlai Chen, et al., *Kinetics and thermodynamics of DNA hybridization on gold nanoparticles*. *Nucleic Acids Research*, 2009. **37**: p. 3756-3765.
28. Larry E. Morrison and L.M. Stols, *Sensitive fluorescence-based thermodynamic and kinetic measurements of DNA hybridization in solution*. *Biochemistry*, 1993. **32**: p. 3095-3104.
29. James G. Wetmur and N. Davidson, *Kinetics of renaturation of DNA*. *Journal of Molecular Biology*, 1968. **31**: p. 349-370.
30. Storhoff, J.J., et al., *Gold nanoparticle-based detection of genomic DNA targets on microarrays using a novel optical detection system*. *Biosens. Bioelectron.*, 2004. **19**: p. 875-883.
31. Eastman, P.S., et al., *Qdot nanobarcodes for multiplexed gene expression analysis*. *Nano Lett.*, 2006. **6**: p. 1059-1064.
32. Hill, H.D., R.A. Vega, and C.A. Mirkin, *Nonenzymatic detection of bacterial genomic DNA using the biobarcode assay*. *Anal. Chem.*, 2007. **79**: p. 9218-9223.
33. Tuttle, J., et al., *Lessons from a large outbreak of Escherichia coli O157:H7 infections: insights into the infectious dose and method of widespread contamination of hamburger patties*. *Epidemiol. Infect.*, 1999. **122**: p. 185-192.
34. www.cdc.gov/ncidod/eid/vol8no4/00-0218.htm.
35. Mao, X., et al., *A nanoparticle amplification based quartz crystal microbalance DNA sensor for detection of Escherichia coli O157:H7*. *Biosens. Bioelectron.*, 2006. **21**: p. 1178-1185.
36. Su, X.-L. and Y. Li, *Quantum dot biolabeling coupled with immunomagnetic separation for detection of Escherichia coli O157:H7*. *Anal. Chem.*, 2004. **76**: p. 4806-4810.
37. Yang, L., Y. Li, and G.F. Erf, *Interdigitated array microelectrode-based electrochemical impedance immunosensor for detection of Escherichia coli O157:H7*. *Anal. Chem.*, 2004. **76**(4): p. 1107-1113.
38. Huang, S., et al., *A wireless, remote-query sensor for real-time detection of Escherichia coli O157:H7 concentrations*. *Sens. Actuators, B* 2008. **131**: p. 489-495.
39. Xue, X., et al., *Fluorescence detection of total count of Escherichia coli and Staphylococcus aureus on water-soluble CdSe quantum dots coupled with bacteria*. *Talanta*, 2009. **77**: p. 1808-1813.
40. Bruno, J.G., et al., *Plastic-adherent DNA aptamer-magnetic bead and quantum dot sandwich assay for Campylobacter detection*. *J. Fluoresc.*, 2009. **19**(3): p. 427-435.
41. Zaytseva, N.V., R.A. Montagna, and A.J. Baeumner, *Microfluidic biosensor for the serotype-specific detection of Dengue virus RNA*. *Anal. Chem.*, 2005. **77**: p. 7520-7527.

Development of an In-situ Capable Method for Detecting Pathogenic Bacteria in the Alabama Water Supplies

Basic Information

Title:	Development of an In-situ Capable Method for Detecting Pathogenic Bacteria in the Alabama Water Supplies
Project Number:	2011AL114B
Start Date:	3/1/2011
End Date:	2/28/2012
Funding Source:	104B
Congressional District:	Third
Research Category:	Engineering
Focus Category:	Surface Water, Water Quality, None
Descriptors:	None
Principal Investigators:	Ahjeong Son

Publications

1. Kim, G. and A. Son, 2010, Development and characterization of a magnetic bead-quantum dot nanoparticles based assay capable of Escherichia coli O157:H7 quantification, *Analytica Chimica Acta*, 677, pp. 90-96.
2. Kim, G. and A. Son, 2010, Quantitative detection of E. coli O157:H7 eaeA gene using quantum dots and magnetic particles, *Biotechnology and Bioprocess Engineering*, 15, pp. 1084-1093.
3. Kim, G.; X. Wang, H. Ahn, and A. Son, 2011, Gene quantification by NanoGene assay is resistant to humic acids, *Environmental Science and Technology*, 45, pp. 8873-8880.
4. Kim, G.; X. Wang, and A. Son, 2011, Inhibitor resistance and in-situ capability of nanoparticle based gene quantification, *Journal of Environmental Monitoring*, 13, pp. 1344-1350.
5. Wang, Xiaofang, 2011, Humic Acids Resistant Gene Quantification Assay in Soils, MS Dissertation, Department of Civil Engineering, Auburn University, Auburn, Alabama, 58.

Annual Technical Report
for
Water Resources Research Institute Program
under
Section 104, Water Resources Research Act of 1984
to the
Alabama Water Resources Research Institute

In support of the
Research Proposal

DEVELOPMENT OF AN IN-SITU CAPABLE METHOD FOR DETECTING PATHOGENIC
BACTERIA IN THE ALABAMA WATER SUPPLIES – *Phase I & II*

March 2010 – February 2012

By

Ahjeong Son (Principal Investigator)
Assistant Professor
Department of Civil Engineering
Auburn University

May 20th 2012

SYNOPSIS OF ANNUAL TECHNICAL REPORT

- A. Title: DEVELOPMENT OF AN IN-SITU CAPABLE METHOD FOR DETECTING PATHOGENIC BACTERIA IN THE ALABAMA WATER SUPPLIES
- B. Primary PI(s): Ahjeong Son, Assistant Professor in Department of Civil Engineering at Auburn University, AL.
- C. OTHER PI(s): None.
- D. START DATE: March 1, 2010
- E. END DATE: February 28, 2012
- F. PROJECT OVERVIEW/SUMMARY:

Proper stewardship of Alabama’s tremendous water resources relies on the amount of data and tools available to formulate and execute management strategies. In other words, the availability of a miniaturized in-situ pathogen detection system will have enormous impact on the way we manage the contamination of our water resources. It will open up numerous possibilities in terms of monitoring, tracing and rectifying the contamination source. However, the development of such an in-situ pathogen detection system is contingent on the availability of a rapid, accurate, and economic detection technology. For this reason, we developed a rapid, accurate, in-situ capable technique for the detection of pathogens (*E. coli* O157:H7) in water at levels as low as 100 organisms per mL. The development of the in-situ capable pathogen system consists of three phases as shown in Figure 1 below.

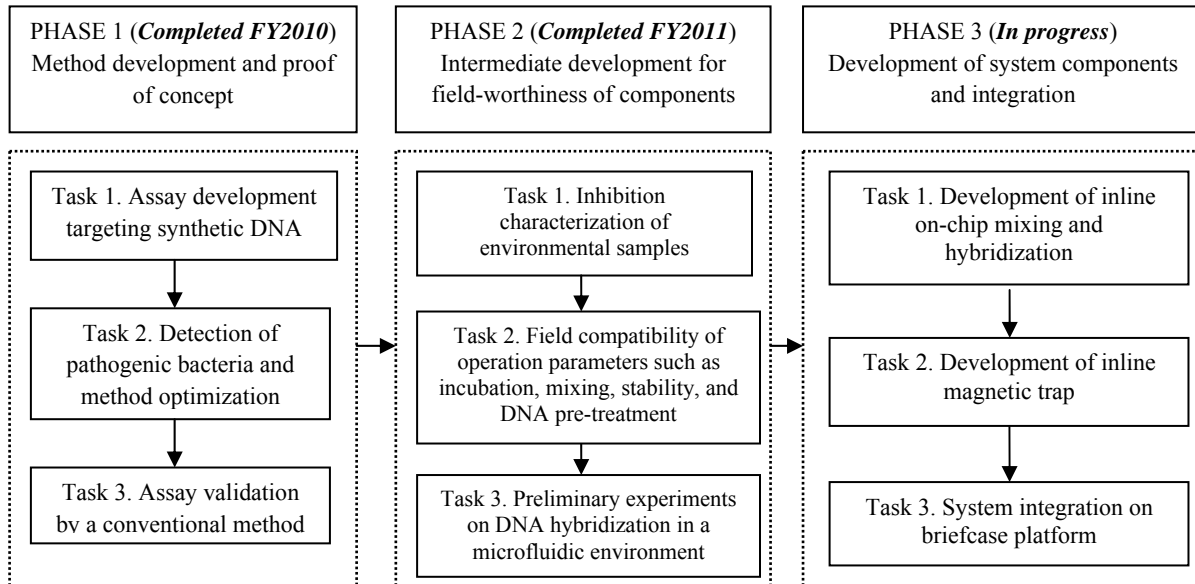


Figure 1. The overall flow scheme of our research objectives in each task for three phases. Phase 1 and 2 have been completed in FY 2010-2011 and Phase 3 is currently being implemented in FY 2012.

Phase 1 (FY2010) was a proof-of-concept study in a laboratory setup to develop a novel, in-situ capable technique for rapid, accurate, and sensitive pathogen detection in water environments. The

methodology is based on the specific DNA hybridization using our custom configured multi-functional nanoparticle labels. Our unique hybridization method was investigated for its ability to quantitatively detect pathogens in the forms of synthetic linear DNA (Task 1) and genomic DNA from bacterial culture (Task 2). Both tasks determined the quantitative parameters for pathogen DNA detection such as linearity (correlation coefficient and range of quantification), assay sensitivity (detection limits), specificity (mismatches), and rapidity of assay (reaction kinetics) in the laboratory. In Task 3, conventional plate counting method was used to verify our proof-of-concept as well as to mitigate the possibility of false positive results. As a result of the research in Phase 1, two scientific papers have been published in the major journals of analytical chemistry and bioengineering (Kim & Son, 2010a; Kim & Son, 2010b).

Phase 2 (FY 2011) consisted of the intermediate development of the technique and the investigation of the compatibility of the developed assay for non-laboratory environment usage. In particular the inhibition effects of environmental samples were identified and we have found that our technology has shown the resistance ability to a number of inhibitors such as humic acids (Task 1). We have identified the key parameters of the techniques that were not field-ready and to perform further investigative studies as well as modifications to enable them for in-situ operation (Task 2). In Task 3, we transformed the format of the method from a microplate format into a microfluidic platform in order to examine the feasibility of in-situ capability of the developed method by testing several operation parameters. Parameters made known from Phase 1 were used as preliminary data for Phase 2 research. The research at this phase is critical for the further development (Phase 3) of the proposed assay into a well-designed, in-situ capable engineered system. As a result of the research in Phase 2, two scientific papers have been published in the major journals of environmental engineering and science (Kim et al., 2011a; Kim et al., 2011b).

Phase 3 (*In progress*, FY2012) includes a development of inline fluidic components, characterization of parameters, and its system integration effort on a portable briefcase platform for the in-situ pathogen detection system.

Finally, the results of this research will lead to a technology that can be patented and commercially developed for *public good*. For regular pathogen monitoring in water, the in-situ pathogen detection system will enable faster response time to trace the source of contamination in the event of an outbreak. For example, park rangers and water officials will be able to perform routine monitoring without the time-consuming need to collect samples and send them to laboratories for analysis. Minimal laboratory expertise will be required to operate the developed in-situ system. With continuous improvement to the system driven by future funding from NIH, NSF, AWWA, WERF or EPA, it will eventually be autonomous without the need of a human operator. Multiple units of the autonomous system can be positioned in the field for ubiquitous monitoring of water pathogens via sensor networks. A real-time, spatially and temporally distributed water quality map will be an invaluable resource to both prevent and control pathogenic outbreaks and their costly aftermath in terms of human lives and resources.

G. PROJECT OBJECTIVE(s):

The research aims to develop an in-situ capable detection system targeting pathogenic *E. coli* O157:H7. The specific research objectives of **Phase 1** were (1) A method development of the quantitative pathogen detection based on the DNA hybridization using nanoparticle labels and a proof-of-concept study using synthetic ssDNA targets; (2) Quantitative detection of pathogenic *E. coli* O157:H7 using bacterial culture and the optimization of the developed method; (3) Assay validation by the comparison to traditional pathogen detection method.

The specific research objectives of **Phase 2** include (1) to examine the effects of common inhibitors in environmental samples for a developed assay via the assay interference test; (2) to examine the compatibility of the assay for in-situ field monitoring via investigating various operational and

quantificational parameters; (3) to perform a preliminary experiments on DNA hybridization with nanoparticles in a microfluidic environment.

H. METHODOLOGIES:

Phase 1 (FY2010). Method development and proof of concept

Phase 1, Task 1: Pathogenic *E. coli* detection targeting synthetic DNA

DNA design and materials: Linear DNA oligonucleotides for probe, target, and signaling probe DNA was designed based on the sequences of *eaeA* gene (Genbank accession: X60439.1) and commercially synthesized (IDT, Coralville, IA). Carboxyl quantum dot nanoparticles (QD₆₅₅, Invitrogen, Carlsbad, CA) was used to encapsulate aminated magnetic beads (M270, Invitrogen) via the formation of amide bond (covalent bond) with the assistance from both ethylcarbodiimide hydrochloride (EDC) and *N*-hydroxysuccinimide (NHS). A DIG easy hybridization buffer (Roche Diagnostic, Basel, Switzerland) was used for the DNA hybridization. All hybridization reactions was implemented in a 96-well PCR tube plate (Applied Biosystems, Foster City, CA). A MPC-96S 96-well magnet (Invitrogen) was used to extract particle-DNA hybrids out of the solution for washing and separation. A hybridization incubator (UVP HB-500 Minidizer Hybridization, Fisher Scientific) provides a constant temperature environment with gentle mixing for the DNA hybridization.

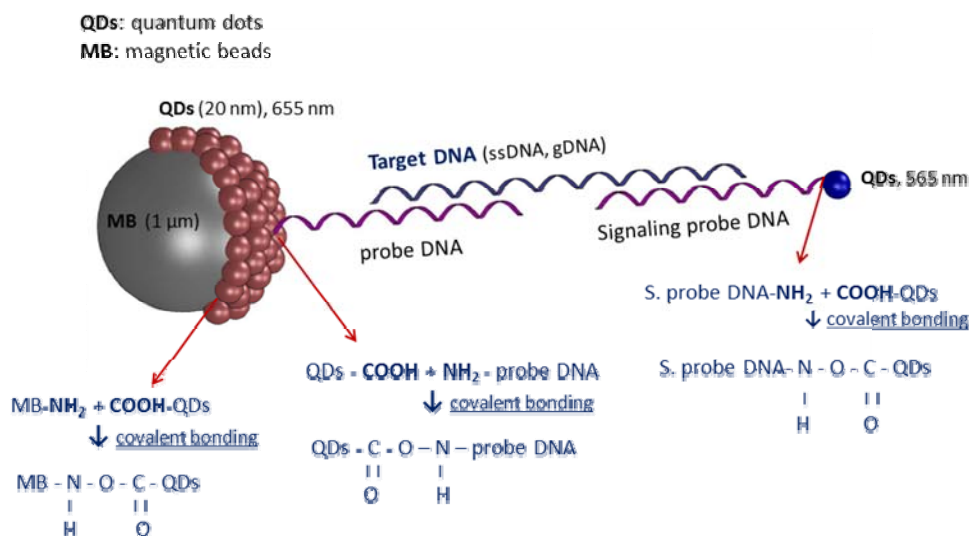


Figure 2. A schematic diagram of nanoparticle based DNA hybridization assay targeting *eaeA* gene of *E. coli* O157:H7 detection

Nanoparticle functionalization and DNA hybridization: The schematic diagram of nanoparticle based hybridization assay for *E. coli* O157:H7 *eaeA* gene quantification is shown in Figure 2. Magnetic beads (2×10^7 beads/mL) are encapsulated with QD₆₅₅ via covalent bond. The probe DNA is subsequently immobilized on the surface of the complex of magnetic beads and QDs. The signaling probe DNA are also prepared by the formation of a covalent bond between the carboxyl group of QD₅₆₅ and the amine group at 3' end of the signaling probe DNA in the same manner as the probe DNA. A desired amount of signaling DNA is added to the solution of QD₅₆₅ nanoparticles (1 μM, 8 μL). After further adding 10 μL of the mixture of EDC and NHS (1:1 in a molar basis), the particles was incubated at ambient temperature with a slow tilt rotation. For the hybridization of *eaeA* ssDNA target, the probe DNA conjugated particle complexes was re-suspended in 100 μL DIG easy Hyb buffer. 500 pmoles of signaling probe DNA and various amounts of target DNA was also added. The mixture was incubated (hybridized) for 8 hrs at 37 °C with gentle mixing. At the end of hybridization, it was washed 3 times with phosphate buffer (0.1

M, pH 7.4). A 96-well external magnet was used to manipulate the paramagnetic particle complex in the solution. As a result of magnetic separation and washing, un-bound DNAs and particles was removed from the suspension. Finally, the target DNA was detected and quantified by the normalized fluorescence of the QDs (i.e., QD_{565}/QD_{655}). Experimental errors resulting from the different particle numbers in each reaction was minimized due to the normalization. The fluorescence of QD_{565} ($\lambda_{ex} = 360$ nm, $\lambda_{em} = 570$ nm) of signaling probe DNA and QD_{655} ($\lambda_{ex} = 360$ nm, $\lambda_{em} = 660$ nm) of probe DNA was determined by a spectrofluorometer (MDS, Sunnyvale, CA).

Kinetics and rapidity of assay: Kinetic experiments was conducted for our DNA hybridization by varying the target DNA concentration and temperature. The main reaction of kinetic experiments is the DNA hybridization that occurs between the probe DNA and target DNA. The signaling probe DNA was added simultaneously with the target DNA. Target DNA concentration was varied at 100, 400, and 800 fM with temperatures of 25, 37, and 42 °C at each concentration. Incubation was carried out for 0.5, 1, 2, 3, 5, and 7 hrs. After each incubation step, fluorescence intensities was measured immediately. Normalized fluorescence (QD_{565}/QD_{655}) was converted to the DNA concentration by using previously established calibration curve between the fluorescence and DNA concentration. The corresponding rate constants for a series of hybridization reactions was obtained using chemical kinetics models and a linear regression analysis.

Phase 1, Task 2: Pathogenic *E.coli* detection targeting cultured bacteria

Culturing bacteria: E. coli O157:H7: Pure culture of *E. coli* O157:H7 (ATCC 43888) was purchased from ATCC (American Type Culture Collection, Rockville, MD) and grown in trypticase soy broth (Difco Laboratories, Detroit, MI) at 37 °C for 20 hrs in a shaking incubator. Since *E. coli* O157:H7 is an organism requires a bio-safety of level 2, all culturing work was performed inside a bio-safety cabinet (Labconco, Kansas City, MO) throughout the experiment. The grown bacterial culture was used for gDNA extraction and plate counting method in Task 3.

Genomic DNA extraction: Genomic DNA from pure bacterial cultures was extracted by a Fast DNA spin kits (Qbiogene, Carlsbad, CA) following the manufacturer's protocol. 10 mL culture sample will be harvested and centrifuged at 5000 rpm for 5 min. The pellet was re-suspended and extracted using the kit. The extracted DNA was dissolved in 75 μ L of H₂O. 5 μ L of gDNA samples was used to measure the DNA concentrations using the optical densities (at 260 nm and 280 nm) obtained via a Nanodrop N100 spectrophotometer (Wilmington, DE). The extracted gDNA was used 1) for PCR amplification to verify the *eaeA* gene presence in the bacterial culture and 2) as a target DNA material in our assay.

PCR amplification: Double-stranded DNA (dsDNA) target fragments was produced by PCR amplification carried out in AB 2720 Thermal Cycler (Applied Biosystems, Foster, CA) with the following program: initial denaturation at 95 °C for 3 min, followed by 40 cycles of denaturation at 95 °C for 30 sec, annealing at 60 °C for 30 sec, and elongation at 72 °C for 1 min, and final extension at 72 °C for 5 min (Mao et al., 2006a). PCRs will be performed by adding 5 μ L of DNA to 45 μ L of mixture consisting of 1x AmpliTaq PCR buffer (Applied Biosystems), 2 mM of AmpliTaq MgCl₂ (Applied Biosystems), 0.2 mM of dNTPs (Takara Bio, Shiga, Japan), 0.4 μ M of F and R primers (IDT), 2.5 units of AmpliTaq Gold DNA polymerase (Applied Biosystems), and DNase/RNase free water (GIBCO[®], Invitrogen). Besides the gDNA sample (positive control), negative control (water) will be included to verify the accuracy of the amplification. The PCR amplicon fragment size will be examined using 1 % agarose gel with 0.5 x TBE (Tris boric acid EDTA, AB) buffer at 65 V for 1.5 hr and visualized with a UV Transilluminator (Fisher Scientific) using ethidium bromide (0.5 μ g/mL) staining. A 100-bp DNA ladder (Promega, Madison, WI) will be used to determine the size of DNA.

Based on the result of PCR amplification, the presence of *eaeA* gene in the gDNA extracted from pure culture will be verified. Following the verification, the PCR products (i.e., amplicons) will be used as the

target material for our hybridization method. The amplicons will be purified using a DNA Clean and Concentrator kit (Zymo, Orange, CA) prior to the hybridization.

Quantitative detection of pathogens: DNA hybridization was performed using gDNA and/or amplified dsDNA. The difference between Task 1 and 2 is that Task 2 uses real bacterial culture instead of synthetic ssDNA. As compared to ssDNA, gDNA has a complicated (i.e., super-coiled) structure embedded with other biomaterials (e.g., carbohydrates, proteins). The target gDNA was denatured (fractionated) for better hybridization result. gDNA was denatured by incubation at 95 °C for 5 min and following ultrasonication for 30 sec (Son et al., 2008). The denaturing conditions will be further optimized to enhance the hybridization of gDNA in Phase 2 research. The optimized denaturation allows us to bypass the DNA extractions when using environmental samples. This process will lay the foundation for preparation of field samples.

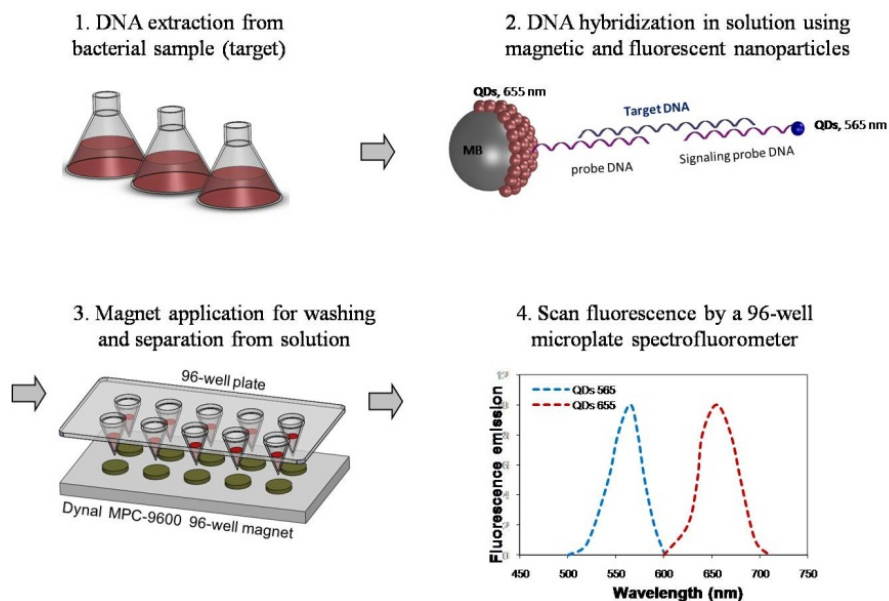


Figure 3. A schematic diagram of our proposed DNA hybridization method using multi-functional nanoparticle labels.

Figure 3 describes the procedure of our proposed quantification method from sampling to detection. The same procedure was performed for both synthetic DNA (Task 1) and real bacterial DNA (Task 2) in the laboratory setup. Various parameters governing hybridization were studied and optimized. These parameters include temperature, time, composition and volume of hybridization buffer, and denaturation conditions. The results of optimization allow the technique to have highest sensitivity within the shortest reaction time for a given concentration of target DNA.

Phase 1, Task 3: Validation of the proposed method by a conventional method

In this task we validated our new detection method – NanoGene assay - by comparing to the conventional method. Currently, under federal regulations, the only detection technique that is specifically used for *E.coli* O157:H7 is a surface plate counting method using an agar plate. Therefore the plate counting method is used as a representation of conventional method. After culturing the bacterial *E. coli* O157:H7 (described in Task 2), the bacterial numbers were calculated based on the conventional plate counting method. The serial dilutions of bacterial culture were inoculated on trypticase soy agar plates and incubated at 37 °C for 24 hrs. Figure 4 shows the picture taken during the plate counting and the yellow dots (i.e., colony) are bacteria grown on the surface of agar plates. The colonies were counted to

determine the number of colony-forming units per mL of culture (CFU/mL). The result based on the plate counting was compared to the numbers obtained from our developed assay for the verification.

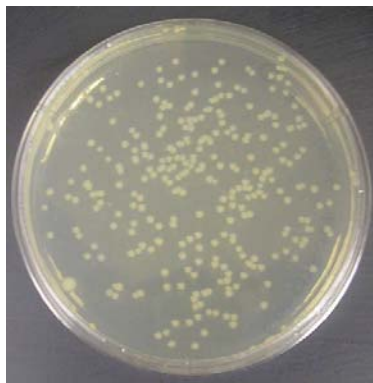


Figure 4. Example of a plate counting method using agar plates. The colonies shown above indicate *E.coli* O157:H7 cultured on trypticase soy agar plates.

Phase 2 (FY2011). Environmental applicability and field readiness of the developed assay

We further developed the technique for use with environmental samples. Prior to the development of the portable biosensor device, the effects of inhibitors that are abundant in environmental samples were examined (Task 1) and the compatibility of the assay for in-situ field application was also examined via various operational and quantificational parameters (Task 2). The conventional plate counting method as well as quantitative PCR assay was used to validate our assay capability using actual environmental samples for both Tasks 1 and 2. We also initiated the work on the microfluidic components to implement the assay in a miniaturized format (Task 3). Figure 5 describes the procedure of our proposed quantification method from sampling to detection. The same procedure was performed for both effects of inhibitors (Task 1) and field compatibility of key parameters (Task 2) in the laboratory setup.

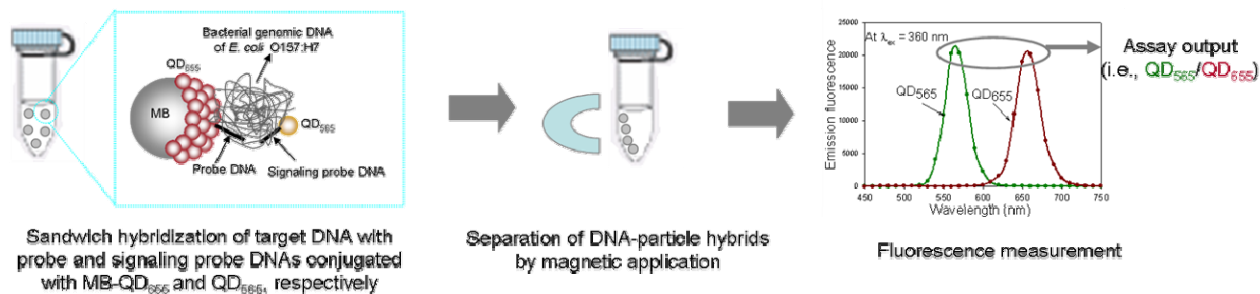


Figure 5. Schematic diagram of gene quantification assay using MB and a set of QD nanoparticles.

Phase 2, Task 1: Effects of common inhibitors from environmental samples on the developed assay

Quantification capability of our NanoGene assay was compared to that of qPCR assay in the presence of inhibitors (6 types). The degree of inhibition by each of these inhibitors will be tested at various concentrations. The inhibition experiments in simple water microcosms will be performed in the laboratory.

Model target bacteria: *E. coli* O157:H7 was used as the target pathogenic bacteria, because (1) the presence of *E. coli* in water is a widely established indicator of recent fecal contamination; (2) in particular, *E. coli* O157:H7 is the most common pathogenic *E. coli* seen in the United States; (3) *E. coli* O157:H7 is notorious due to its pathogenicity (i.e., fewer than 100 organisms of infective dose per mL water) (Singleton, 2004; Tuttle et al., 1999a) that can infect both human and animals; and (4) thus it poses a serious risk when present in animal waste or reclaimed wastewater. (Lin et al., 2008; Mao et al., 2006b; Shriver-Lake et al., 2007)

Sample preparation and standard DNA templates: Samples for the assays consisted of blank (water), series of standard DNA (a serial dilution of PCR amplicons targeting *eaeA* gene, 151 bp), and microcosm sample (pathogen culture, water, and 6 inhibitors with varying concentration). For calibration curve construction, the standard templates of *eaeA* gene were generated by a standard PCR (Mao et al., 2006b) and the subsequent serial dilution of the PCR amplicon (e.g., 2×10^1 to 2×10^9). As for the microcosm sample, the bacterial culture of *E. coli* O157:H7 (ATCC, 43888) was incubated in trypticase soy broth at 37°C. The overnight culture was transferred to sample water in order to simulate pathogen-containing water.

Inhibitor spiking and DNA extraction: Varying amounts of 6 inhibitors was added to the microcosm samples. The amounts of inhibitors that are added to each sample were based on their abundance in the environment. A wide range of inhibitors in the environmentally relevant concentration range was used in Task 1. The gDNA was extracted from the water containing both pathogen and inhibitor by a FastDNA® SPIN for Soil kit (MP Biomedicals). DNA concentration and purity was determined by UV absorption at 260 nm and 280 nm using a Nanodrop ND-1000 spectrophotometer. The gDNA was the template for both assays.

Gene quantification based on DNA hybridization: The extracted gDNA from each microcosm was denatured by the combination of ultra-sonication and high-temperature incubation (95°C). The preparation of particle-DNA complex was previously optimized. The denatured target gDNA was hybridized with MB-QD₆₅₅-probe DNA and QD₅₆₅-signaling probe DNA at 37°C using a gentle tilt rotation. The DNA sequences of probe and signaling probe DNA oligonucleotides are listed in Table 2. Prior to the fluorescence measurement, the DNA-particle hybrids was subsequently separated by the magnet (MPC®-96S, Invitrogen) and washed three times with phosphate buffer (pH=7.5). The fluorescence measurement will be implemented by a MDS spectramax M2 spectrofluorometer, which is available in the PI's laboratory.

Table 1. The sequences and the modification of *E. coli* O157:H7 *eaeA* DNA oligonucleotides.

DNA oligonucleotides	Assays	Sequence (5' → 3') and modification	Reference
Probe DNA	<i>Our assay</i>	NH ₂ -CGGATAAGACTTCGGCTAAA	Designed by the PI
Signaling probe DNA	<i>Our assay</i>	CTTATACCGCGACGGTGAAA -NH ₂	Designed by the PI
Fwd. primer	Real-time	GGCGGATAAGACTTCGGCTA	Carey <i>et al.</i> (2009) (Carey <i>et al.</i> , 2009)
Rev. primer	Real-time	CGTTTTGGCACTATTTGCC	Carey <i>et al.</i> (2009) (Carey <i>et al.</i> , 2009)

qPCR assay: qPCR assay was implemented by the SYBR based method. The reaction mixture includes 1× Universal SYBR Green master mix (Applied Biosystems), 0.5 μM of *eaeA* targeting forward and reverse primers (Table 1), 2 μL of standard or sample DNA template, and filter-sterilized DNase/RNase free water (GIBCO®, Invitrogen) to bring the final reaction volume to 25 μL. (Sharma et al., 1999) The qPCR reaction will be performed using a StepOne™ Real-Time PCR system (Applied Biosystems) based on the thermal cycles cited in the study by Carey et al. (Carey et al., 2009) Following PCR amplification, melting curve analysis of amplified DNA products will be performed to confirm product purity with the temperature at a rate of 0.3 °C/s from 55°C to 95°C.

Extra purification of gDNA: As a control, the extra step of purification for environmental samples, which is additionally used for the removal of inhibitors in PCR assays, was employed to demonstrate the level of inhibitor purification as a control. PCR purification kit and gDNA purification kit (Zymo) was used to remove the organic inhibitors from the extracted gDNA before the DNA hybridization.

Phase 2, Task 2: Compatibility of key assay parameters for in-situ field application

We examined the key assay parameters to identify their levels of field-readiness and to initiate further development where necessary. The output from this task will allow us to formulate the system design required for carrying out the Phase 3 research. The focus of this task is to identify and mitigate potential technical challenges during the development of the in-situ capable system. By investigating and pushing the operating limits of each key assay parameters, design rules can be established prior to Phase 3. For example the hybridization step can be further developed such that it only requires ambient temperature and therefore in-situ compatible.

Various parameters were tested to investigate the compatibility of the proposed assay for *in-situ* application.

1) *Specificity:* The specificity of the MB-QD assay was demonstrated by quantifying the *eaeA* gene of *E. coli* O157:H7's gDNA from a mixed pool of target and non-target gDNA. Non-pathogenic *E. coli* K12 (ATCC) was used as a non-specific target that is phylogenetically close with *E. coli* O157:H7. Mixed (non-specific target) microorganisms was obtained from the mixed liquor in the aeration basin of an activated sludge process (Auburn wastewater treatment plant, Auburn, AL). Genomic DNAs extracted from pure *E. coli* O157:H7, *E. coli* K12 and mixed liquor samples was mixed in various ratios. The gDNA mixture was denatured and used for the subsequent DNA hybridization.

2) *Rapidity dependence on temperature & agitation:* The heated incubation and agitation are critical parameters to determine the rapidity of DNA hybridization. Kinetic experiments were used to investigate the assay's performance at ambient temperature. 40 ng of gDNA per reaction was hybridized at 15, 25, and 37 °C. Normalized fluorescence (i.e., QD_{565}/QD_{655}) was measured at 0.5, 1, 2, 4, 6, and 8 hrs. Kinetic order shall be determined via the R^2 values of regression equations for various kinetic reactions. The effect and necessity of mechanical agitation on the gDNA hybridization were also investigated. 40 ng of gDNA per reaction was hybridized at 37°C for 8 hrs with three different mixing conditions: continuous agitation, pulsed agitation (i.e., agitation for only 10 min in every 2 hrs), and no agitation. The hybridization capability (%) was calculated based on the assumption that 100% of gDNA hybridization is achieved under the continuous agitation.

3) *Stability of pre-made reagents:* The stability of the MB-QD particle complex will be examined under various storage conditions (i.e., ambient and refrigeration temperature). Storage stability will enable the reagents to be prepared in advance and stored prior to DNA hybridization. Pre-incubations for covalent bonding formation are required for making MB-QD particle complex and immobilizing probe DNA on QDs. QD_{655} only and MB- QD_{655} complex will be stored in phosphate buffer at 4°C and ambient temperature for 30 days. The storage stability shall be monitored by measuring the fluorescence of QD_{655} for the MB- QD_{655} complex. The stability of MB- QD_{655} will be an indication of the covalent bonding stability between particles. The fluorescence of QD_{655} itself will also be monitored in parallel to investigate the photobleaching effect of QD nanoparticles.

Phase 2, Task 3: Preliminary experiments for NanoGene assay in a microfluidic environment

Based on the results from Task 2, we have brought one of our key technical challenges, which is in-situ mixing and hybridization of DNA-nanoparticle complexes, to the next level of development. This involved the investigation, optimization and demonstration of DNA hybridization in a microfluidic

environment at in-situ field conditions. It was essential to obtain preliminary information on the hybridization efficiency in a microfluidic environment. For this purpose, commercial off-the-shelf microfluidic rhombic chamber chips were adopted and incorporated into the proposed assay protocol. In this task, the inflow to the microfluidic chamber included synthetic ssDNA obtained from Integrated DNA Technologies. After hybridization, the sample was collected and the bench-top spectrofluorometer was used to measure the fluorescence.

1) *Preparation of reagents, samples, and microfluidic components.* As with the non-microfluidic NanoGene assay, the components required for hybridization, and thus the reagents to be injected into the chip, included particle-probe DNA complexes, a target ssDNA, and hybridization buffer. The particle-probe DNA complexes were prepared according to the protocol dictated in Phase 1, Task 1. Based on the results from Phase 2, Task 2 pertaining to the stability of reagents, the particle-probe DNA complex can be prepared in advance and stored until hybridization. The components of the customized hybridization buffer included SSC (saline-sodium citrate, Fisher-Scientific, Fair Lawn, NJ), BSA (bovine serum albumin, New England Biolabs, Ipswich, MA), and SDS (Sodium dodecyl sulfate, MP Biomedicals, Solon, OH).

The experimental components for the microfluidic setup included a microfluidic chip, a magnetic trap, miniature peristaltic pumps, and a DC power supply. The commercial off-the-shelf microfluidic chip selected for the purpose was the Rhombic Chamber Chip (Part Number 12-0901-0172-01) with a volume of 120 μL (Microfluidic ChipShop, Jena, Germany, see Figure 6a). Strong rare earth Neodymium (NdFeB) magnets (Part Number D52-N52, K&J Magnetics, Bethlehem, PA) were placed over the chip to act as an inline magnetic trap. The reagents were injected into the chip via commercial off-the-shelf Miniature Peristaltic Pumps (Part Number 3200024, Dolomite, Hertfordshire, United Kingdom, see Figure 6b). Silicone pump tubing (Part Number 3200173, Dolomite, 1.5 mm inner diameter, 2.5 mm outer diameter) and PTFE connection tubing (Part Number 3200067, Dolomite, 0.5 mm inner diameter, 1/16" outer diameter) were connected between the microfluidic chip and the miniature peristaltic pump. To aid in the connection between the chip and the tubing, mini luer connectors were also purchased (Part Number 09-0541-0000-09, Microfluidic ChipShop). The flow rates of the pump were controlled via a Mastech HY1803D Variable DC Power Supply (San Jose, CA, Figure 6c).



Figure 6. (a) A schematic of Microfluidic ChipShop Rhombic chamber chip, (b) Dolomite miniature peristaltic pump and (c) Mastech HY1803D variable DC power supply.

2) *Optimization of hybridization buffer components.* Preliminary experiments for hybridization using a microfluidic format were conducted using the same hybridization buffer used in the well-plate format (Roche, DIG Easy hybridization buffer). This buffer created a plethora of bubbles in the chip that were determined to be detrimental to hybridization. In order to eliminate the problem of bubble formation, it was imperative that a different hybridization buffer be used for hybridization in the microfluidic chip. The alternative buffer should demonstrate the similar hybridization capability with less bubble created in the microfluidic chip. Therefore five buffers were tested and the main parameter was the SDS (surfactant)

contents by varying it as 0, 0.05%, 0.1%, and 0.2%. To evaluate whether or not each buffer would create bubbles in the chip, 200 μL of each buffer was circulated through the chip for 30 min at a flow rate of 9 $\mu\text{L}/\text{min}$. After 30 minutes, each chip was analyzed for the presence of bubbles. The pictures were taken for the bubble creation in each buffer examined in the microfluidic platform. In order to evaluate the efficiency of each buffer on hybridization, each of the five buffers were used for hybridization in the well-plate method (volume = 400 μL) as well as in the microfluidic format. Each buffer was used for the hybridization of 0 mol/L (negative control) and 10^{-12} mol/L of target ssDNA. The NanoGene assay protocol dictated in Phase 1/Task 1 was followed for hybridization. For microfluidic hybridization, two strong rare earth Neodymium magnets were placed on opposite sides of the microfluidic chip to act as a stationary magnetic trap. Ten μL of the magnetic bead-QD₅₆₅-probe DNA complexes, 4 μL (6.2×10^{-8} mol/L) of the signaling DNA-QD₆₅₅ complexes, 2 μL (10^{-12} mol/L) of target DNA, and 184 μL of hybridization buffer were injected into the chip. The magnetic bead complexes were held by the magnet and the target and signaling DNAs were circulated through the chip. Hybridization was allowed for 60 min at flow rates of 5, 9, 15, 21 and 27 $\mu\text{L}/\text{min}$. Various flow rates were applied to determine the working flow rate range of each buffer. The sample was then washed with 1.5 mL of phosphate buffer (PB, pH = 7.4) to remove any untethered particles. After hybridization, the magnets were removed, the sample was collected, and fluorescence was immediately measured using the MDS SpectraMax spectrofluorometer.

3) *Optimization of Flow Rate and Retention Time.* More experiments to optimize flow rate and retention time were conducted to examine our microfluidic NanoGene assay as a viable option for rapid, in-situ gene detection. The 0.01% BSA, 0.10% SDS in $10\times$ SSC hybridization buffer and 1×10^{-12} mol/L of target DNA were used. Hybridization was conducted in the same manner described above. Experiments were conducted for retention times of 0, 2.5, 5, 10, 20, 30, and 45 minutes at flow rates of 5, 9, 15, and 21 $\mu\text{L}/\text{min}$. Normalized fluorescence was plotted for each retention time and flow rate to create curves to compare the effect of retention time and flow rate on hybridization efficiency. Based on these curves, the optimum flow rate and retention time was selected.

I. PRINCIPAL FINDINGS/RESULTS:

Results and findings for Phase 1

Preliminary (a)-Optimization of particle configuration

The QD nanoparticles that are bonded to the MB serves as internal calibration for the assay by providing stable and long-lasting fluorescence. The stability of the MB-QD bonding is critical for successful quantification. The ratio of MB to the number of QDs together with the washing protocol was optimized to ensure maximum bonding of the QDs to the MB. Figure 7 (Kim & Son, 2010b) shows the presence of QDs encapsulated on the surface of MB. Field emission scanning electron microscopic (FE-SEM) energy disperse spectroscopy (EDS) mapping images of CdSe/ZnS QDs have shown four elements (Cd, Se, Zn, S) with four different colors. The results indicate that the covalent bonding between QDs and MB was successful, which also imply that the QDs were successfully immobilized on the surface of the MB. (Kim & Son, 2010b)

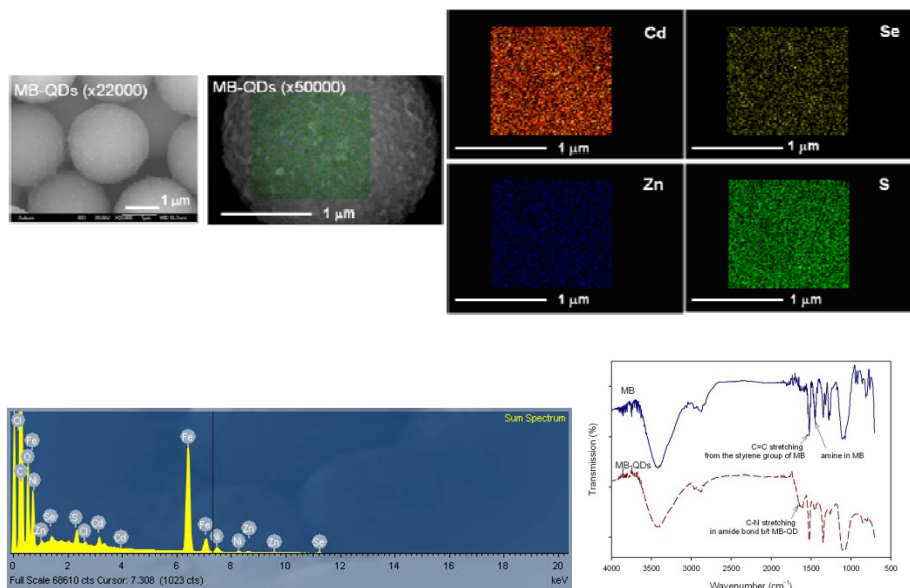


Figure 7. FE-SEM images of MB-QD complex (two in left, upper line) and corresponding energy disperse spectrometry (EDS) mapping images (right, upper line) of CdSe/ZnS QDs on the MB surface (scale bar = 1 μm). The color images of each elements (Cd: brown; Se: dark green; Zn: navy; S: light green) indicated the immobilization of QDs on the MB surface via covalent bonding was successful. (Kim & Son, 2010b)

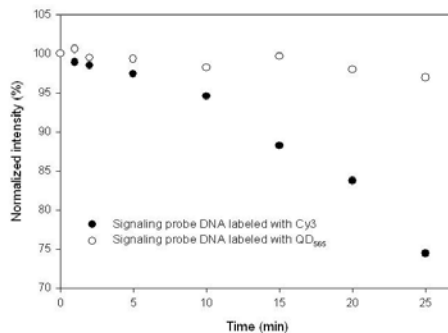


Figure 8. Comparison of signal photostability obtained by using signaling probe DNA labeled with Cy3 and QD565. The QDs nanocrystals that are made of semi-conducting materials have shown the excellent photostability over organic fluorophore, Cy3.

Preliminary (b)-Photostability

The main advantage of using QD over organic fluorophore as a label for the assay is its photostability, which is defined as the resistance to photobleaching. Photostability of both QDs and Cy3 labeled DNAs was monitored via continuous measurement of the fluorescence intensity for 25 min. As shown in Figure 8, the fluorescence intensity of the signaling probe DNA with QDs maintained its initial intensity for the duration of the experiment, but that obtained from the DNA with Cy3 decreased to 75% after 25 min. The results showed that the **QD nanoparticles label has better stability for hybridization as compared to organic fluorophore, Cy3.**

Preliminary (c)-Assay optimization

Washing. For further hybridization, the probe DNA conjugated MB-QDs particle complexes were washed with PB. The washing is required to remove non-hybridized DNA, non-bound QDs and residual hybridization reagents. However harsh washing could affect the bonds between particle and DNA or within DNA hybrids. In order to optimize the washing stringency, the fluorescence intensity was monitored in response to varying washing duration. As shown in Figure 9a, the similar fluorescence values were observed in the range of 100 through 500 pmoles of probe DNA labeled with Cy3 after a single wash. After 5 washes, there was no linear relationship between fluorescence signal and the concentration of probe DNA labeled with Cy3. After 3 washes, the normalized fluorescence values linearly increased and there was clear discrimination as the concentration of probe DNA labeled with Cy3 increased. Based on the experimental observations, even though stringent washing is advantageous for the complete removal of non-bound QDs and probe DNA, but it could also cause a loss of already bound QDs and probe DNA. In this regard the optimum washing stringency was determined to 3 times for the following experiments.

Passivation. Passivation is a common method for avoiding a non-specific binding (i.e., particle coagulations in this case) by inactivating the functional groups. The signaling probe DNA labeled with QD₅₆₅ was incubated in a NaBH₄ based blocking solution (0.5 g of NaBH₄ in the mixture of 10 mL 20×SSC, 0.5 mL 10% SDS, and 90 mL H₂O) at 42°C for 20 min to passivate the remained functional groups on the QD₅₆₅ surface, and washed with 1× SSC and 0.2× SSC twice. The signaling probe DNA with QD₅₆₅ was subsequently collected by centrifuging twice at 10,000 rpm for 5 min. In order to examine the passivation effect of the nanoparticle labels on DNA hybridization, both treated and non-treated QD₅₆₅ - signaling probe DNAs were compared during hybridization. The effect of passivation treatment for QD₅₆₅ labels (i.e., conjugated with a signaling probe DNA) is presented in Figure 9b. The passivation of QD₅₆₅ labels allowed the fluorescence output to increase accordingly when the amount of target ssDNA increases. This indicated that the quantification is only feasible with the use of passivated nanoparticle labels. For non-passivated labels, no change of fluorescence was observed with a various amount of target ssDNA. One possible cause involves particle aggregation via non-specific binding which can be induced by the remaining functional groups on the surface of non-treated QD₅₆₅ labels. The passivation of QDs in the signaling probe DNA can prevent particle agglomeration which is caused by the unoccupied functional groups of QD₅₆₅.

Molar ratio of QDs and signaling probe DNA. The molar ratio effect of QD₅₆₅ to signaling probe DNA (i.e., 1:3, 1:10, and 1:30) on the hybridization efficiency was examined. The optimum molar ratio of signaling probe DNA and QD₅₆₅ was determined by the highest output signal of fluorescence after hybridization. The quantification of target DNA is based on sandwich hybridization between the probe and signaling probe DNAs. The capturing MB-QD₅₆₅ particles' functional groups (i.e., carboxyl) should be linked to a large number of probe DNAs' functional groups (i.e., amine) to maximize available counterparts for the target DNA. Since the target and signaling probe DNAs are simultaneously hybridized with the probe DNA, the successful hybridization between the target and the signaling probe DNAs is essential for the complete hybridization. The ratio between the numbers of signaling probe DNA and label has to be optimized to maximize the output of the assay. The effect of QD₅₆₅ to signaling probe DNA molar ratio on DNA quantification is shown in Figure 9c. The maximum output of assay was

observed at the signaling probe DNA to QD₅₆₅ molar ratio of 10. For our assay format the optimum molar ratio was established at 10. The signaling probe DNA and labels were optimized in terms of molar ratio and passivation prior to the subsequent quantification experiments in later sections.

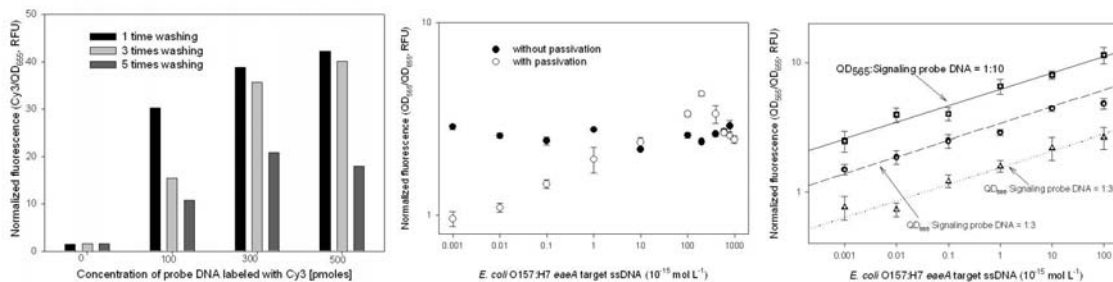


Figure 9. (a) The washing effect, (b) passivation effect, and (c) optimized molar ratio between QDs and probe DNAs for MB-QD assay.

Phase I, Task 1 – Synthetic DNA (ssDNA) quantification

Quantification results and assay sensitivity. In order to characterize the quantification range and linearity of the MB-QD assay, hybridization was performed using ssDNA as the target. The quantification result is presented in Figure 10. A linear quantitative relationship was observed in the range of 10^{-18} to 10^{-13} mol L⁻¹. The normalized fluorescence (i.e., QD₅₆₅/QD₆₅₅) showed a linearity ($R^2 = 0.929$) of over 5 orders of magnitude with the LOD of 890 zeptomolar concentration (i.e., zM = 10^{-21} mol L⁻¹). The detection of ssDNA in various formats was reported in several prior literatures: 2×10^{-9} mol L⁻¹ in the gold nanoparticle based fluorescence quenching method (Wu et al., 2006); 1×10^{-10} mol L⁻¹ by MB-functionalized fluorescent microspheres (Ferguson et al., 2000); 1×10^{-12} mol L⁻¹ in the format of gold nanoparticles coupled light scattering (Dai et al., 2008); 8×10^{-13} mol L⁻¹ in the dye-doped silica nanoparticle based hybridization (Zhao et al., 2003); 5×10^{-15} mol L⁻¹ in the silver nanoparticle based chemiluminescent method (Liu et al., 2006); and 8.3×10^{-18} mol L⁻¹ by the magnetic particles with electrogenerated chemiluminescent detection (Patolsky et al., 2003). Recently Liu *et al.* (Liu et al., 2008) reported the feasibility of detecting ssDNA of 250 zM (i.e., 2.5×10^{-19} mol L⁻¹) by QD nanoparticle labeling. The result however was preliminary. The assay had only three points examined and no LOD reported. More importantly there was no internal standard to normalize the assay output, thereby potentially resulting in the poor reproducibility of the assay. As compared to the previous studies listed above, the MB-QD assay demonstrated excellent sensitivity for the detection of ssDNA.

Table 2. The linear equation and concentration range, R², and detection limit of nanoparticle-based gene quantification assay.

Parameters	
Regression equation	$y = 0.0329x + 3.391$
Correlation coefficient (R^2)	0.992
Linear range	10 – 1000 fM
Detection limit	9.72 fM

Assay specificity. In order to evaluate the discrimination capability of DNA sequence variations of our assay, 1-, 2-, and 41-bp mismatched (out of total 55-bp) ssDNAs targets were hybridized with probe DNA as compared to perfectly matched target DNA. DNAs of different concentrations (50 - 400 fM) were analyzed based on the normalized fluorescence signal (Figure 10b). The various mismatched DNAs were clearly discriminated from perfectly matched target for the range of concentration. Assuming the difference of fluorescence signals between perfectly matched and 41-bp mismatched DNA at 400 fM is 100%, the fluorescence intensity of 1- and 2-bp mismatched DNA target corresponded to 30 and 20% of that of the perfectly matched target, respectively. The significant difference among them was verified by a

statistical test. All the obtained P -values were smaller than 0.1 by the two-sided t -test with 95% confidence level. Moreover, the fluorescence signal among mismatches tended to be consistent regardless of varying concentrations of target DNA (50 - 400 fM). Bacteria represented by 1- and 2-bp mismatched DNAs are phylogenetically close but not identical to the bacterium represented by perfectly matched DNA. In contrast, the 41-bp mismatched DNA is of entirely different species. This demonstrates that our developed technique is capable of screening through the DNA sequences of pathogenic and non-pathogenic bacteria species and detecting the pathogens. Our assay has shown excellent selectivity in discriminating a phylogenetically similar gene to *eaeA* gene. Furthermore, the use of our technique can be expanded to encompass the detection of single-nucleotide polymorphisms (SNPs) in biomedical science.

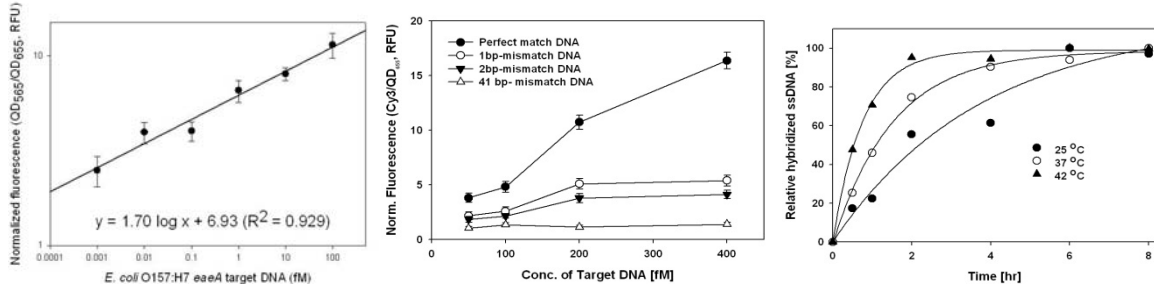


Figure 10. (a) Linearity, dynamic range, and sensitivity of the assay, (b) specificity using mismatch DNAs, and (c) rapidity of the assay based on the kinetics in various temperatures.

Assay rapidity (kinetics). In order to examine the kinetic parameters of the presented technique, the effects of target DNA concentration and hybridization temperature were investigated as described earlier. The results are illustrated in Figure 10c and detailed in Table 3. The rate constants of hybridization reactions were obtained from the linear regression analysis based on second-order kinetic model with the assumption of negligible dissociation reaction and excess signaling probe DNA concentration. The governing equation is as follows:

$$\ln\left(\frac{C_{i,p} - C_{h,p}}{C_{i,t} - C_{h,t}}\right) = -k_h \cdot (C_{i,t} - C_{i,p}) \cdot t$$

where, $C_{i,t}$ and $C_{h,t}$ is the initial and hybridized concentration of target DNA, respectively, $C_{i,p}$ and $C_{h,p}$ is the initial and hybridized concentration of probe DNA, t is time, and k_h is the hybridization rate constant. Herein, the initial concentration of probe DNA was 1.25 μM . As shown in Table 3, the correlation coefficient (R^2) indicated that the kinetics of DNA hybridization follows the second-order reaction. Please note that the result is consistent with the previous studies (Chunlai Chen et al., 2009; Larry E. Morrison & Stols, 1993). It was due to the rate-limiting step of DNA hybridization is the prior formation of a few base pairs from each strand into a transient intermediate (i.e., nucleus). Then the remaining base quickly forms a complete helix (James G. Wetmur & Davidson, 1968). The hybridization rate increased with the concentration of target DNA, indicating the target concentration is another rate-limiting factor in a hybridization reaction.

Figure 10c shows the normalized hybridized amount of ssDNA target depending on the various hybridization temperatures. The percentage was calculated by assuming each plateau value as 100%. This assumption is reasonable because each measurement is relative. The result indicated that the reaction rate constant increased as the hybridization temperature increased, which is consistent with Table 3. In other words, the higher hybridization temperature would allow hybridization equilibrium to be reached in a shorter period of time. For example, the equilibrium time for hybridization was 5 hrs at 25 °C, and it was 2 h at 42 °C. From a practical perspective, it is concluded that at sufficiently high target concentration, the required amount of target DNA could be hybridized at ambient temperature. However higher temperature will be required to expedite DNA hybridization for low DNA concentrations. The adjustment of

hybridization temperature in accordance to the amount of target DNA is required for the maximum efficiency of DNA hybridization.

Table 3. The hybridization rate constants and R^2 values measured from the linear regression analysis based on the second order kinetic models. R^2 values were presented in brackets.

Target DNA (fM)	Second order rate constant (k_h) ($\times 10^6 \text{ M}^{-1} \text{ h}^{-1}$)		
	25°C	37°C	25°C
100	0.211 (0.929)	0.450 (0.781)	0.676 (0.902)
400	0.366 (0.971)	0.699 (0.998)	0.801 (0.908)
800	0.335 (0.957)	0.682 (0.995)	1.073 (0.931)

Phase 1, Task 2 – Bacterial DNA (dsDNA) quantification

Assay sensitivity. The characterization of the MB-QD assay’s sensitivity was carried out via dsDNA quantification. The standard curve constructed by the serial dilution of dsDNA fragments (i.e., 151 bp of PCR amplicon) and the quantification result are presented in Figure 11a and Table 4. The linear quantification range was $2 \times 10^2 - 2 \times 10^7$ with the LOD of 87 gene copies. The dynamic range was 5 orders of magnitude. The lower detection limit of dsDNA in the developed MB-QD assay (i.e., 87 gene copies) presented here is a significant improvement over previously reported assay for the nanoparticle based DNA quantification. For example, Storhoff *et al.* (Storhoff et al., 2004) demonstrated the detection of at least 6×10^6 gene copies of the PCR product from human gDNA using silver amplified gold nanoparticles in DNA microarray format; Eastman *et al.* (Eastman et al., 2006) developed a QD nanobarcode-based magnetic microbead array for gene expression analysis with a sensitivity of $10^4 - 10^6$ gene copies; and Hill *et al.* (Hill et al., 2007) reported that $2.5 \times 10^{-15} \text{ mol L}^{-1}$ (i.e., 7.5×10^4 gene copies) of bacterial gDNA was detected at the bio-bar-code assay using gold nanoparticles. To evaluate the quantification capability of the MB-QD assay, real-time PCR analysis was conducted. The linear range of real-time PCR was $2 \times 10^2 - 2 \times 10^9$ with the LOD of 47 gene copies.

Table 4. Quantification performance of the MB-QD assay. (CV: coefficient of variation)

Parameters	
Dynamic range (gene copies)	$2 \times 10^2 - 2 \times 10^7$
Regression equation	$\text{RFU} = 0.670 \log(\text{gene copies}) - 0.729$
Correlation coefficient (R^2)	0.929
Limit of detection (gene copies)	87
Inter-assay CV (%)	2.01
Intra-assay CV (%)	5.74

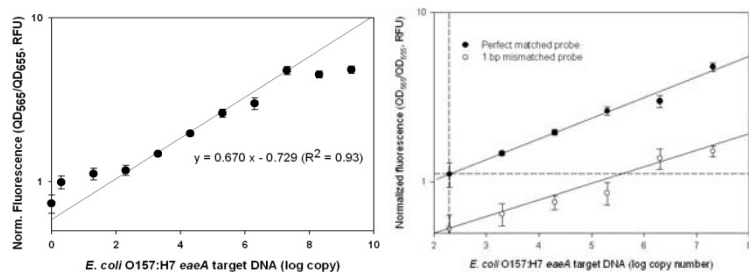


Figure 11. (a) Quantification of *E. coli* O157:H7 *eaeA* target dsDNA in the MB-QDs assay. The normalized fluorescence is plotted against the corresponding *E. coli* O157:H7 *eaeA* gene copy numbers. (b) Assay specificity of the MB-QDs assay.

Assay specificity. The specificity of the MB-QD assay was characterized by varying the amount of PCR amplicon hybridized with both perfectly matched and 1 bp nucleotide mismatched probe DNAs. The specificity result is presented in Figure 11b. By comparing the fluorescence signal, 1 bp mismatched probe DNA was clearly discriminated from the perfectly matched probe DNA. When the 1 bp mismatch was used, the quantification results were observed to be below the LOD (i.e., RFU = 1.17) in the range of $2 \times 10^2 - 2 \times 10^5$ target gene copies. This result demonstrated our developed method is capable of screening and detecting pathogenic bacteria with an excellent selectivity among other non-pathogenic but phylogenetically similar bacteria. Real-time PCR assay (graph not shown) was implemented to validate the specificity of MB-QD assay. In the real-time PCR assay, 1 bp nucleotide mismatched forward primer was adopted to simulate the 1 bp nucleotide mismatch effect. When the 1 bp mismatched primer was used, the limit of quantification increased from 2×10^2 to 2×10^4 and the dynamic range shifted accordingly.

Phase 1, Task 3 - Validation of the assay using *E. coli* O157:H7 bacteria culture

Genomic DNA quantification. In order to demonstrate the assay's capability to perform quantification without the need of amplification, non-amplified genomic DNA of *E. coli* O157:H7 culture was used as the target. Target gDNA with various gene copies were hybridized and the quantification result is shown in Figure 12.

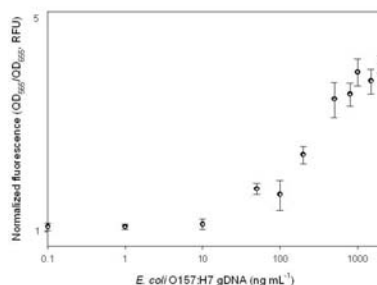


Figure 12. Quantitative detection of *E. coli* O157:H7 using gDNA without amplification.

Comparison with the traditional plate counting method. A standard culture based bacteria quantification method (plate counting) was employed to correlate the DNA-based quantification and conventional bacterial cell counts. The output of the assay, depicted in the y-axis (Figure 13a), is the normalized fluorescence. The serial dilutions of bacterial culture was inoculated on trypticase soy agar plates and incubated at 37°C for 24 hrs. Figure 13b shows the picture taken during the plate counting and the yellow dots (i.e., colony) are bacteria grown on the surface of agar plates. The colonies were counted to determine the number of colony-forming units per mL of culture (CFU/mL).

Gene copy numbers (i.e., a variable of assay) were converted to the number of bacterial cells (CFU mL⁻¹) based on the result of the plate counting method and subsequently depicted in the x-axis. Plate counting method was implemented using active *E. coli* O157:H7 cells and correlated with gene quantification results. 4×10^9 CFU per mL was determined to be equivalent to 2×10^{12} gene copy numbers of the *eaeA* per mL. The dynamic range of the assay was $4 \times 10 - 4 \times 10^5$ CFU mL⁻¹ ($R^2 = 0.980$) with the LOD of 25 CFU mL⁻¹. The infectious dose (> 100 organisms) (Tuttle et al., 1999b; www.cdc.gov/ncidod/eid/vol18no4/00-0218.htm) was indicated by the vertical dashed line in Figure 13a. The minimum infectious dose of *E. coli* O157:H7 was within the range of quantification of the MB-QD assay. In comparison, other studies have shown that their LODs were similar or more than 100 CFU mL⁻¹ (Huang et al., 2008; Mao et al., 2006b; Su & Li, 2004; Xue et al., 2009; Yang et al., 2004), indicating the MB-QD assay has higher sensitivity for the detection of pathogens. Similar techniques have been recently developed and they are based on DNA aptamer or liposome. Bruno *et al.* (Bruno et al., 2009) have developed DNA aptamer based sandwich hybridization approach with magnetic bead and QDs. Zaytseva *et al.* (Zaytseva et al.,

2005) used fluorescent liposome as a reporter for the detection of viral nucleic acids. Even though these developments have demonstrated the integration of the assay with portable devices such as microfluidics, they are still in the early stage of development.

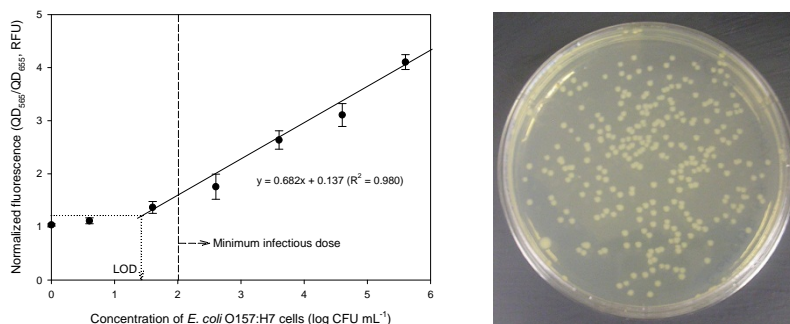


Figure 13. (a) Quantitative detection of *E. coli* O157:H7 using genomic DNA without amplification (y-axis) in comparison to the conventional plate counting methods (x-axis). This technique is able to detect below the minimum infectious limit (100 cells) as indicated by the vertical dashed line. (b) Example of a plate counting method using agar plates. The colonies shown above indicate *E. coli* O157:H7 cultured on trypticase soy agar plates.

We have developed a highly sensitive DNA assay using magnetic and quantum dot nanoparticles for the quantification of pathogenic *E. coli* O157:H7 bacteria in water. The use of QD₅₆₅ for the label of signaling probe DNA resulted in increased photostability and also allowed the assay to be used with a single, short-wavelength excitation source. The new format of QDs configuration (i.e., QD₅₆₅/QD₆₅₅) as both a fluorescence label and an internal standard increased the sensitivity of the assay. This MB-QD assay was able to detect ssDNA and dsDNA fragment up to 890 zeptomolar concentration and 87 gene copies, respectively. The specificity of the assay was also demonstrated via the discrimination of target DNA with 1 bp nucleotide mismatch. Finally the MB-QD assay was able to detect *E. coli* O157:H7 with 25 cells/mL of the detection limit which is below the minimum infectious dose in water. This sensitive nanoparticle based DNA quantification assay is potentially applicable for in-situ monitoring of pathogenic bacteria in the aquatic environment.

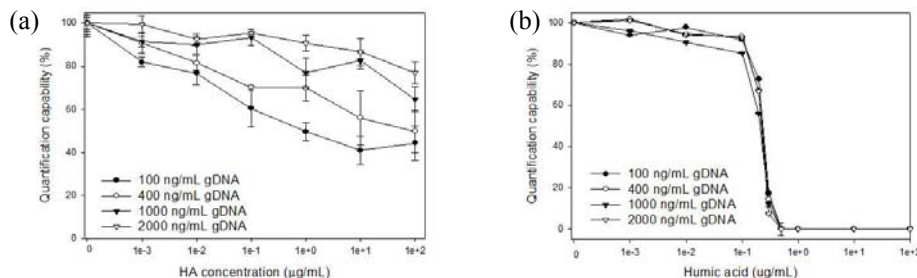


Figure 14. Comparison of the quantification of the *eaeA* gene of *E. coli* O157:H7 by (a) NanoGene and (b) qPCR assays in the presence of various concentrations of humic acids.

Phase 2, Task 1: Effects of common inhibitors from environmental samples on the developed assay.

Inhibition resistance of NanoGene assay to humic acids. The quantification capability (%) of the NanoGene assay was not completely inhibited by the presence of humic acids (Figure 14a). But the quantification capability of qPCR reduced to 0% over 1 µg/mL humic acids, although it maintained 90% at 0.1 µg/mL humic acids (Figure 14b). The output (fluorescence) of NanoGene assay slightly decreased

at the high concentration of humic acids, however it maintained the gene quantification capability of more than 50% at all concentration ranges of humic acids (0.001 - 1000 $\mu\text{g/mL}$) and target gDNA. Note the range of environmental relevant concentration of humic acids is 0.02 - 30 $\mu\text{g/mL}$. Therefore, quantification of raw environmental samples using a qPCR assay may not be plausible because the inhibition is very significant and the result will show no signal at humic acid levels greater than 1 $\mu\text{g/mL}$. In order to further increase the inhibition resistance of NanoGene assay at high humic acid concentrations, we identified the specific mechanisms that are responsible for the inhibition as described in Figure 15.

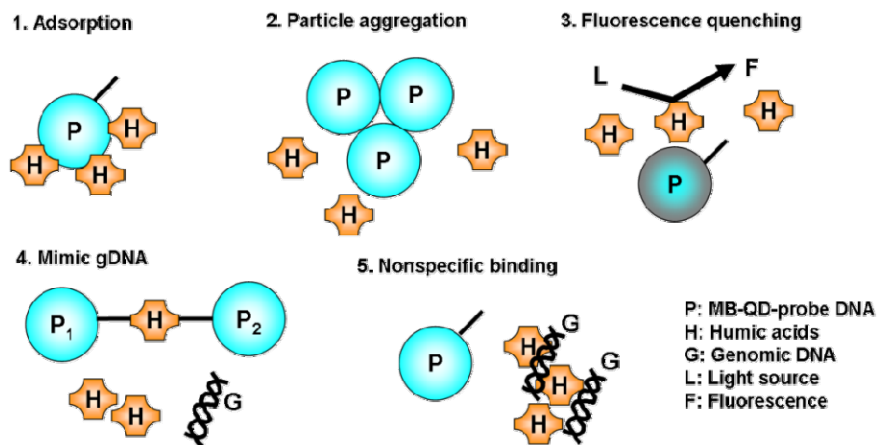


Figure 15. Five hypotheses that describe the possible mechanisms of humic acids-resistance of the NanoGene assay. 1. Adsorption of humic acids on the particle surface, 2. Particle aggregation induced by humic acids, 3. Fluorescence quenching of QDs by humic acids during hybridization, 4. Humic acids mimicking target DNA, 5. Random nonspecific binding between humic acids and target gDNA.

Adsorption of humic acids on the particles. FE-SEM analysis was performed to visualize the interaction of humic acids with the components (MB-QD) of the NanoGene assay. As shown in Figure 16, the humic molecules were observed as a coagulated pattern and resided on the surface of MB-QD at higher concentrations (100 and 1000 $\mu\text{g/mL}$). It was reported that the humic molecules can be held together in supramolecular conformations by weak hydrophobic bonds at neutral and alkaline pH (Österberg, 1993). Since humic substances have both hydrophobic and hydrophilic functional groups (i.e., amphiphilic), they can form aggregates which have the hydrophobic interior with the highly charged exterior (Wershaw, 1993) and reside on the particle surface. However, the amount of information that can be derived from the image pertaining to the interactions (e.g., quantitative data of adsorption) between humic acids and MB-QD is limited. Therefore, we performed the following experiment in order to measure the adsorption of humic acids on the surface of particles.

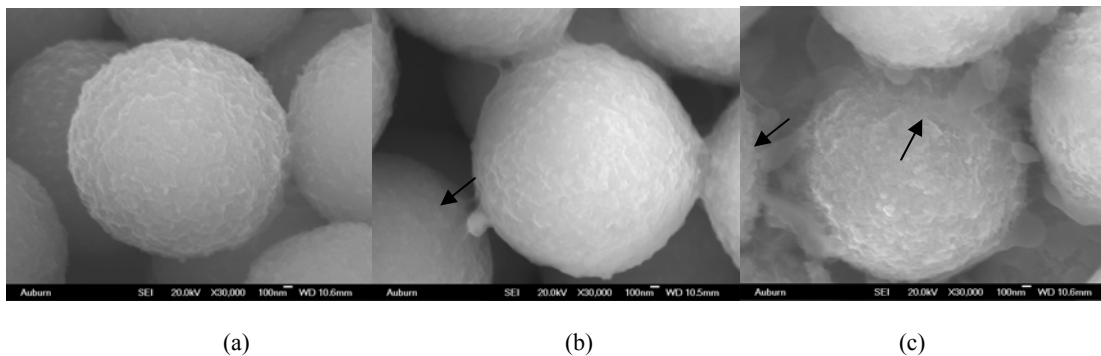


Figure 16. FE-SEM image of MB-QDs (a) without humic acids, (b) with 100 $\mu\text{g/mL}$ humic acids and (c) 1000 $\mu\text{g/mL}$ humic acids. The locations of putative humic molecules are indicated by the arrows. The scale bar represents 100 nm.

During DNA hybridization, humic acids may be adsorbed on the components of the NanoGene assay. Therefore, it causes the interruption of DNA hybridization and further gene quantification of the assay. Various amounts of humic acids were incubated with the particles (i.e., MB, MB-QD, and MB-QD-DNA) under hybridization condition to examine the adsorption of humic acids. Table 4 shows the amounts of adsorbed humic acids on the particles. No humic acids were adsorbed on the particles at lower concentrations (< 10 µg/mL of reaction), and a slight adsorption occurred at higher concentrations (10 - 1000 µg/mL). To determine the degree of humic acids adsorption at higher concentrations, the initial amount (µg/mL) and remaining (the initial amount – the adsorbed amount) portion of humic acids were compared using the paired *t* test. All tests were non-significant ($P > 0.01$, $n = 3$). In other words, there was no significant adsorption of humic acids throughout all the concentrations applied (0.1 - 1000 µg/mL) on all particles tested: MB, MB-QD and MB-QD-DNA particle complex.

Table 4. The adsorption of humic acids on the particle of NanoGene assay: (a) MB, (b) MB - QD, and (c) MB - QD - DNA.

Humic acids (µg/mL)	MB		MB - QD		MB - QD - DNA	
	Adsorbed (µg HA/mL/particle)	<i>P</i> - value	Adsorbed (µg HA/mL/particle)	<i>P</i> - value	Adsorbed (µg HA/mL/particle)	<i>P</i> - value
0	0.0	-	0.0	-	0.0	-
0.1	0.0	-	0.0	-	0.0	-
1	0.0	-	0.0	-	0.0	-
10	0.34 ± 0.31	0.2244	0.05 ± 0.08	0.4226	0.0	-
100	4.24 ± 3.26	0.1538	2.31 ± 2.07	0.2018	3.34 ± 4.20	0.2811
1000	21.98 ± 7.67	0.0205	22.66 ± 21.77	0.2138	31.49 ± 5.57	0.0192

Particle aggregation: surface charge and particle size distribution. We hypothesized the particle complexes may aggregate in the presence of humic acids, as humic acids have various functional groups. In order to investigate particle aggregation, particle size distribution was determined using dynamic light scattering spectroscopy. Figure 17a shows the hydrodynamic diameter measurement of the particles (i.e., MB, MB-QD, and MB-QD-DNA). The diameter of particles (Figure 17a) was approximately 4 µm regardless of various amount of humic acids and the particle combinations. The particle size was uniform and less than 5.6 µm (depicted by the line in Figure 17a), which is twice of MB's diameter. The result showed that no significant particle aggregation was induced by humic acids.

The stability of particle dispersion in the presence of humic acids was also investigated. The stability of particles in solution decreases as the particle aggregation occurs due to charge neutralization. Surface charge values $> \pm 30$ mV indicates well dispersed particles with no aggregation (Zeta potential of colloids in water and waste water). In the absence of humic acids (negative control), the surface charges of particle conjugates were around - 60 mV. As shown in Figure 17b, the surface charges of all three particle conjugates were approximately - 60 mV over the range (0.001 - 1000 µg/mL) of humic acids used in the experiment. This meant no aggregation of particles occurred in the presence of humic acids. In other words, the humic acids do not function as the bridge between particles for further coagulation. In addition, the pH was maintained at 7.4 without being affected by the amount of humic acids.

Fluorescence quenching of quantum dots by humic acids. To examine the fluorescence quenching effect of humic acids, the fluorescence of MB-QD in the presence of various humic acids was measured. The relative fluorescence intensities of samples were calculated based on the assumption that the initial fluorescence intensity of MB-QD in the absence of humic acids was 100%. As shown in Figure 18a, the fluorescence intensity of MB-QD was sustained at 80% of its initial value when exposed to humic acids concentration range from 0.001 to 10 µg/mL. However, at the higher concentration of humic acids (100 and 1000 µg/mL), the fluorescence decreased to 40%. One way ANOVA test indicated that the relative

fluorescence (%) at higher concentrations of humic acids was significantly different ($P < 0.05$, $n = 16$). In addition, the probability of collisional encounters between humic acids and particles increases with higher concentration of humic acids. The collision between humic acids and MB-QD may generate the loss of excitation energy in the form of heat instead of photon emission (fluorescence), resulting in the decrease of the MB-QD fluorescence. This loss in fluorescence is known as collisional (or dynamic) quenching. The collisional quenching is the interaction of transient excited state and does not affect the absorption spectrum (Lakowicz, 1991; Zipper et al., 2003).

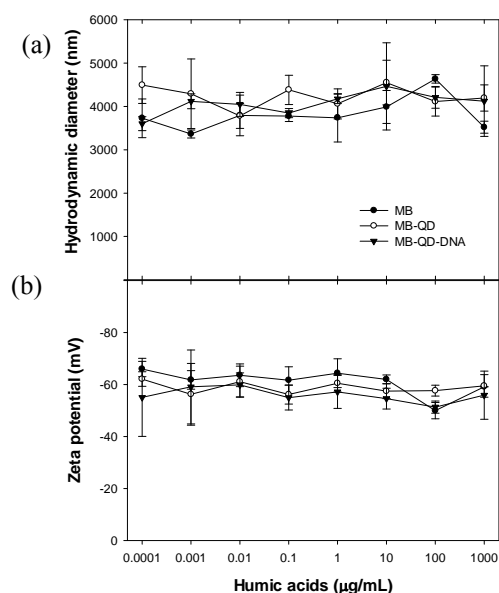


Figure 17. Particle aggregation effect by humic acids. (a) Hydrodynamic diameters and (b) zeta potential (surface charge) distribution of the particle complex of the NanoGene assay (MB, MB - QD, and MB - QD - DNA) in the presence of varying humic acids.

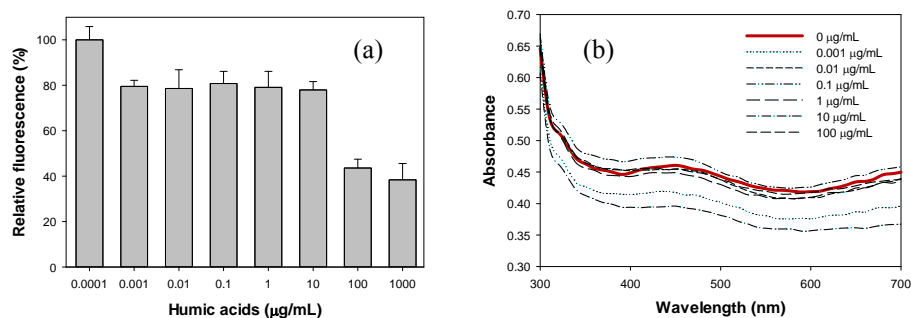


Figure 18. Fluorescence quenching effects by humic acids. (a) Collisional quenching: fluorescence intensity of MB-QD₆₅₅ with various concentrations of humic acids. (b) Static quenching: UV-vis absorbance spectra of MB-QD₆₅₅ incubated with varying humic acids (0.001 - 1000 $\mu\text{g/mL}$).

On the other hand, the interaction of the fluorophore with quencher can form a non-fluorescent complex, resulting in static quenching. Since the complex may have a different spectrum from the fluorophore, the change of absorption spectra would indicate static quenching (Lakowicz, 1991). As a result of UV-vis absorbance scanning, no peak shift was observed in the absorption spectrum of MB-QD incubated with

various concentrations of humic acids relative to the absence of humic acids (Figure 18b). The spectra of negative control (no humic acids), which is depicted as a thick line in Figure 18b, showed a similar pattern for all tested samples over the entire concentration range of humic acids. One way ANOVA was used to test the significance of the absorbance peak shift. The ANOVA result showed no significant difference ($P > 0.05$, $n = 7$) between the wavelengths for the absorbance peak for all the samples tested. In other words, the presence of humic acids did not affect the optical characteristic of MB - QD by creating other complexes which would be represented by peaks in absorption spectra. This indicated that no static quenching occurred between humic acids and particle complex.

Humic acids mimicking target genomic DNA. The possibility of humic acids mimicking target gDNA was examined by incubating the particles with humic acids instead of target gDNA. Figure 19 shows the normalized fluorescence obtained by the hybridization of humic acids with the probe DNAs. The DNA hybridization in the NanoGene assay was carried out using humic acids in place of target gDNA. In the event that the humic acids mimic target gDNA, fluorescence (QD_{565}/QD_{655}) will be detected as a result of the hybridization between humic acids and probe/signaling probe DNAs. However, all the signals (Figure 19) were lower than the background level (1.17 RFU) and it is the limit of detection of the NanoGene assay (Kim, 2010). All the signals, except 1000 $\mu\text{g/mL}$ ($P > 0.05$, $n = 7$), were significantly different from the limit of detection ($P < 0.05$, $n = 7$, Student's t -test). Thus, the humic acids except 1000 $\mu\text{g/mL}$ did not mimic the target gDNA and no hybridization would occur between humic acids and probe/signaling DNAs.

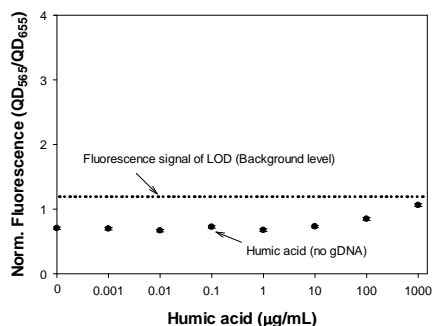


Figure 19. Mimicking effect of humic acids. The fluorescence, which is lower than background fluorescence, indicate that the mimicking effect of humic acids like gDNA is not significant. That means no humic acids were bound to probe and signaling probe DNAs conjugated with MB-QD₆₅₅ and QD₅₆₅, respectively.

Nonspecific binding between humic acids and target genomic DNA. An adsorption test was used to investigate the degree of nonspecific binding between humic acids and target gDNA. Figure 20a shows the adsorption isotherm of target gDNA on the surface of humic acids encapsulated MB. C_s on the y-axis indicates the mass of target gDNA over the mass of humic acids ($\text{ng}/\mu\text{g}$) and C_e on the x-axis indicates the concentration of target gDNA added ($\text{ng}/\mu\text{L}$), where the volume is the reaction volume of the assay. The adsorbed amount of target gDNA per unit amount of humic acids on MBs increased initially and reached a plateau value ($5.5 \text{ ng}/\mu\text{g}$). The adsorption isotherm of target gDNA onto the humic acids coated on MBs was fitted using the Langmuir equation (eq. 1):

$$q = \frac{q_{\max} K_A C}{1 + K_A C} \quad (\text{eq. 1})$$

where q = the adsorbed target gDNA concentration ($\text{ng gDNA}/\mu\text{g}$ humic acids on MBs), q_{\max} = the maximum concentration of adsorbed target gDNA, K_A = constant, and C = the residual concentration of target gDNA in solution. The constants K_A and q_{\max} were evaluated from the linearized form represented by the eq. 2:

$$\frac{1}{q} = \frac{1}{q_{\max}} \frac{1}{K_A C} + \frac{1}{q_{\max}} \quad (\text{eq. 2})$$

A plot of $1/q$ against $1/C$ gives a straight line with a slope of $1/(q_{\max} K_A)$ and an intercept of $1/q_{\max}$. The correlation coefficient (R^2) describing the goodness of fit to the linearized Langmuir model was 0.99. The q_{\max} and K_A were 5.71 (ng/ μ g) and 1.50×10^{-2} , respectively. This means a maximum of 5.71 ng of gDNA can be adsorbed by 1 μ g of humic acids (bounded on MBs).

The binding between target gDNA and humic acids is likely due to passive adsorption. Passive adsorption can occur via the combination of both electrostatic and hydrophobic interactions. Humic acids have various hydrophilic functional groups as well as hydrophobic centers. Similarly, gDNA has hydrophilic groups such as amine and phosphate as well as hydrophobic impurities such as proteins. Since humic acids contain organic groups with variable aromaticity, the hydrophobic part of humic acids may attract the hydrophobic impurities of gDNA. In addition, the phenolic groups of humic substances can also denature biological molecules by forming amide bonds or oxidizing to form a quinone which covalently bonds to DNA or proteins (Alm, 2000; Young, 1993). These various functional sites may induce the nonspecific binding between gDNA and humic acids.

To further examine the nonspecific binding between gDNA and humic acids, additional quantification experiment (NanoGene assay) was performed with test samples containing varying amounts of gDNA and the same amount of humic acids (1 μ g/ μ L: the highest humic acids concentration (1000 μ g/mL) in the previous graphs). As shown in Figure 20b, as the amount of gDNA increases, the quantification capability (percentage) of the NanoGene assay also increases. This observation is consistent with the hypothesis that humic acids compete with the NanoGene assay components to bind with the gDNA via non-specific binding. In addition, the results showed that the humic acids were able to bind a larger absolute amount, but lower overall percentage, of the gDNA at a higher gDNA concentration. Therefore it is indicative that the binding efficiency between humic acids and gDNA is on the same order of magnitude as that between components of NanoGene assay (MB-QDs) and gDNA.

In order to mitigate inhibition via non-specific binding between humic acids and gDNA, the binding efficiency between MB-QDs and gDNA can be increased via increasing the concentration of MB-QDs. Another mitigation strategy can involve the use of the additional interceptor molecules (e.g., polymers), which can preferably bind with humic acids, prior to the quantification. The interceptor molecule will be chosen such that it will not bind to the MB-QDs. In this way, the humic acids in the sample will be bound to the interceptor molecule and therefore unable to further bind to the target gDNA. These methods are reasonable propositions because the binding efficiency between gDNA and the competing humic acids and MB-QDs are in the same order of magnitude. They will be investigated in our follow up studies.

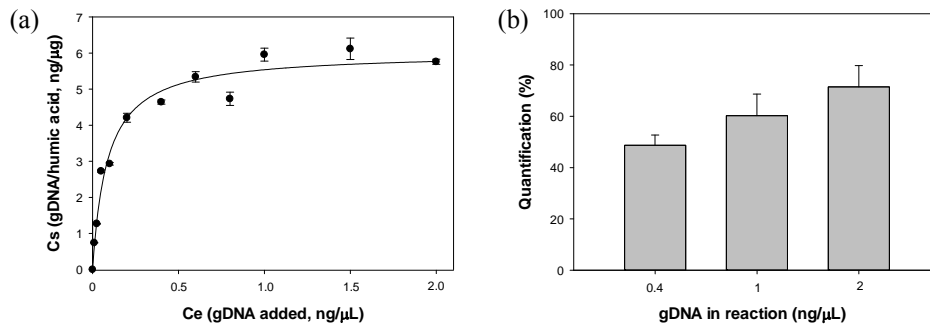


Figure 20. Nonspecific binding of gDNA and humic acids via passive adsorption. (a) The adsorption isotherm of gDNA on the humic acids-encapsulated MB. (b) Relative gene quantity that are obtained as a function of gDNA (0.4, 1, 2 ng/ μ L).

Phase 2, Task 2: Compatibility of key assay parameters for in-situ field application

Specificity of assay. The sensitivity of the assay has been previously demonstrated for both ssDNA and dsDNA (Kim, 2010). In this study, the specificity of the MB-QD assay was examined by using the gDNA mixture of both *E. coli* O157:H7 and mixed microbial cultures in activated sludge. The result is presented in Figure 21a. The gDNA of activated sludge was used as a negative control and it had a negligible fluorescence signal.

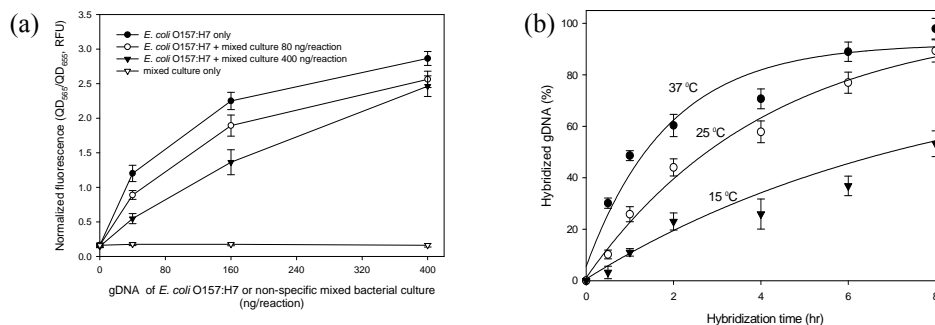


Figure 21. (a) Specificity of the MB-QD assay. The ability of assay that can specifically detect *eaeA* gene was demonstrated in the presence of non-specific gDNA in the hybridization reaction. The signal and error bars represent mean and standard deviation based on five measurements of fluorescence. (b) The effect of various temperatures on the DNA hybridization kinetics.

In other words, the MB-QD-probe did not capture any non-target gDNA during hybridization. Various amounts of non-target gDNA (0, 80, 400 ng/reaction) were mixed with the target gDNA (0, 40, 160, 400 ng/reaction) to simulate real environmental condition. The assay output decreased about 50% of initial fluorescence signal as the amount of non-target gDNA increased from 0 to 160 ng/reaction. However, the assay output was almost recovered at the 400 ng of target gDNA per reaction. It seems that the hybridization kinetics of target gDNA in the presence of nonspecific target may affect the quantification output of assay.

The effect of temperature and mixing condition. In order to examine the suitability of the MB-QD assay for on-site measurement without the benefit of an incubator, kinetic experiments were performed with the target gDNA at three different temperatures: 15, 25 (i.e., ambient condition), and 37 °C. The three temperatures were selected to represent ambient temperature in different regions. Figure 21b shows the hybridized amount of gDNA at various temperatures for 8 hours. The y-axis of Figure 21b indicated the relative hybridized amount of gDNA (%). In order to better visualize the kinetic result, the concentration unit of hybridized gDNA was converted to the percentile unit. The amount of hybridized gDNA at 37 °C and 8 h was assumed to be the maximum possible for hybridization, since it was shown as the plateau (i.e., reaching the equilibrium) in the original kinetic plot. Thus the gDNA value at 37 °C and 8 h was assumed to represent 100% hybridization. Although the higher temperature accelerates the gDNA hybridization process, the gDNA hybridization could also be achieved at the ambient temperature or lower. For example, at the temperature of 25 °C, 3 h was required to achieve 50% hybridization. At 15 °C, 50% hybridization was achieved after 8 h incubation.

The hybridization rate constants measured from the linear regression analysis using the second-order kinetic model are shown in Table 5. Since the target concentration is another rate-limiting factor in a hybridization reaction based on the second order kinetics, the hybridization efficiency at ambient temperature can be increased by using a higher amount of target gDNA. This kinetic result indicates that hybridization incubator may not be required for the MB-QD assay as DNA hybridization can also be achieved at ambient temperature.

Table 5. The hybridization rate constants (k_h) and the correlation co-efficient (R^2) measured by the linear regression analysis based on the second order kinetics model.

Temperature (°C)	$k_h (\times 10^6 \text{ M}^{-1} \text{ h}^{-1})$	Second-order kinetics	R^2
25	0.140		0.991
37	0.571		0.943
42	0.643		0.964

Thorough mixing is also beneficial for the successful DNA hybridization (Figure 22). Compared to the amount of hybridization achieved via continuous agitation for 8 h, 20% hybridization was achieved without agitation and 50% of gDNA was hybridized using pulsed agitation.

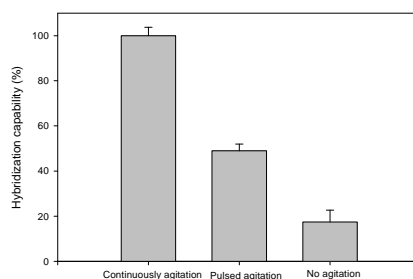


Figure 22. The effect of mechanical strength agitation on the DNA hybridization efficiency.

It is interesting to note that 50% hybridization is achieved with 10 minutes agitation every 2 h for a total of 8 h. This finding can be beneficial for actual on-site application where the agitation device is not available.

Stability of reagents. In order to observe the stability of reagents used for DNA hybridization, the stability of covalent bonding and the photobleaching effect of labels were monitored at two temperature conditions (ambient and 4 °C) for 30 days. Figure 23a shows the photobleaching effect of QD₆₅₅ at two different storage temperatures over time for 30 days. After 10 days, the fluorescence of the QDs was at 60% and 40% of the initial value at 4 °C and ambient temperature, respectively. The remained intensity subsequently sustained for the last 20 days. The covalent bond between MB and QD₆₅₅ was observed to be stable for 30 days. Its fluorescence intensity remained over 80% throughout the experiment (Figure 23b). The remaining fluorescence (%) in the y-axis of Figure 23b was obtained based on the subtraction of the fluorescence loss by photobleaching (Figure 23a) from the total fluorescence loss. It is interesting to note that temperature is not an important factor for the stability of the covalent bonding. The stability of covalent bonding is more critical for the assay performance than the photobleaching of QDs. If the covalent bond between MB and QDs is disrupted, the magnetic separation may not yield the QD-DNA hybrids. The incomplete separation of hybrids will result in poor quantification by the assay.

Based on our findings, the covalent bonds between particle-particle is stable (i.e., maintain at least 80% of the fluorescence) at ambient temperature for a month. The fluorescence intensity of the QD label decreased due to natural photobleaching; however, it is still acceptable to use QDs as photostable labels for storage duration of a minimum 10 days. Therefore, the reagents of the MB-QD assay (i.e., particle complex and particle-DNA conjugate) can be prepared ahead of time and stored for a minimum of 10 days without the need of refrigeration. Producing all of the reagents for the MB-QD assay requires ~ 6 h. The MB-QD assay requires 8 h to perform for DNA hybridization and detection at 25 and 37 °C. In total, reagent synthesis, probe preparation and detection require 1 d. It should be noted that the particle reagents can be stored at 4 °C for weeks at a time, the total assay time will be decreased to 8 h.

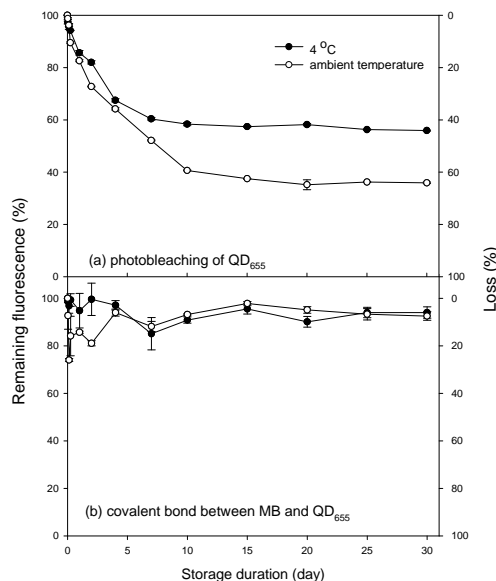


Figure 23. Stability of reagents: (a) photobleaching effect of QD₆₅₅ and (b) covalent bond between MB and QD₆₅₅ at both ambient and refrigeration (4 °C) temperature. The change of fluorescence (y-axis) observed for the storage duration (x-axis) is presented in percentage relative to initial fluorescence value.

Assay interference test. The applicability of the MB-QD assay to environmental samples was demonstrated by its inhibitors resistance. The inhibitory change of gene quantification capability for both MB-QD and real-time PCR assays targeting gDNAs in the presence of four inhibitors was shown in Figure 24. Here, the pure target gDNA was spiked with four inhibitors to simulate environmentally contaminated samples before purification. The incubation of four inhibitors without gDNA (i.e., negative control) resulted in no significant fluorescence signal. It indicated that the inhibitors did not behave like the target DNA which hybridizes with probe DNA. In other words, the inhibitors did not mimic gDNA as target material in the MB-QD assay.

(1) Humic acids. The effect of various amounts of humic acids on the MB-QD assay was observed. Due to the ubiquity and abundance of humic acids in the environment, they are often co-extracted along with the nucleic acids from soil, sediment, and water samples. Humic acids can be partially removed by time-consuming purification techniques, and the complete removal of humic acids from the sample is nearly impossible. During the extensive purification technique of humic acids, DNA loss is also common. The presence of humic acids has drastically decreased the quantification efficiency of real-time PCR assays. We found that the MB-QD assay is resistant to humic acids (Figure 24a). Even though the output (fluorescence) of the MB-QD assay slightly decreased (from 100% to 80%) at the high concentration of humic acids (100 ng per μL reaction), it maintained the linearity of gene quantification at all concentration ranges of humic acids. In comparison to the presented MB-QD assay, the real-time PCR assay was completely inhibited by humic acids at more than 1 ng per μL reaction although it showed no inhibition (i.e., 100% of output) in the low concentration range of humic acids (i.e., 0.001-0.1 ng μL^{-1} of reaction). The inhibition mechanisms of humic acids in real-time PCR assay may be due to the inhibited *Taq* polymerase by humic acids and/or complexation of humic acids with Mg^{2+} ions. Mg^{2+} are vital cofactor for *Taq* polymerase in the PCR reaction. As compared to the real-time PCR assay, the MB-QD assay maintained stable signals at the corresponding concentration of humic acids. More than 90% of the quantification capability was maintained without the drastic change of assay output. Overall, the MB-QD assay is more suitable for the environmental samples that contain high levels of humic acids than the real-time PCR assay.

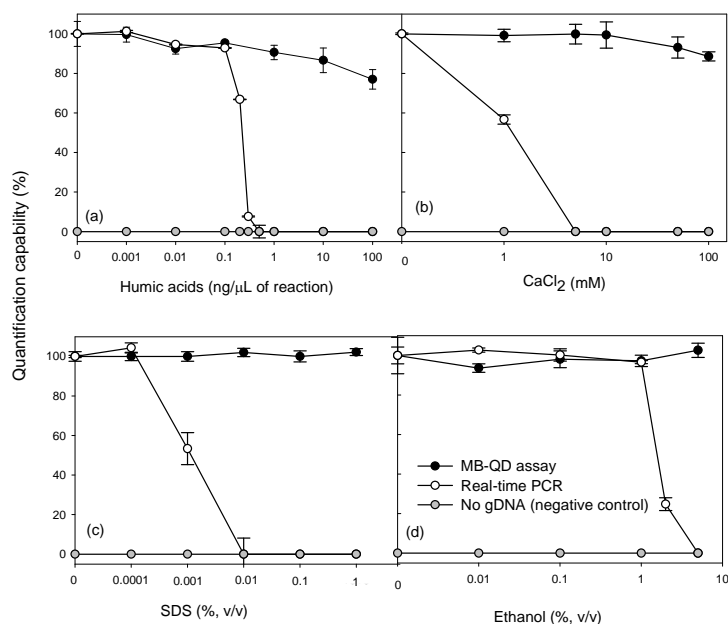


Figure 24. The inhibitory change of gene quantification capability for both MB-QD assay and real-time PCR assay in the presence of various inhibitors: humic acids, CaCl₂, SDS, and ethanol. Gene quantifications targeting *ea*A gene in pure *E. coli* O157:H7 bacterial gDNA were performed by measuring the normalized fluorescence (i.e., QD₅₆₅/QD₆₅₅) and the gene copies for MB-QD assay and real-time assay, respectively.

(2) *Multivalent ions.* Calcium is one of the abundant cations in the environment because of its natural occurrence in the earth's crust. The river in lime areas may contain amounts of Ca²⁺ as high as 100 ppm (i.e., 2.5 mM). Since there is a possibility of Ca²⁺ to be carried over from environmental samples to the extracted gDNA, the inhibitory effect of Ca²⁺ was examined for both the MB-QD assay and real-time PCR assay. The output of the MB-QD assay was found to be stable for the entire range of Ca²⁺ concentration tested (i.e., 1-100 mM). This indicates that there is no major inhibitive effect of amplification reaction failed (i.e., zero signal) at a concentration of more than 5 mM of Ca²⁺ and only 60% of the quantification was achieved at 1 mM of Ca²⁺. This is mainly due to the competitive interaction of Ca²⁺ with Mg²⁺, which is the vital cofactor for *Taq* polymerase in PCR reactions. Recent literature also indicated that the high concentration of divalent cations such as Ca²⁺ can induce a decrease (i.e., bleaching) in the fluorescence values of organic fluorophore dye. Hybridization based MB-QD assay recruit neither polymerase nor organic fluorophores. Thus, the MB-QD assay is more suitable than real-time PCR for the samples from an environment with large quantities of multivalent cations.

(3) *SDS and ethanol.* The DNA extraction step is necessary prior to the MB-QD assay. Residual amount of reagents used for DNA extraction may remain in the gDNA and may impair gene quantification. In order to examine the effect of residual reagents on the gene quantification, varying amounts of SDS (surfactant) and ethanol were added to the hybridization reaction. The assay was severely inhibited by the presence of Ca²⁺ for the MB-QD assay. In comparison, the real-time PCR quantification output of the MB-QD assay was consistently maintained without any inhibition over the range of SDS (i.e., 0.001-1%, v/v) used (Figure 24c). However, the real-time PCR assay was severely inhibited by SDS. The amplification reaction completely failed at over 0.01% SDS concentration. Even the lowest amount of SDS (i.e., 0.001%) can cause 50% inhibition of the real-time PCR assay. The Figure 24d shows that the MB-QD assay continued to function with the

presence of increasing ethanol concentration. In contrast, the real-time PCR assay was completely inhibited by 5% ethanol and 60% inhibited by 2% ethanol. No inhibition was observed at the lower range of ethanol concentration (0.01-1%). The results indicated that the MB-QD assay can be used directly on gDNA extracted from environmental sample without further purification steps.

Genomic DNA denaturation. In order to develop a simple DNA preparation that allows in-situ DNA preparation by bypassing tedious gDNA extraction, various denaturation processes have been applied for gDNA. The optimum denaturation process will be straightforwardly used for in-situ DNA preparation that is currently in progress.

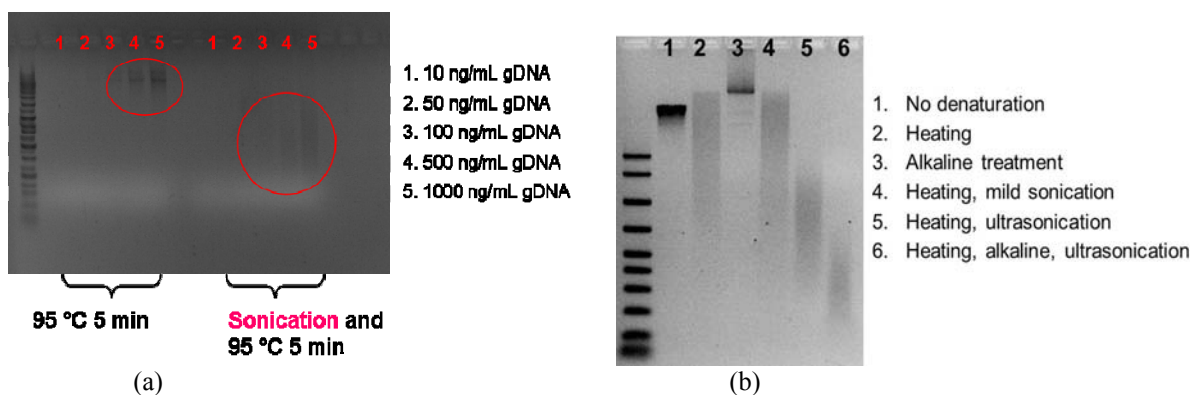


Figure 25. (a) Effectiveness of physical disruption (ultrasonication) in the denaturation of genomic DNA; (b) Optimization of gDNA denaturation among heating, alkaline treatment, and sonication in the NanoGene assay.

Figure 25a describes the efficiency of physical disruption in the fragmentation of DNA. Using gel electrophoresis of genomic DNA, we are able to demonstrate the successful fragmentation of DNA after sonication as shown on the right-hand side of the gel picture. The bands represent various sizes of DNA fragments (several hundred bp to several thousand bp) after denaturation, while the band on the left hand side represents intact gDNA (over 10,000 bp). In the result presented in Figure 25a, we were able to scrutinize the efficiency of mechanical treatment for the manipulation of gDNA. We will investigate the mechanical treatment by comparing to that of extracted gDNA as a target of the assay. A particular challenge is associated with the difficulty of microbial cell wall lysis. In contrast to mammalian cell, the microbial cell has a rigid cell wall exterior to the cell membrane. We will also test chemical addition such as lysozyme, pH buffer, and surfactant during physical disruption of cells to increase the efficiency of using cell crude extract. In the Figure 25b, the range and intensity of smeared bands, which indicated the fragmented gDNA, present the efficiency of each denaturation treatment: lane 1, 100 bp ladder; lane 2, no denaturation (negative control); lane 3, heating; lane 4, alkaline treatment; lane 5, heating and mild sonication; lane 6, heating and ultrasonic treatment; lane 7, heating, alkaline and ultrasonic treatments. As a result, the combination of heating, alkaline, and ultrasonic treatment generated the most smeared bands (lane 7) in the gel, indicating the best fragmentation of gDNA.

Phase 2, Task 3: Preliminary experiments for a microfluidic NanoGene assay

The microfluidic NanoGene assay is being developed for pathogen detection in water systems. A magnetic bead and quantum dot nanoparticle based NanoGene assay has been proved (Kim et al., 2011a; Kim et al., 2011b) for a sensitive gene quantification that is robust and specific in environmental samples. In order to further develop the NanoGene assay in a portable, in-situ capable system, a microfluidic

platform has been applied. The ability to mix and hybridize the nanoparticles within a microfluidic chip and hybridization buffer composition, flow rate, and residence time have been optimized. Parameters determined during component optimization will be used to begin incorporating the microfluidic NanoGene assay into a portable, in-situ detection system (Phase 3).

Prototype setup of a microfluidic NanoGene assay: In order to incorporate the developed NanoGene assay into a microfluidic format, commercial off-the-shelf components were selected for the prototype setup for proof-of-concept purposes. These components included a rhombic chamber chip, Neodymium magnets, miniature peristaltic pumps, and a variable DC power supply. The commercial off-the-shelf microfluidic chip selected for the purpose was the Rhombic Chamber Chip with a volume of 120 μL (Microfluidic ChipShop). Strong rare earth Neodymium (NdFeB) magnets (K&J Magnetics) were placed over the chip to act as an inline magnetic trap. The reagents were injected into the chip via Dolomite Miniature Peristaltic Pumps. The miniature peristaltic pumps were found to be operational between 5 to 27 $\mu\text{L}/\text{min}$. The flow rates of the pump were controlled via Mastech HY1803D Variable DC Power Supply. The actual experimental has been shown in Figure 26.

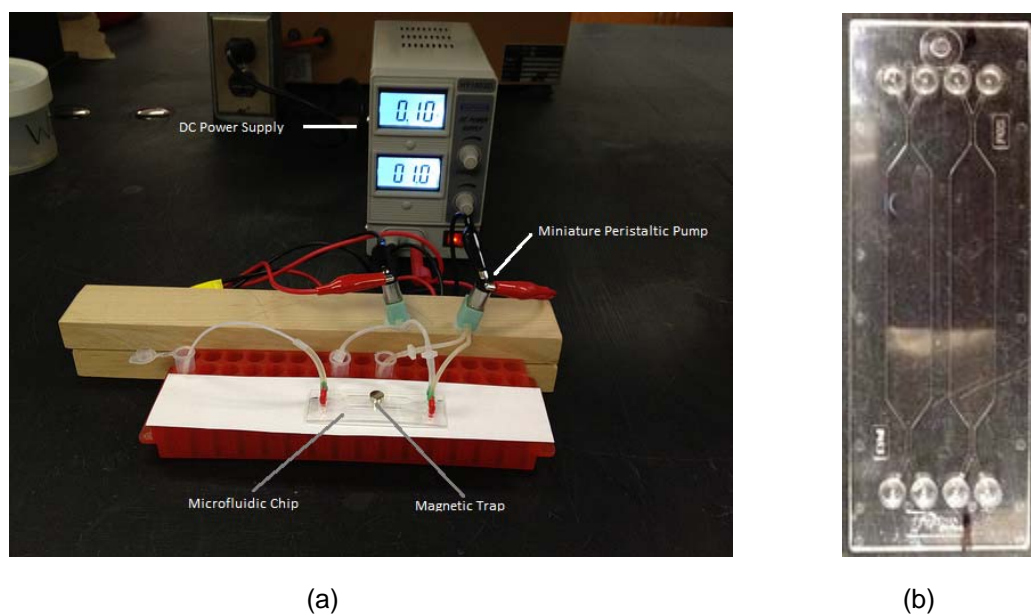


Figure 26. (a) Experimental set-up for a microfluidic NanoGene assay (power supply, miniature peristaltic pumps, microfluidic chip, magnetic trap); (b) Rhombic Chamber Microfluidic Chip

Optimization of Hybridization Buffer Components: In order to optimize the buffer composition for microfluidic hybridization, five hybridization buffers were tested. The first buffer that applied was 50% DIG Easy hybridization buffer. This combination was selected to be a close representation of the buffer used for the well-plate NanoGene assay. However a number of bubbles were created and persisted in the chip when the buffer was passed through the chip at a flow rate of 9 $\mu\text{L}/\text{min}$ for 30 min (Figure 27a). The presence of bubbles in the microfluidics can disrupt the physical contact between particles and DNA during DNA hybridization in the chip.

Therefore, other hybridization buffers were applied to mitigate the bubble formation in the chip by controlling the amount of surfactant in the buffer. The customized buffer consisted of a combination of SSC (saline-sodium citrate), BSA (bovine serum albumin), and SDS (Sodium dodecyl sulfate). SSC provides the salinity as well as the pH buffering capacity as a salt. BSA, as a eukaryotic protein, prohibits a nonspecific binding and SDS is an anionic surfactant that helps to make a better dispersion of components. The composition of the remaining buffers included: 0.01% BSA in 10 \times SSC (Figure 27b),

0.01% BSA and 0.05% SDS in 10× SSC (Figure 27c), 0.01% BSA and 0.10% SDS in 10× SSC (Figure 27d), and 0.01% BSA and 0.20% SDS in 10× SSC (Figure 27e). The persistence of bubbles created by each buffer in the microfluidic chip was observed for 30 min (9 μ L/min) and presented in Figure 27. No bubbles were created with four hybridization buffers applied. Because bubbles would be detrimental to the hybridization ability, it was determined that the original hybridization buffer (50% DIG Easy hybridization buffer) that was used for NanoGene assay, was not optimal for microfluidic DNA hybridization.

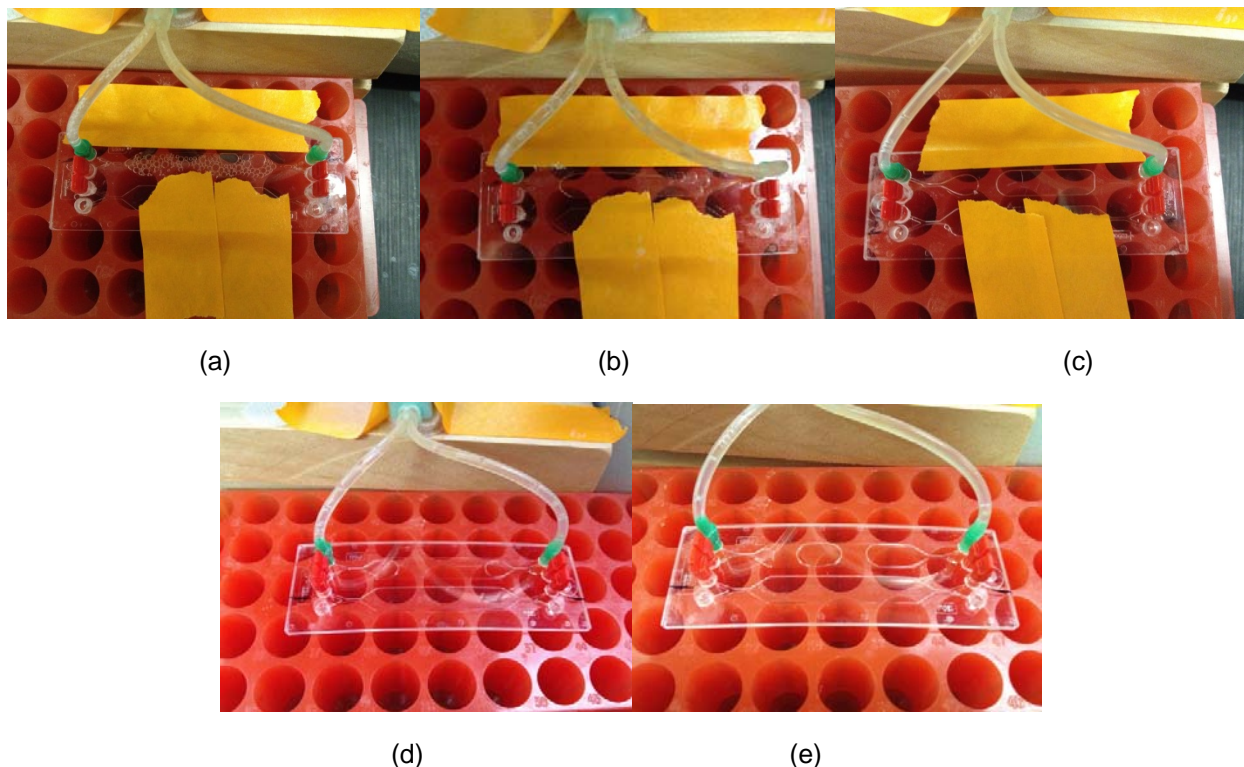


Figure 27. Observation of bubble formation in various hybridization buffers at 9 μ L/min for 30 min. (a) 50% DIG Easy hybridization buffer and 50% deionized water; (b) 0.01% BSA in 10x SSC; (c) 0.01% BSA and 0.05% SDS in 10x SSC; (d) 0.01% BSA and 0.10% SDS in 10x SSC; (e) 0.01% BSA and 0.20% SDS in 10x SSC.

To test the performance ability of new customized hybridization buffers, NanoGene assay was conducted with all five buffers using the traditional well-plate method. These hybridization results can be seen in Figure 28. As is evident, the 0.01% BSA and 0.10% SDS in 10× SSC and 0.01% BSA and 0.20% SDS in 10× SSC buffers performed best in the well-plate method (Figure 28a). Because they did not form bubbles in the microfluidic chip (Figure 27d and e) and they performed well in the well-plate based DNA hybridization (Figure 28a), these two buffers were selected for following testing as potential hybridization buffers for the microfluidic method.

In order to choose the optimal buffer from two selected buffers (0.10% SDS and 0.20% SDS), hybridization was conducted at various flow rates in the microfluidic chip (60 min retention time, 10^{-12} mol/L ssDNA). Because of its superior hybridization performance of 0.10% SDS at all flow rate applied (Figure 28b), 0.10% SDS was selected as the optimum composition for the hybridization buffer to be used in the chip.

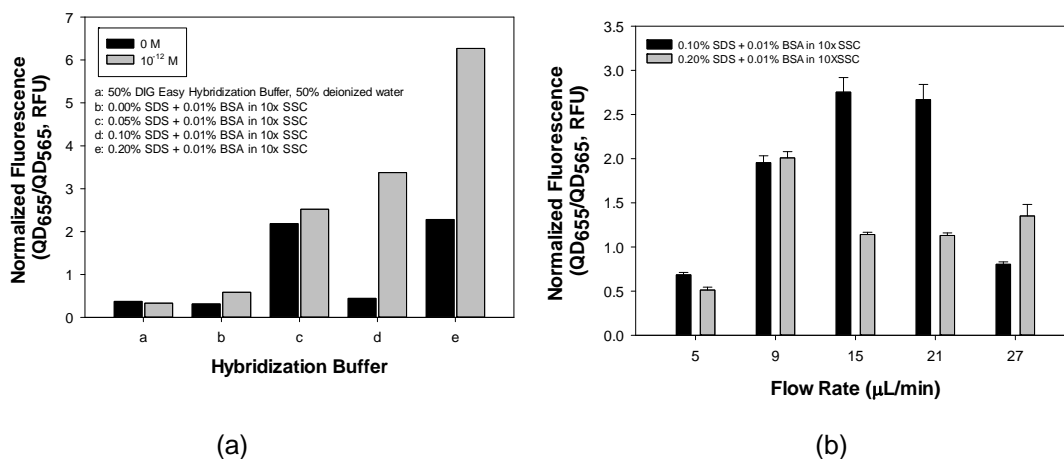


Figure 28. (a) Hybridization results with five applied hybridization buffers (well-plate method) (b) Hybridization results with two buffers selected from Figure 28a under various flow rate in microfluidic format (retention time=60 minutes, 10^{-12} mol/L ssDNA used)

Optimization of Flow Rate and Retention Time: In order to optimize flow rate (retention time) for hybridization, the microfluidic NanoGene assay was performed at flow rates of 5, 9, 15, and 21 $\mu\text{L}/\text{min}$ at retention times of 0, 2.5, 5, 10, 20, 30, and 45 minutes. The retention times indicated the amount of time the fluid was circulated through the chip. Since the volume of the tubing is negligible, the whole circulation time was considered as the retention time in the chip. This was conducted using a ssDNA target concentration of 10^{-12} mol/L and the previously determined hybridization buffer composition of 0.01% BSA, 0.10% SDS in $10\times$ SSC. Because the results were obtained using the proven NanoGene assay, the results from Figure 28a were used as a control. Figure 28a shows that using a buffer composition of 0.01% BSA, 0.10% SDS in $10\times$ SSC and a ssDNA target concentration of 10^{-12} mol/L should yield normalized fluorescence results of approximately 3 RFU.

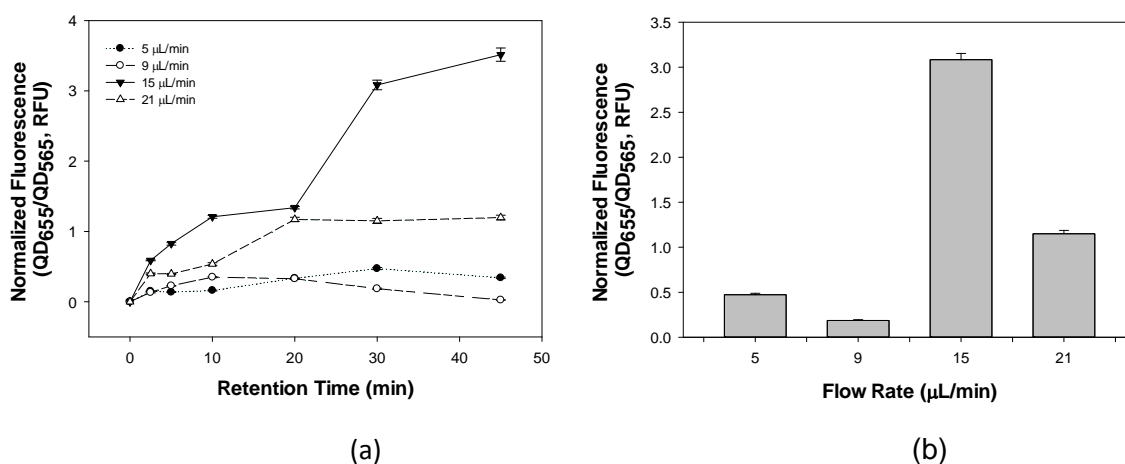


Figure 29. (a) Microfluidic hybridization kinetic results at various flow rate conditions (10^{-12} mol/L, 0.01% BSA, 0.1% SDS in $10\times$ SSC) (b) Microfluidic hybridization kinetic results at fixed retention time, 30 min (10^{-12} mol/L, 0.01% BSA, 0.1% SDS in $10\times$ SSC)

Hybridization results seen in Figure 29a indicate that hybridization was optimized at a flow rate of 15 $\mu\text{L}/\text{min}$ and a retention time of 30 minutes. At this flow rate and retention time, the normalized fluorescence reached 3 RFU and the results plateaued for greater retention times. The results shown in

Figure 28b also indicate that hybridization at a flow rate of 15 $\mu\text{L}/\text{min}$ yield a normalized fluorescence of approximately 3 RFU. Because results from the microfluidic NanoGene assay shown in Figure 28b and Figure 29 both indicate that normalized fluorescence from complete hybridization yields results of 3 RFU, evidence suggests that this method is capable of yielding repeatable results. Flow rates of 5, 9, and 21 $\mu\text{L}/\text{min}$ each plateaued at values much less than 3 RFU. The trend in hybridization results for all four flow rates at a retention time of 30 minutes can be seen in Figure 29b. It is hypothesized that there is a narrow range of optimum flow rates for microfluidic hybridization. Flow rates less than optimum (5 and 9 $\mu\text{L}/\text{min}$) allowed the particles to precipitate from the flow and did not allow the appropriate amount of time for contact between the complexes for complete hybridization. Because the retention time was fixed, lower flow rates caused a decreased number of passes of the complexes through the magnetic trap. Flow rates greater than optimum (21 $\mu\text{L}/\text{min}$) were too fast and may not allow sufficient time for hydrogen bonds formation during hybridization.

A retention time of 30 minutes (using a flow rate of 15 $\mu\text{L}/\text{min}$) for the microfluidic NanoGene assay is significantly less than the previously used retention time of 6-8 hours for the well-plate method. Because of its ability to allow rapid hybridization and its capability of generating repeatable results, the microfluidic NanoGene assay has the potential to be ideal for the use of in-situ pathogen detection.

J. NOTABLE AWARDS AND ACHIEVEMENTS. List any awards or recognitions for this research NSF CAREER award (January, 2011): “Development of a novel inhibitor-resistant genomic assay in environmental samples” funded for \$430,000

K. PUBLICATIONS GENERATED:

Number of Research Publications generated from this research project:	
Publication Category	Number
Articles in Refereed Journals	4
Book Chapters	0
Theses and Dissertations	1
Water Resources Institute Reports	0
Articles in Conference Proceedings	0
Other Publications	0

PROVIDE A CITATION FOR EACH PUBLICATION USING THE FOLLOWING FORMATS:

1. Articles in Refereed Scientific Journals Citation

1. Kim, G. and A. Son, 2010, Development and characterization of a magnetic bead-quantum dot nanoparticles based assay capable of *Escherichia coli* O157:H7 quantification, *Analytica Chimica Acta*, 677, pp. 90-96.
2. Kim, G. and A. Son, 2010, Quantitative detection of *E. coli* O157:H7 eaeA gene using quantum dots and magnetic particles, *Biotechnology and Bioprocess Engineering*, 15, pp. 1084-1093.
3. Kim, G.; X. Wang, H. Ahn, and A. Son, 2011, Gene quantification by NanoGene assay is resistant to humic acids, *Environmental Science and Technology*, 45, pp. 8873-8880.
4. Kim, G.; X. Wang, and A. Son, 2011, Inhibitor resistance and in-situ capability of nanoparticle based gene quantification, *Journal of Environmental Monitoring*, 13, pp. 1344-1350.

2. Book Chapter Citation

None

3. Dissertations Citation

Wang, Xiaofang, 2011, Humic Acids Resistant Gene Quantification Assay in Soils, “MS Dissertation,” Department of Civil Engineering, Auburn University, Auburn, Alabama, 58.

4. Water Resources Research Institute Reports Citation

None

5. Conference Proceedings Citation

None

6. Other Publications Citation

None

L. PRESENTATIONS MADE:

1. Kim, G., X. Wang, and A. Son, 2010, Quantitative detection of *E. coli* O157:H7 *eaeA* gene using quantum dots and magnetic particles, *ASM 2010*, The 210th General Meeting of American Society for Microbiology, San Diego, CA, USA, May 23-27, 2010, *Poster presentation*.
2. Kim, G., X. Wang, and A. Son, 2010, Separation and quantification of *E. coli* O157:H7 using magnetic bead-quantum dot nanoparticles, *ACS 2010*, The 240th General Meeting of American Chemical Society, Boston, MA, USA, August 22-26, 2010, *Poster presentation*.
3. Wang, X., G. Kim,, and A. Son, 2010, Development of an inhibitor resistant gene monitoring method for the bacteria detection in water systems, The 24th Annual Alabama Water Resources Conference, Orange Beach, AL, USA, September, 2010, *Poster presentation*.
4. Son, A. and G. Kim, 2011, *In-situ* capable gene quantification using quantum dots and magnetic beads, *ASM 2011*, The 211th General Meeting of American Society for Microbiology, New Orleans, LA, USA, May 21-24, 2011, *Poster presentation*.
5. Wang, X. and A. Son, A, 2011, Humic acid resistant gene quantification assay in soils, *ASM 2011*, The 211th General Meeting of American Society for Microbiology, New Orleans, LA, USA, May 21-24, 2011, *Poster presentation*.
6. Wang, X. and A. Son, 2011, Humic acid resistant assay for bacteria quantification in environmental samples, *AEESP conference 2011: Global sustainability and environmental engineering & science: Implications for research, education, & practice*, Tampa, FL, USA, July 10-12, 2011, *Poster presentation*.
7. Wang, X. and A. Son, 2012, Genomic DNA denaturation optimized for DNA hybridization, *ACS 2012*, The 244th General Meeting of American Chemical Society, Philadelphia, PA, USA, August 19-23, 2012, Accepted for *poster presentation*.
8. Son, A. and X. Wang, 2012, NanoGene assay: Sensitive and inhibition resistant gene quantification using quantum dots and magnetic beads, *ACS 2012*, The 244th General Meeting of American Chemical Society, Philadelphia, PA, USA, August 19-23, 2012, Accepted for *platform presentation*.
9. Kilpatrick, K. and A. Son, 2012, Development of a microfluidic NanoGene assay for the pathogen detection in water, *ACS 2012*, The 244th General Meeting of American Chemical Society, Philadelphia, PA, USA, August 19-23, 2012, Accepted for *platform presentation*.

M. STUDENTS SUPPORTED (Complete the following table)

Number of Students Supported, by Degree	
Type	Number of students funded through this research project:
Undergraduate	1
Masters	2
Ph.D.	0
Post Doc	1

Number of Theses and Dissertations Resulting from Student Support:	
Master's Theses	1
Ph.D. Dissertations	0

N. RESEARCH CATEGORIES: (In column 1 mark all that apply)

	Research Category
x	Biological Sciences
	Climate and Hydrological Processes
x	Engineering
	Ground Water Flow and Transport
	Social Sciences
x	Water Quality
x	Other: biosensors, nanobiotechnology, environmental microbiology, public health

O. FOCUS CATEGORIES (mark all that apply with "X" in column 1):

	ACID DEPOSITION	ACD
x	AGRICULTURE	AG
	CLIMATOLOGICAL PROCESSES	CP
	CONSERVATION	COV
	DROUGHT	DROU
	ECOLOGY	ECL
	ECONOMICS	ECON
	EDUCATION	EDU
	FLOODS	FL
	GEOMORPHOLOGICAL PROCESSES	GEOMOR
	GEOCHEMICAL PROCESSES	GEOCHE
x	GROUNDWATER	GW
	HYDROGEOCHEMISTRY	HYDGEO
	HYDROLOGY	HYDROL
	INVASIVE SPECIES	INV
	IRRIGATION	IG

	LAW, INSTITUTIONS, & POLICY	LIP
	MANAGEMENT & PLANNING	M&P
x	METHODS	MET
	MODELS	MOD
	NITRATE CONTAMINATION	NC
	NONPOINT POLLUTION	NPP
	NUTRIENTS	NU
	RADIOACTIVE SUBSTANCES	RAD
	RECREATION	REC
	SEDIMENTS	SED
	SOLUTE TRANSPORT	ST
x	SURFACE WATER	SW
	TOXIC SUBSTANCES	TS
	TREATMENT	TRT
	WASTEWATER	WW
x	WATER QUALITY	WQL
	WATER QUANTITY	WQN
	WATER SUPPLY	WS
	WATER USE	WU
	WETLANDS	WL

P. DESCRIPTORS: (Enter keywords of your choice, descriptive of the work)

Pathogenic bacteria, *E. coli* O157:H7, nanoparticle, DNA, in-situ detection, microfluidics, gene quantification

REFERENCES

- Alm, E.W., et al. 2000. The presence of humic substances and DNA in RNA extracts affects hybridization results. *Applied and Environmental Microbiology*, **66**, 4547-4554.
- Bruno, J.G., Phillips, T., Carrillo, M.P., Crowell, R. 2009. Plastic-adherent DNA aptamer-magnetic bead and quantum dot sandwich assay for *Campylobacter* detection. *J. Fluoresc.*, **19**(3), 427-435.
- Carey, C.M., Kostrzynska, M., Thompson, S. 2009. *Escherichia coli* O157:H7 stress and virulence gene expression on Romaine lettuce using comparative real-time PCR. *Journal of Microbiological Methods*, **77**(2), 235-242.
- Chunlai Chen, Wenjuan Wang, Jing Ge, Zhao, X.S. 2009. Kinetics and thermodynamics of DNA hybridization on gold nanoparticles. *Nucleic Acids Research*, **37**, 3756-3765.
- Dai, Q., Liu, X., Coutts, J., Austin, L., Huo, Q. 2008. A one-step highly sensitive method for DNA detection using dynamic light scattering. *J. Am. Chem. Soc.*, **130**, 8138-8139.
- Eastman, P.S., Ruan, W., Doctolero, M., Nuttall, R., Feo, G.d., Park, J.S., Chu, J.S.F., Cooke, P., Gray, J.W., Li, S., Chen, F.F. 2006. Qdot nanobarcode for multiplexed gene expression analysis. *Nano Lett.*, **6**, 1059-1064.
- Ferguson, J.A., Steemers, F.J., Walt, D.R. 2000. High-density fiber-optic DNA random microsphere array. *Anal. Chem.*, **72**, 5618-5624.
- Hill, H.D., Vega, R.A., Mirkin, C.A. 2007. Nonenzymatic detection of bacterial genomic DNA using the biobarcode assay. *Anal. Chem.*, **79**, 9218-9223.
- Huang, S., Pang, P., Xiao, X., He, L., Cai, Q., Grimes, C.A. 2008. A wireless, remote-query sensor for real-time detection of *Escherichia coli* O157:H7 concentrations. *Sens. Actuators, B* **131**, 489-495.
- James G. Wetmur, Davidson, N. 1968. Kinetics of renaturation of DNA. *Journal of Molecular Biology*, **31**, 349-370.
- Kim, G.-Y., Wang, X., Son, A. 2011a. Inhibitor resistance and in-situ capability of nanoparticle based gene quantification. *J. Environ. Monit.*, **13**, 1344-1350.
- Kim, G.Y., et al. 2010. Development and characterization of a magnetic bead-quantum dot nanoparticles based assay capable of *Escherichia coli* O157:H7 quantification. *Analytica Chimica Acta*, **677**, 90-96.
- Kim, G.Y., Son, A. 2010a. Development and characterization of a magnetic bead-quantum dot nanoparticles based assay capable of *Escherichia coli* O157:H7 quantification. *Analytica Chimica Acta*, **677**, 90-96.
- Kim, G.Y., Son, A. 2010b. Quantitative detection of *E.coli* O157:H7 *eaeA* gene using quantum dots and magnetic particles. *Biotechnology and Bioprocess Engineering*, **15**(6), 1084-1093.
- Kim, G.Y., Wang, X., Ahn, H., Son, A. 2011b. Gene quantification by the NanoGene assay is resistant to inhibition by humic acids. *Environmental Science & Technology*, **45**, 8873-8880.
- Lakowicz, J.R. 1991. *Fluorescence quenching: theory and applications*. 2nd ed. Kluwer Academic/Plenum, New York, NY.
- Larry E. Morrison, Stols, L.M. 1993. Sensitive fluorescence-based thermodynamic and kinetic measurements of DNA hybridization in solution. *Biochemistry*, **32**, 3095-3104.
- Lin, Y.-H., Chen, S.-H., Chuang, Y.-C., Lu, Y.-C., Shen, T.Y., Chang, C.A., Lin, C.-S. 2008. Disposable amperometric immunosensing strips fabricated by Au nanoparticles-modified screen-printed carbon electrodes for the detection of foodborne pathogen *Escherichia coli* O157:H7. *Biosens. Bioelectron.*, **23**, 1832-1837.
- Liu, C.-H., Li, Z.-P., Du, B.-A., Duan, X.-R., Wang, Y.-C. 2006. Silver nanoparticle-based ultrasensitive chemiluminescent detection of DNA hybridization and single-nucleotide polymorphisms. *Anal. Chem.*, **78**, 3738-3744.
- Liu, Y.-J., Yao, D.-J., Chang, H.-Y., Liu, C.-M., Chen, C. 2008. Magnetic bead-based DNA detection with multi-layers quantum dots labeling for rapid detection of *Escherichia coli* O157:H7. *Biosens. Bioelectron.*, **24**, 558-565.

- Mao, X., Yang, L., Su, X.-L., Li, Y. 2006a. A nanoparticle amplification based quartz crystal microbalance DNA sensor for detection of *Escherichia coli* O157:H7. *Biosensors and Bioelectronics*, **21**, 1178-1185.
- Mao, X., Yang, L., Su, X.-L., Li, Y. 2006b. A nanoparticle amplification based quartz crystal microbalance DNA sensor for detection of *Escherichia coli* O157:H7. *Biosens. Bioelectron.*, **21**, 1178-1185.
- Österberg, R., et al. 1993. Particle size of humic acid. *Soil Science Society of America Journal*, **57**, 283-285.
- Patolsky, F., Weizmann, Y., Katz, E., Willner, I. 2003. Magnetically amplified DNA assays (MADA): sensing of viral DNA and single-base mismatches by using nucleic acid modified magnetic particles. *Angew. Chem. Int. Ed.*, **42**, 2372-2376.
- Sharma, V.K., Dean-Nystrom, E.A., Casey, T.A. 1999. Semi-automated fluorogenic PCR assays (TaqMan) for rapid detection of *Escherichia coli* O157:H7 and other *Shiga* toxicogenic *E. coli*. *Mol. Cell. Probes* **13**, 291-302.
- Shriver-Lake, L.C., Turner, S., Taitt, C.R. 2007. Rapid detection of *Escherichia coli* O157:H7 spiked into food matrices. *Anal. Chim. Acta*, **584**, 66-71.
- Singleton, P. 2004. *Bacteria in Biology, Biotechnology and Medicine*. 6th ed. Wiley.
- Son, A., Dhirapong, A., Dosev, D., Kennedy, I.M., Weiss, R.H., Hristova, K. 2008. Rapid and quantitative DNA analysis of genetic mutations for polycystic kidney disease (PKD) using magnetic/luminescent nanoparticles. *Analytical and Bioanalytical Chemistry*, **390**(7), 1829-1835.
- Storhoff, J.J., Marla, S.S., Bao, P., Hagenow, S., Mehta, H., Lucas, A., Garimella, V., Patno, T., Buckingham, W., Cork, W., Müller, U.R. 2004. Gold nanoparticle-based detection of genomic DNA targets on microarrays using a novel optical detection system. *Biosens. Bioelectron.*, **19**, 875-883.
- Su, X.-L., Li, Y. 2004. Quantum dot biolabeling coupled with immunomagnetic separation for detection of *Escherichia coli* O157:H7. *Anal. Chem.*, **76**, 4806-4810.
- Tuttle, J., Gomez, T., Doyle, M.P., Wells, J.G., Zhao, T., Tauxe, R.V., Griffin, P.M. 1999a. Lessons from a large outbreak of *Escherichia coli* O157:H7 infections: Insights into the infectious dose and method of widespread contamination of hamburger patties. *Epidemiology and Infection*, **122**(2), 185-192.
- Tuttle, J., Gomez, T., Doyle, M.P., Wells, J.G., Zhao, T., Tauxe, R.V., Griffin, P.M. 1999b. Lessons from a large outbreak of *Escherichia coli* O157:H7 infections: insights into the infectious dose and method of widespread contamination of hamburger patties. *Epidemiol. Infect.*, **122**, 185-192.
- Wershaw, R.L. 1993. Model for humus in soils and sediment. *Environmental Science and Technology*, **27**, 814-816.
- Wu, Z.-S., Jiang, J.-H., Fu, L., Shen, G.-L., Yu, R.-Q. 2006. Optical detection of DNA hybridization based on fluorescence quenching of tagged oligonucleotide probes by gold nanoparticles. *Anal. Biochem.*, **353**(1), 22-29.
- Xue, X., Pan, J., Xie, H., Wang, J., Zhang, S. 2009. Fluorescence detection of total count of *Escherichia coli* and *Staphylococcus aureus* on water-soluble CdSe quantum dots coupled with bacteria. *Talanta*, **77**, 1808-1813.
- Yang, L., Li, Y., Erf, G.F. 2004. Interdigitated array microelectrode-based electrochemical impedance immunosensor for detection of *Escherichia coli* O157:H7. *Anal. Chem.*, **76**(4), 1107-1113.
- Young, C., et al. 1993. Polyvinylpyrrolidone-agarose gel electrophoresis purification of polymerase chain reaction-amplifiable DNA from soils. *Applied and Environmental Microbiology*, **59**, 1972-1974.
- Zaytseva, N.V., Montagna, R.A., Baeumner, A.J. 2005. Microfluidic biosensor for the serotype-specific detection of Dengue virus RNA. *Anal. Chem.*, **77**, 7520-7527.
- Zeta potential of colloids in water and waste water, A.S.D.-., American Society for Testing and Materials, 1985
- Zhao, X., Tapeç-Dytioco, R., Tan, W. 2003. Ultrasensitive DNA detection using highly fluorescent bioconjugated nanoparticles. *J. Am. Chem. Soc.*, **125**, 11474-11475.

Zipper, H., Buta, C., Lammle, K., Brunner, H., Bernhagen, J., Vitzthum, F. 2003. Mechanisms underlying the impact of humic acids on DNA quantification by SYBR Green I and consequences for the analysis of soils and aquatic sediments. *Nucleic Acids Research*, **31**, e39.

Forage and Fertilization Management Practices to Ensure Quality of Runoff from Pasture Under Grazing Beef Cattle

Basic Information

Title:	Forage and Fertilization Management Practices to Ensure Quality of Runoff from Pasture Under Grazing Beef Cattle
Project Number:	2011AL115B
Start Date:	3/1/2011
End Date:	2/28/2012
Funding Source:	104B
Congressional District:	Third
Research Category:	Water Quality
Focus Category:	Water Quality, Non Point Pollution, Agriculture
Descriptors:	None
Principal Investigators:	Russell B. Muntifering, Yucheng Feng, Thomas A. McCaskey, Frank F. Owsley, Charles Wesley Wood

Publications

There are no publications.

ANNUAL TECHNICAL REPORT SYNOPSIS

A. PROJECT TITLE: Forage and fertilization management practices to ensure quality of runoff from pasture under grazing beef cattle

B. PRIMARY PI: Dr. Russell B. Muntifering, Professor of Animal Sciences

C. OTHER PIs: Drs. W. Frank Owsley (Associate Professor of Animal Sciences), Thomas A. McCaskey (Professor of Animal Sciences), C. Wes Wood (Professor of Agronomy & Soils) and Yucheng Feng (Associate Professor of Agronomy & Soils)

D. START DATE: May 1, 2011

E. END DATE: April 30, 2012 (no-cost extension through September 30, 2012)

F. PROJECT OVERVIEW/SUMMARY:

The project quantifies effects of nitrogen (N)-fertilization regime on forage nutrient uptake, microbial and nutrient returns in grazing-cattle excreta, and water quality of runoff from pastures with high background soil-test phosphorus (P). The experimental system comprises six 0.28-ha, instrumented runoff plots located at the Stanley P. Wilson Beef Teaching Unit on the Auburn University campus. Nutrient concentrations in runoff from grazing paddocks are evaluated over summer and winter grazing seasons, and seasonal transport of nutrients is calculated for all major runoff events during each grazing season. Samples of runoff from each major rainfall event are analyzed for concentrations of *E. coli*, fecal coliforms and enterococci.

G. PROJECT OBJECTIVES:

We hypothesize that, by using differing N application rates and application schedules in conjunction with overseeding of a N-fixing legume into a permanent pasture sod, patterns of plant uptake of P, P excretion by grazing cattle, and P loss via water runoff are altered. Also, we hypothesize that botanical composition and productivity of the pastures differ among treatments in a manner that modulates loss of N and pathogenic microbes via runoff.

H. METHODOLOGIES:

In May of 2011, annual cowpea (*Vigna unguiculata*) was broadcast-seeded in the runoff plots, and replicate plots (2/fertilizer treatment) received either no N fertilizer (0-N), 34 kg N/ha (34-N) in a single application as ammonium nitrate, or 68 kg N/ha (68-N) in a split application of 34 kg N/ha as ammonium nitrate at time of seeding and again in early July. These fertilizer treatments represent 0, 50 and 100% of the agronomic recommendation for the permanent summer sod of bermudagrass (*Cynodon dactylon*) within the plots. The summer-grazing period began in mid-July when forage had achieved a mean height of approximately 15 cm (corresponding to approximately 1,500 kg DM/ha). At that time, 2 steers from the Beef Teaching Unit herd were turned into each of the experimental plots for grazing such that stocking rate and steer-grazing days were uniform across the plots. Forage mass within each plot was determined prior to the beginning of grazing and then monthly throughout the grazing period by clipping representative forage to a 5-cm height within 0.25-m² quadrats. Freshly cut forage was

immediately weighed on a portable field scale, and subsamples were placed into tared paper bags, dried at 60°C for 48 hr, and then re-weighed for dry weight determination. Dry matter (DM) yield was then calculated for each sample. Grazing was discontinued when forage DM availability had declined to 500 kg DM/ha in late September. Cattle had *ad libitum* access to water and salt, and shade was provided well in excess of the 1.4–1.8 m²/head recommended for beef cattle.

In late September/early October of 2011, replicate plots (2/fertilizer treatment) were drill-seeded with triticale (*Triticum secale*) and crimson clover (*Trifolium incarnatum*) in a ratio of 80:20 and receive either no N fertilizer (0-N), 56 kg N/ha (56-N) at time of planting as ammonium nitrate, or 112 kg N/ha (112-N) in a split application as ammonium nitrate at time of seeding and again after 120 days post-seeding. These fertilizer treatments represent 0, 50 and 100% of the agronomic recommendation for tall fescue (*Lolium arundinacea*), the predominant perennial forage in the plots during the winter and spring months. The 0, 50 and 100% treatments were applied to the same plots that had received these treatments in the summer-grazing portion of the experiment. When forage achieved a mean height of approximately 20 cm, corresponding to forage dry matter (DM) availability of approximately 2,000 kg DM/ha, 2 steers from the Beef Teaching Unit herd were turned into each experimental plot for grazing such that stocking rate and steer-grazing days were uniform across the plots. Forage samples were collected for mass determination, and plots were grazed through April 2012.

Forage samples are being separated manually into predominant species in the plots during the summer (bermudagrass and cowpea, some tall fescue) and winter/spring (tall fescue, triticale and crimson clover) grazing seasons. Total C and N in forage samples will be determined via dry combustion on a LECO TruSpec CN analyzer. Samples will be dry-ashed, evaporated with 10 mL 1N nitric acid, dissolved with 10 mL 1N HCl, and analyzed for total P, K, Ca, Mg, Cu and Zn using inductively coupled argon plasma (ICAP) spectroscopy (Hue and Evans, 1986). Nutrient uptake will be calculated as the product of forage nutrient concentration and DM yield.

Prior to chemical analyses, runoff water samples will be filtered through a 0.45- μ m filter. Nitrate-N and NH₄-N will be determined in filtered runoff samples via standard colorimetric procedures (Sims et al., 1995). Dissolved P, K, Ca, Mg, Mn, Cu and Zn will be determined in filtered runoff samples by digesting a 25-mL sample with 10 mL of 70:30 nitric acid:perchloric acid mix for 2 hr at 200°C followed by addition of 10 mL 1.0 N HCl prior to ICAP spectroscopy. Sediment from 250 mL of runoff water will be collected on a 0.45- μ m filter. The filter and sediment will be dried to a constant weight and then weighed to determine suspended solids. To perform nutrient analyses on the sediment, the filter and sediment will be ashed in a muffle furnace at 450°C for 12 hr followed by addition of 10 mL 1N HNO₃ and heating at 200°C until dryness, and addition of 10 mL 1.0 N HCl with further heating at 200°C prior to ICAP analyses for P, K, Ca, Mg, Mn, Cu and Zn (Hue and Evans, 1986). Unfiltered runoff water samples will be analyzed for Kjeldahl N (AOAC, 1995). For this procedure, a 50 mL water sample will be digested with 10 mL concentrated H₂SO₄ and a K₂SO₄ catalyst tablet for 12 hours at 200°C without an aspirator, followed by 2 hours of digestion with an aspirator at 450°C. Samples will then be distilled with a Kjeltex system 1028 Distilling Unit for determination of Kjeldahl N. Flow-weighted nutrient concentrations are defined as the amount of nutrient in runoff divided by the total runoff volume collected within a specific period. Runoff concentrations will be evaluated over each forage-growing season (summer season, May to October; winter/spring season, December through April). Seasonal transport of each nutrient is defined as the sum of the transport for all runoff events during each forage-growing season.

Guidelines established by the U.S. Environmental Protection Agency recommend that *E. coli* be used as an indicator of fecal contamination in fresh recreation waters (USEPA, 1986). The use of indicator organisms circumvents the need to assay for every pathogen. Samples of runoff from each major rainfall event will be analyzed for *E. coli* concentrations by using Colilert reagents in Quantitray-2000 format (IDEXX Corporation, Westbrook, ME) in accordance with Method 9223 (Eaton et al., 2005). In addition, the intermittent stream that receives runoff from the plots drains into Parkerson Mill Creek will be sampled after each heavy-rainfall event and analyzed for *E. coli* concentrations. Water samples will also be analyzed for *E. coli* by EPA method 1603 (EPA, 2002), which is a membrane-filtration method that allows for analysis of variable amount of water depending upon bacterial density, and enables a timely and relevant comparison of interest with values from Method 9223. Fecal coliforms in water samples will be determined by APHA/AWWA/WEF (2005) procedures, and enterococci by EPA method 1600 (EPA, 2002).

Data will be analyzed initially using mixed model procedures for a completely randomized design with 3 treatments (2 runoff plots/treatment) using PROC MIXED procedures of SAS and standard least-squares model fit (SAS Inst., Inc., Cary, NC). Single degree-of-freedom contrasts between 0-N and N-fertilizer treatments within grazing seasons (34-N + 68-N in summer, and 56-N + 112-N in winter/spring) and between 50 and 100% agronomic rates of N fertilization within grazing seasons (34-N vs. 68-N in summer, and 56-N vs. 112-N in winter/spring) will enable evaluation of N fertilization and time-of-application effects. Statistical associations between runoff characteristics, precipitations patterns and amounts, fecal microbial and nutrient loads, and forage uptake of nutrients will be determined by correlation analysis using PROC CORR procedures, and by stepwise regression analysis using PROC REG procedures (SAS Inst., Inc., Cary, NC). Multivariate analysis of data will be employed to apportion variance among factors and establish their predictive relationships with nutrient, microbiological and sediment loading in runoff.

I. PRINCIPAL FINDINGS/RESULTS TO DATE

Forage DM availability ($P = 0.002$) and uptake of P ($P = 0.01$) were greater for cool- than warm-season forage (4,441 vs. 2,311 kg/ha and 8.44 vs. 5.30 kg P/ha, respectively), but were not different among N-fertilization treatments. Foliar P concentrations were not different among treatments. Daily P intake and excretion by cattle were not different among treatments (12.2, 11.3 and 13.3 g/d, and 14.8, 15.0 and 11.9 g/d for 0N, 50N and 100N, respectively). Results indicate that manipulation of N-fertilization regime did not affect P removal from plots with high soil P beyond that from overseeded small-grain and annual legumes, and seasonal differences in P removal were not reflected in patterns of P utilization by grazing cattle.

There were no differences among N-fertilization treatments for soil acid ($P > 0.417$) or base phosphatase ($P > 0.225$). Cool-season acid and base phosphatase activities were lower (0.09 and 0.13 $\mu\text{g pNP/g/h}$, respectively) than warm-season (0.22 and 0.24 $\mu\text{g pNP/g/h}$, respectively) ($P = 0.034$ and $P = 0.045$, respectively). Results indicate that growing season and grazing of seasonally adapted forage species greatly affected soil phosphatase activity, but these were not affected by manipulation of N fertilization regime.

Prior to imposition of N-fertilization treatments, concentrations of generic *E. coli* and enterococci were determined in freshly voided feces of cattle grazing the experimental plots. These data will help establish baseline populations of the indicator bacteria in feces prior to determining their regrowth and survival on pastureland. The *E. coli* populations in 20 samples

collected averaged 1.71×10^4 /g wet weight with a range of less than 10^3 to 1.1×10^5 /g wet weight. Thirty percent of the fecal samples had no detectable *E. coli* in the 1:1000 diluted samples. These samples are therefore being reported as less than 10^3 /gram, but how much less than 10^3 /g is not known. Usually *E. coli* counts in cattle feces are reported to be about 4×10^6 /g wet weight or 5×10^6 /g dry weight. Based on a 25-gram sample size of each of the 20 fecal samples, *Salmonella* bacteria were not detected in any of the samples.

Feces collected from grazing cattle initially contained 0.68, 0.84 and 0.89% P (dry basis) for 0N, 50N and 100N treatments, respectively. Fecal P concentration decreased ($P < 0.07$) from day 0 to day 28 in the 0N treatment, and was different ($P < 0.036$) in 50N between day 0 and days 28, 84 and 112; fecal P concentrations tended to decrease after 28 days in all N-fertilization treatments. Soil P concentrations were not different among treatments. Soil P concentration was greater ($P < 0.0001$) at 0 – 5 cm (70 mg P /kg) than 5 – 10 cm (34 mg P/kg) and 10 – 20 cm (35 mg P/kg) depths, and tended to increase from day 0 to 112 in all treatments. Results are interpreted to mean that differing temporal patterns of decrease in fecal P concentration among the N-fertilization regimes were inconsequential to soil P concentrations under winter/spring grazing.

J. NOTABLE AWARDS AND ACHIEVEMENTS

This research was featured recently as a cover story in the Fall 2011 issue of the Auburn University Graduate School Magazine.

K. PUBLICATIONS GENERATED:

Number of Research Publications generated from this research project to date:	
Publication Category	Number
Articles in Refereed Journals	0
Book Chapters	0
Theses and Dissertations	0
Water Resources Institute Reports	0
Articles in Conference Proceedings	0
Other Publications	0

L. PRESENTATIONS MADE:

The following is scheduled for presentation at the annual meeting of the American Society of Animal Science, July 15-19, 2012 in Phoenix, AZ:

Dillard, Sandra L., Walter F. Owsley, C.Wes Wood, Brenda H. Wood and Russell B. Muntifering. Foliar uptake and utilization of phosphorus by grazing cattle as influenced by nitrogen fertilization regime.

The following have been submitted for presentation at the annual meeting of American Society of Agronomy/Crop Science Society of America/Soil Science Society of America, October 21-24, 2012 in Cincinnati, OH:

Dillard, Sandra L., Walter F. Owsley, C.Wes Wood, Brenda H. Wood, Yucheng Feng and Russell B. Muntifering. Soil phosphatase activity and foliar uptake of phosphorus as influenced by nitrogen fertilization regime in a grazed pasture system.

Dillard, Sandra L., Walter F. Owsley, C.Wes Wood, Brenda H. Wood and Russell B. Muntifering. Phosphorus release from fecal pats in grazed pasture as influenced by nitrogen fertilization regime.

M. STUDENTS SUPPORTED

Number of Students Supported, by Degree	
Type	Number of students funded through this research project:
Undergraduate	1
Masters	0
Ph.D.	1
Post Doc	0
Number of Theses and Dissertations Resulting from Student Support:	
Master's Theses	
Ph.D. Dissertations	1

N. RESEARCH CATEGORIES:

	Research Category
√	Biological Sciences
	Climate and Hydrological Processes
	Engineering
	Ground Water Flow and Transport
	Social Sciences
√	Water Quality
	Other: Explain

O. FOCUS CATEGORIES:

	ACID DEPOSITION	ACD
X	AGRICULTURE	AG
	CLIMATOLOGICAL PROCESSES	CP
	CONSERVATION	COV
	DROUGHT	DROU
X	ECOLOGY	ECL
	ECONOMICS	ECON
	EDUCATION	EDU
	FLOODS	FL
	GEOMORPHOLOGICAL PROCESSES	GEOMOR
	GEOCHEMICAL PROCESSES	GEOCHE
	GROUNDWATER	GW
	HYDROGEOCHEMISTRY	HYDGEO
	HYDROLOGY	HYDROL
	INVASIVE SPECIES	INV
	IRRIGATION	IG
	LAW, INSTITUTIONS, & POLICY	LIP
	MANAGEMENT & PLANNING	M&P
	METHODS	MET
	MODELS	MOD
	NITRATE CONTAMINATION	NC
X	NONPOINT POLLUTION	NPP
X	NUTRIENTS	NU
	RADIOACTIVE SUBSTANCES	RAD
	RECREATION	REC
	SEDIMENTS	SED
	SOLUTE TRANSPORT	ST
X	SURFACE WATER	SW
	TOXIC SUBSTANCES	TS
	TREATMENT	TRT
	WASTEWATER	WW
X	WATER QUALITY	WQL
	WATER QUANTITY	WQN

	WATER SUPPLY	WS
	WATER USE	WU
	WETLANDS	WL

P. DESCRIPTORS: Water, Soil, Forage, Cattle, Phosphorus

Utilizing Greywater for Landscape and Green Roof Irrigation

Basic Information

Title:	Utilizing Greywater for Landscape and Green Roof Irrigation
Project Number:	2011AL117B
Start Date:	3/1/2011
End Date:	2/28/2012
Funding Source:	104B
Congressional District:	Third
Research Category:	Water Quality
Focus Category:	Wastewater, Water Use, Irrigation
Descriptors:	None
Principal Investigators:	Amy N. Wright, Charlene M LeBleu

Publications

1. Lecompte, J., A.N. Wright, J. R. Kessler, and C. LeBleu. 2012. Saline irrigation of five landscape species for the Southeast. Proc. SNA Res. Conf. in press.
2. LeCompte, J.S., A.N. Wright, J.R. Kessler, and C. Lebleu. 2012. Saline irrigation of three green roof species for the Southeast. HortScience in press. (Abstr.)

ANNUAL TECHNICAL REPORT SYNOPSIS

The Terms and Conditions of the grants awarded under the Water Resources Research Act state that each institute shall prepare an Annual Program Report summarizing its activities during the reporting period under its base grant, and National Competitive Grant Program awards. The reporting period is March 1, through February 28. All Annual Reports must be submitted by 5:00 PM, Eastern Daylight Time, June 1, and must be submitted electronically. In order to do this we need your assistance by providing the following information about your current or recent WRRRI-funded research project:

- A. PROJECT TITLE: UTILIZING GREYWATER FOR LANDSCAPE AND GREEN ROOF IRRIGATION
- B. PRIMARY PI(s): Name(s), Title(s) & Academic Rank(s) Amy Wright, Associate Professor
- C. OTHER PI(s): Name(s), Title(s) & Academic Rank(s) Charlene LeBleu, Associate Professor
- D. START DATE: March 1, 2011
- E. END DATE: February 27, 2013
- F. PROJECT OVERVIEW/SUMMARY: Provide a brief narrative overview or summary of the project. Results from this study include quantitative data from controlled greenhouse experiments on the effect of greywater application rates on growth and survival of selected species of landscape and green roof plants. Results also include analysis of greywater generated on campus. Results will yield information regarding greywater reuse in terms of tolerance of selected landscape and green roof plants to surfactants and salinity. It will also set a basis for the future collection of greywater on campus and its possibilities for reuse.
- G. PROJECT OBJECTIVE(s): Briefly explain the project objectives.
 - (1) Establish the potential for greywater reuse as a substitute for potable water for landscape and green roof irrigation, (2) Evaluate the tolerance of selected landscape and green roof plants to surfactants and salinity, and (3) Establish baseline data to characterize chemical properties of greywater samples collected from on-campus buildings.
- H. METHODOLOGIES: Briefly explain the research methodology used. Selected landscape and green roof species were evaluated for tolerance to salt concentrations found in greywater. Species included one grass, one evergreen shrub, one deciduous shrub, two bedding plants, and two green roof species. Greywater was also collected from a hand washing station on campus, and different concentrations of that greywater were used to irrigate one species of bedding plant. Chemical analysis of greywater was completed. One species of bedding plant was evaluated for tolerance to surfactant concentrations found in greywater.
- I. PRINCIPAL FINDINGS/RESULTS: Explain the results of findings of this research project.

All five landscape species *Begonia x semperflorens-cultorum*, *Portulaca oleracea*, *Illicium parviflorum*, *Itea virginica*, and *Muhlenbergia capillaris* were tolerant of NaCl concentrations higher than what would be expected from greywater, with *Itea virginica* being the least tolerant. Three green roof species *Sedum spurium* 'Tricolor', *Sedum rupestre* 'Angelina', and *Coreopsis auriculata* 'Nana' were also tolerant of NaCl concentrations higher than what would be expected from greywater with *Coreopsis auriculata* 'Nana' being least tolerant. Mortality was observed in *Begonia x semperflorens-cultorum*, *Itea virginica*, and *Coreopsis auriculata* 'Nana' at higher NaCl concentrations; however these concentration levels were four times higher than expected in greywater. The concentration of collected greywater used for irrigation did not affect plant growth or leachate pH and EC of *Portulaca oleracea*. Plant growth and leachate pH and EC of *Echinacea purpurea* were not affected by surfactant concentration. Thus, both *P. oleracea* and *E. purpurea* would be tolerant of irrigation using greywater. In collected greywater, surfactant concentration in collected greywater ranged from 25-90 mg/L, Na concentration ranged from 22-24 mg/L, and Cl concentration ranged from 12-25 mg/L.

- J. NOTABLE AWARDS AND ACHIEVEMENTS. List any awards or recognitions for this research
None
- K. PUBLICATIONS GENERATED:

Number of Research Publications generated from this research project:	
Publication Category	Number
Articles in Refereed Journals	
Book Chapters	
Theses and Dissertations	
Water Resources Institute Reports	
Articles in Conference Proceedings	1
Other Publications	1

PROVIDE A CITATION FOR EACH PUBLICATION USING THE FOLLOWING FORMATS:

1. Articles in Refereed Scientific Journals Citation

None

2. Book Chapter Citation

None

3. Dissertations Citation

None

4. Water Resources Research Institute Reports Citation

Author (first author; last name, first name; all others: first name, last name), Year, Title, Name of WRRRI, University, City, State, Number of Pages.

5. Conference Proceedings Citation

Paper:

Lecompte, J., A.N. Wright, J. R. Kessler, and C. LeBleu. 2012. Saline irrigation of five landscape species for the Southeast. Proc. SNA Res. Conf. *in press*.

6. Other Publications Citation

Abstract:

LeCompte, J.S., A.N. Wright, J.R. Kessler, and C. Lebleu. 2012. Saline irrigation of three green roof species for the Southeast. HortScience *in press*. (Abstr.)

PRESENTATIONS MADE:

Lecompte, J., A.N. Wright, J. R. Kessler, and C. LeBleu. 2012. Saline irrigation of five landscape species for the Southeast. Southern Nursery Association Research Conference.

LeCompte, J.S., A.N. Wright, J.R. Kessler, and C. Lebleu. 2012. Saline irrigation of three green roof species for the Southeast. American Society for Horticultural Science – Southern Region Annual Meeting.

L. STUDENTS SUPPORTED (Complete the following table)

Number of Students Supported, by Degree	
Type	Number of students funded through this research project:
Undergraduate	
Masters	2 (in progress)
Ph.D.	
Post Doc	
Number of Theses and Dissertations Resulting from Student Support:	
Master’s Theses	2 (in progress)
Ph.D. Dissertations	

M. RESEARCH CATEGORIES: (In column 1 mark all that apply)

Research Category

	Biological Sciences
	Climate and Hydrological Processes
	Engineering
	Ground Water Flow and Transport
	Social Sciences
X	Water Quality
	Other: Explain

N. FOCUS CATEGORIES (mark all that apply with "X" in column 1):

	ACID DEPOSITION	ACD
X	AGRICULTURE	AG
	CLIMATOLOGICAL PROCESSES	CP
	CONSERVATION	COV
	DROUGHT	DROU
	ECOLOGY	ECL
	ECONOMICS	ECON
	EDUCATION	EDU
	FLOODS	FL
	GEOMORPHOLOGICAL PROCESSES	GEOMOR
	GEOCHEMICAL PROCESSES	GEOCHE
	GROUNDWATER	GW
	HYDROGEOCHEMISTRY	HYDGEO
	HYDROLOGY	HYDROL
	INVASIVE SPECIES	INV
X	IRRIGATION	IG
	LAW, INSTITUTIONS, & POLICY	LIP
	MANAGEMENT & PLANNING	M&P
	METHODS	MET
	MODELS	MOD
	NITRATE CONTAMINATION	NC
	NONPOINT POLLUTION	NPP
	NUTRIENTS	NU
	RADIOACTIVE SUBSTANCES	RAD
	RECREATION	REC
	SEDIMENTS	SED
	SOLUTE TRANSPORT	ST

	SURFACE WATER	SW
	TOXIC SUBSTANCES	TS
	TREATMENT	TRT
X	WASTEWATER	WW
	WATER QUALITY	WQL
	WATER QUANTITY	WQN
X	WATER SUPPLY	WS
X	WATER USE	WU
	WETLANDS	WL

- O. DESCRIPTORS: (Enter keywords of your choice, descriptive of the work)
Sustainable, landscape, water reuse, greywater, green infrastructure

Forecasting toxic cyanobacterial blooms throughout the southeastern U.S.

Basic Information

Title:	Forecasting toxic cyanobacterial blooms throughout the southeastern U.S.
Project Number:	2011AL121G
Start Date:	9/1/2011
End Date:	8/31/2014
Funding Source:	104G
Congressional District:	3rd
Research Category:	Water Quality
Focus Category:	Models, Nutrients, Surface Water
Descriptors:	None
Principal Investigators:	Alan Elliott Wilson, Kevin Schrader, Russell Alan Wright

Publication

1. Wilson, Alan E.; Michael F. Chislock. In press. Ecological control of cyanobacterial blooms in freshwater ecosystems. in ed. Aloysio Ferrão-Filho, Cyanobacteria: Toxicity, ecology, and management. Hauppauge, New York, Nova Science Publishers, xx-xx.

ANNUAL TECHNICAL REPORT SYNOPSIS

- A. PROJECT TITLE:
USGS Project 2011AL121G – Forecasting toxic cyanobacterial blooms throughout the southeastern U.S.
Project website - http://wilsonlab.com/bloom_network/
- B. PRIMARY PI(s): Name(s), Title(s) & Academic Rank(s)
Alan E. Wilson, Assistant Professor, Ph.D.
- C. OTHER PI(s): Name(s), Title(s) & Academic Rank(s)
Russell A. Wright, Associate Professor, Ph.D.
Kevin Schrader, Microbiologist, Ph.D.
- D. START DATE:
1 October 2011
- E. END DATE:
30 September 2014
- F. PROJECT OVERVIEW/SUMMARY: Provide a brief narrative overview or summary of the project.
Using a novel collaborative approach, we are collecting water quality samples and associated data from 400+ diverse freshwater systems, including lakes, reservoirs, ponds, and rivers, throughout much of the eastern U.S. These samples will be analyzed by the PIs for phycocyanin (cyanobacteria), cyanobacterial toxins, off-flavors, and phytoplankton enumeration. Data generated from these efforts will be used to refine and build models aimed at forecasting blooms of freshwater cyanobacterial blooms. Although the focus of the current project is on the Southeast, we have quickly expanded our efforts beyond this region. We hope to continue this expansion throughout the 3-year project.
- G. PROJECT OBJECTIVE(s): Briefly explain the project objectives.
To enhance our network of water quality managers and scientists throughout the southeastern U.S. aimed at monitoring sites for toxic cyanobacterial blooms.
To test and refine current models that forecast toxic cyanobacterial blooms and off-flavor events in freshwater lakes, reservoirs, rivers, and ponds throughout the Southeast.
To train state and federal scientists, water quality managers, and aquaculturists on standard techniques to measure cyanobacterial toxin and phycocyanin concentrations and to identify and enumerate phytoplankton.
To train graduate and undergraduate students on field sampling and laboratory-based water quality analytical analyses.
To enhance our existing, user-friendly, interactive website where water quality managers and aquaculturists can determine the risk of their waterbodies for toxic cyanobacterial blooms and/or off-flavor events.
To create a model collaborative network that can be extended to other U.S. regions.

H. **METHODOLOGIES:** Briefly explain the research methodology used.

Sample sharing is central to the success of our project. We are also planning to share data among collaborators, but we are most excited about our approach for bringing together scientists in academia, agencies, and industry who all share a common concern – algal blooms. We are leveraging resources provided by our many colleagues throughout the eastern U.S. to collect and analyze water quality samples for us. In turn, we will analyze these samples for phytoplankton, cyanobacteria, and cyanobacterial toxins and off-flavors in order to build algal bloom forecasting models.

I. **PRINCIPAL FINDINGS/RESULTS:** Explain the results of findings of this research project.

Despite being in our first project year, we have observed a huge interest in our project by agency and academic scientists throughout the eastern U.S. We proposed to get samples and data from 200 sites per year. We will double that estimate in our first year! All of our sampling gear has been shipped to our colleagues (60+ individuals in 13 states and Puerto Rico). Our colleagues will return their samples to us this fall when we will begin our own analyses. We have held two water quality workshops this spring (Orlando and Auburn). Both were well attended (16-17 students each), and we received feedback showing that our students learned a lot about the project and our analytical and modelling approaches. We will be organizing similar workshops next spring. We have also given several presentations at regional and national conferences showcasing this project, and all have generated more excitement about our project and our analytical techniques (especially the phycocyanin analysis). One of Wilson’s students is in the process of running a laboratory experiment further validating the utility of our phycocyanin analyses, which we expect to submit for publication later this year. Given the feedback we have received from others, we expect these data to be of broad interest to scientists interested in quickly quantifying cyanobacterial abundance.

J. **NOTABLE AWARDS AND ACHIEVEMENTS.** List any awards or recognitions for this research
None

K. **PUBLICATIONS GENERATED:**

Number of Research Publications generated from this research project:	
Publication Category	Number
Articles in Refereed Journals	0
Book Chapters	1
Theses and Dissertations	0
Water Resources Institute Reports	0
Articles in Conference Proceedings	0
Other Publications	0

PROVIDE A CITATION FOR EACH PUBLICATION USING THE FOLLOWING FORMATS:

1. Articles in Refereed Scientific Journals Citation

Author (first author; last name, first name; all others; first name, last name), Year, Title, Name of Journal, Volume(Number), Page Numbers.

None

2. Book Chapter Citation

Author (first author; last name, first name; all others: first name, last name), Year, Title of chapter, "in" Name(s) of Editor "ed.", Title of Book, City, State, Publisher, Page Numbers.

Wilson, Alan E.; Michael F. Chislock. *In press*. Ecological control of cyanobacterial blooms in freshwater ecosystems. in ed. Aloysio Ferrão-Filho, *Cyanobacteria: Toxicity, ecology, and management*. Hauppauge, New York, Nova Science Publishers, xx-xx.

3. Dissertations Citation

Author (last name, first name), Year, Title, "MS (Ph.D.) Dissertation," Department, College, University, City, State, Number of Pages.

None

4. Water Resources Research Institute Reports Citation

Author (first author; last name, first name; all others: first name, last name), Year, Title, Name of WRRRI, University, City, State, Number of Pages.

None

5. Conference Proceedings Citation

Author (first author; last name, first name; all others: first name, last name), Year, Title of Presentation, "in" Title of Proceedings, Publisher, City, State, Page Numbers.

None

6. Other Publications Citation

Author (first author; last name, first name; all others: first name, last name), Year, Title, other information sufficient to locate publications, Page Numbers (if in publication) or Number of Pages (if monograph).

None

L. PRESENTATIONS MADE:

Presenter(s) (last name, first name; all others presentation authors: first name, last name), Year, Title, other information sufficient to identify the venue in which the presentation was made.

- Wilson, Alan E.; Russell A. Wright; Kevin. K. Schrader; Gina L. Curvin; Barry H. Rosen; Jennifer L. Graham, 2012, Creating cost-effective regional algal bloom monitoring networks: Extending beyond Alabama. Alabama Water Resources Conference, Orange Beach, Alabama.
- Wilson, Alan E.; Russell A. Wright; Kevin. K. Schrader; Gina L. Curvin; Barry H. Rosen; Jennifer L. Graham, 2012, Creating cost-effective regional algal bloom monitoring networks: The Southeast as a case study. 21st SE NALMS Southeastern Lake and Watershed Management Conference. Columbus, Georgia.
- Wilson, Alan E.; RajReni B. Kaul; Michael F. Chislock; Gina L. Curvin, 2012, Towards an improved understanding of the factors mediating toxic cyanobacterial blooms throughout the Southeast. Association of Southeastern Biologists, Athens, Georgia.
- Wilson, Alan E.; Russell A. Wright; Kevin. K. Schrader; Gina L. Curvin; Barry H. Rosen; Jennifer L. Graham, 2012, Creating cost-effective regional algal bloom monitoring networks. 8th National Monitoring Conference. Portland, Oregon.

M. STUDENTS SUPPORTED (Complete the following table)

Number of Students Supported, by Degree	
Type	Number of students funded through this research project:
Undergraduate	4
Masters	1
Ph.D.	0
Post Doc	0
Number of Theses and Dissertations Resulting from Student Support:	
Master's Theses	0
Ph.D. Dissertations	0

N. RESEARCH CATEGORIES: (In column 1 mark all that apply)

	Research Category
X	Biological Sciences
	Climate and Hydrological Processes
	Engineering
	Ground Water Flow and Transport
	Social Sciences
X	Water Quality
X	Other: Modelling

O. FOCUS CATEGORIES (mark all that apply with "X" in column 1):

	ACID DEPOSITION	ACD
	AGRICULTURE	AG
	CLIMATOLOGICAL PROCESSES	CP
X	CONSERVATION	COV
	DROUGHT	DROU
	ECOLOGY	ECL
	ECONOMICS	ECON
X	EDUCATION	EDU
	FLOODS	FL
	GEOMORPHOLOGICAL PROCESSES	GEOMOR
	GEOCHEMICAL PROCESSES	GEOCHE
	GROUNDWATER	GW
	HYDROGEOCHEMISTRY	HYDGEO
	HYDROLOGY	HYDROL
	INVASIVE SPECIES	INV
	IRRIGATION	IG
	LAW, INSTITUTIONS, & POLICY	LIP
X	MANAGEMENT & PLANNING	M&P
X	METHODS	MET
X	MODELS	MOD
X	NITRATE CONTAMINATION	NC
	NONPOINT POLLUTION	NPP
X	NUTRIENTS	NU
	RADIOACTIVE SUBSTANCES	RAD
	RECREATION	REC
	SEDIMENTS	SED
	SOLUTE TRANSPORT	ST
X	SURFACE WATER	SW
X	TOXIC SUBSTANCES	TS
	TREATMENT	TRT
	WASTEWATER	WW
X	WATER QUALITY	WQL
X	WATER QUANTITY	WQN
	WATER SUPPLY	WS

	WATER USE	WU
	WETLANDS	WL

- P. DESCRIPTORS: (Enter keywords of your choice, descriptive of the work)
Algal blooms, cyanobacteria, off-flavor, toxin, microcystin, BMAA, cylindrospermopsin, saxitoxin, phytoplankton, modeling, forecasting, monitoring, network, collaboration

Information Transfer Program Introduction

None.

USGS Summer Intern Program

None.

Student Support					
Category	Section 104 Base Grant	Section 104 NCGP Award	NIWR-USGS Internship	Supplemental Awards	Total
Undergraduate	2	4	0	0	6
Masters	2	1	0	0	3
Ph.D.	3	0	0	0	3
Post-Doc.	1	0	0	0	1
Total	8	5	0	0	13

Notable Awards and Achievements